US007219087B2

(12) **United States Patent**
Panfilov et al.

(10) **Patent No.: US 7,219,087 B2**
(45) **Date of Patent: *May 15, 2007**

(54) **SOFT COMPUTING OPTIMIZER OF INTELLIGENT CONTROL SYSTEM STRUCTURES**

(75) Inventors: **Sergey A. Panfilov**, Crema (IT); **Ludmila Litvintseva**, Crema (IT); **Sergey V. Ulyanov**, Crema (IT); **Viktor S. Ulyanov**, Moscow (RU); **Kazuki Takahashi**, Crema (IT)

(73) Assignee: **Yamaha Hatsudoki Kabushiki Kaisha** (JP)

(*) Notice: Subject to any disclaimer, the term of this patent is extended or adjusted under 35 U.S.C. 154(b) by 299 days.

This patent is subject to a terminal disclaimer.

(21) Appl. No.: **10/897,978**

(22) Filed: **Jul. 23, 2004**

(65) **Prior Publication Data**

US 2005/0119986 A1 Jun. 2, 2005

Related U.S. Application Data

(60) Provisional application No. 60/490,397, filed on Jul. 25, 2003.

(51) **Int. Cl.**

G05B 13/00	(2006.01)
G05B 13/04	(2006.01)
G05B 15/00	(2006.01)
G05B 17/00	(2006.01)

(52) **U.S. Cl.** **706/23**; 706/1; 706/19; 700/28; 700/50

(58) **Field of Classification Search** 706/59, 706/8, 50, 1, 23, 19; 700/28, 50
See application file for complete search history.

(56) **References Cited**

U.S. PATENT DOCUMENTS

5,111,531	A		5/1992	Grayson et al.
5,142,877	A		9/1992	Shimizu
5,159,660	A		10/1992	Lu et al.
5,204,718	A		4/1993	Morita
5,208,749	A		5/1993	Adachi et al.
5,214,576	A		5/1993	Tani et al.
5,263,123	A	*	11/1993	Hayashi 706/45
5,268,835	A		12/1993	Miyagaki et al.
5,285,377	A		2/1994	Sugasaka et al.
5,305,230	A		4/1994	Matsumoto et al.
5,324,069	A		6/1994	Ogawa
5,349,646	A	*	9/1994	Furuta et al. 706/23
5,361,628	A		11/1994	Marko et al.
5,367,612	A		11/1994	Bozich et al.
5,372,015	A		12/1994	Suzuki et al.
5,434,951	A		7/1995	Kuwata
5,471,381	A		11/1995	Khan
5,483,450	A		1/1996	Titli et al.
5,488,562	A		1/1996	Otterbein et al.
5,539,638	A		7/1996	Keeler et al.
5,557,520	A		9/1996	Suissa et al.
5,740,323	A	*	4/1998	Nomura et al. 706/13
5,815,198	A		9/1998	Vachtsevanos et al.
5,877,954	A		3/1999	Klimasauskas et al.
5,912,821	A		6/1999	Kobayashi
5,928,297	A		7/1999	Murata et al.
5,943,660	A		8/1999	Yesildirek et al.
5,971,579	A		10/1999	Kim
6,021,369	A		2/2000	Kamihira et al.
6,064,996	A		5/2000	Yamaguchi et al.
6,188,988	B1	*	2/2001	Barry et al. 705/3
6,411,944	B1	*	6/2002	Ulyanov 706/13
6,463,371	B1	*	10/2002	Ulyanov et al. 701/40
6,490,237	B1	*	12/2002	Supino 369/59.1
6,496,761	B1	*	12/2002	Ulyanov et al. 701/37
6,701,236	B2	*	3/2004	Ulyanov et al. 701/40
6,711,556	B1	*	3/2004	Sepe et al. 706/6
6,721,718	B2	*	4/2004	Ulyanov 706/2
6,735,576	B1	*	5/2004	Kaji et al. 706/1
6,829,604	B1	*	12/2004	Tifft 707/5
2002/0016665	A1	*	2/2002	Ulyanov et al. 701/106
2002/0099673	A1	*	7/2002	Pappalardo et al. 706/1
2003/0078899	A1	*	4/2003	Shanahan 706/8

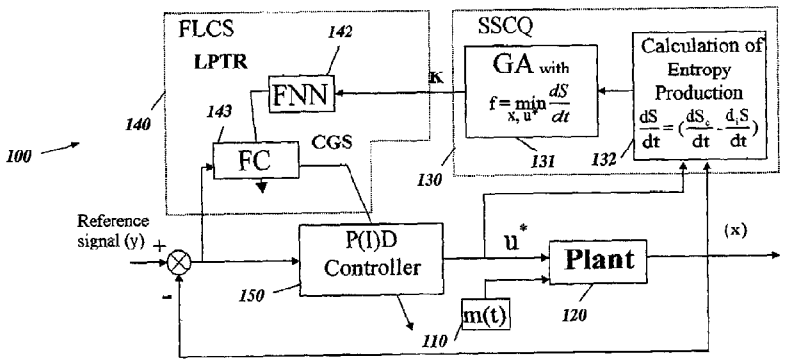

2003/0093392	A1	5/2003	Ulyanov	
2004/0024750	A1*	2/2004	Ulyanov et al.	707/3
2004/0030420	A1*	2/2004	Ulyanov et al.	700/48

FOREIGN PATENT DOCUMENTS

EP	1 085 460	3/2001
JP	10268904 A	10/1998

OTHER PUBLICATIONS

Fuzzy Control of Rider-Motorcycle System Using Genetic Algorithm and Auto-Tuning. J.C. Wu and T.S. Liu. Mechatronics vol. 5, No. 4, pp. 441-455. 1995.*

A Model for a Rider-Motorcycle System Using Fuzzy Control. T.S. Lui and J.C. Wu. IEEE Transactions on Systems, Man, and Cybernetics, vol. 23, No. 1, pp. 267-276, 1993.*

J.C. Wu and T.S. Liu, Fuzzy Control of Rider-Motorcycle System Using Genetic Algorithm and Auto-Tuning, Mechatronic vol. 5, pp. 441-455. 1995.*

Antony Satyadas and K. Krishnakumar, GA-optmized Fuzzy Controller for Spacecraft Attitude Control, IEEE, pp. 1979-1984. 1994.*

Bose, Bimal K., (1994), "Expert System, Fuzzy Logic, and Neural Network Applications in Power Electric and Motion Control," Processing of the IEEE, vol. 82, No. 8, pp. 1303-1323.

Chen, Jen-Yang, "An Integration Design Approach in PID Controller," IEEE, 1999, pp. 901-907.

Dote, Y., "Real Time Nonlinear Learning Control for Robotic Manipulator Using Novel Fuzzy Neural Network," IEEE International Conference on System, Man, and Cybernetics, Oct. 1998.

Feng Q and Yamafuji K., (1988), "Design and Simulation of Control System of An Inverted Pendulum," Robotica, vol. 6, No. 3, pp. 235-241.

Gradetsky V.G. and Ulyanov S.V., (1993), "Mobile System With Wall Climbing Robots," Intern. J. of Computer and Systems Sciences, vol. 31, No. 1, pp. 126-142.

Johansson R., Magnusson M. and Fransson P.A., (1995), "Galvanic Vestibular Stimulation for Analysis of Postural Adaptation and Stability," IEEE Transactions on Biomedical Engineering, vol. 42, No. 3, pp. 282-292.

Ju M.S., Yi S.G., Tsuei Y.G, and Chou Y.L., (1995), "Fuzzy Control of Electrohydraulic Above-Knee Prostheses," JSME International Journal, vol. 38, No. 1, pp. 78-85.

Lee Y.N., Kim T.W. and Suh I.H., (1994), "A Look-Up Table-Based Self Organizing Fuzzy Plus Linear Controller," Mechatronics, vol. 4, Vo. 1, pp. 71-90.

Liu T.S. and Wu J.C., (1993), "A Model For Rider-Motorcycle System Using Fuzzy Control," IEEE Transactions on Systems, Man and Cybernetics, vol. 23 SMC, No. 1, pp. 267-276.

Mendel, Jerry M., (1995), "Fuzzy Logic Systems for Engineering: A Tutorial", Proceeding of the IEEE, vol. 83, No. 3, pp. 345-377.

Nakajima R., Tsubouchi T., Yuta S. and Koyanagi E., (1997), "A development of a new mechanism of an autonomous unicycle", Proc. IEEE/RSJ International Conference on Intelligent Robots and Systems (IROS '97), vol. 2, Grenoble, France, pp. 906-912.

Perround M. and Saucier A., (1987), "Thermodynamics of dissipative systems", Helvetica Physica, vol. 60, No. 8, pp. 1038-1051.

Sheng Z.Q. and Yamafuji K., (1995), "Realization of a human riding a unicycle by a robot", Proc. of '95 IEEE Intern. Conf. on Robotics & Automation, Japan, vol. 2, pp. 1319-1326.

Sheng Z.Q. and Yamafuji K., (1997), "Postural stability of a human riding a unicycle and its emulation by a robot", IEEE Trans. on Robotics and Automation, vol. 13, No. 5, pp. 709-720.

Sheng, Z.Q. and Yamafuji K., (1995), "Study on the stability and motion control of a unicycle, 1st Report: Dynamics of a human riding a unicycle and its modeling by link mechanism", JSME International Journal, vol. 38C, No. 2, pp. 249-259.

* cited by examiner

Primary Examiner—Anthony Knight
Assistant Examiner—Adrian L. Kennedy
(74) *Attorney, Agent, or Firm*—Knobbe, Martens, Olson & Bear, LLP

(57) **ABSTRACT**

The present invention involves a Soft Computing (SC) optimizer for designing a Knowledge Base (KB) to be used in a control system for controlling a plant such as, for example, an internal combustion engine or an automobile suspension system. The SC optimizer includes a fuzzy inference engine based on a Fuzzy Neural Network (FNN). The SC Optimizer provides Fuzzy Inference System (FIS) structure selection, FIS structure optimization method selection, and teaching signal selection and generation. The user selects a fuzzy model, including one or more of: the number of input and/or output variables; the type of fuzzy inference model (e.g., Mamdani, Sugeno, Tsukamoto, etc.); and the preliminary type of membership functions. A Genetic Algorithm (GA) is used to optimize linguistic variable parameters and the input-output training patterns. A GA is also used to optimize the rule base, using the fuzzy model, optimal linguistic variable parameters, and a teaching signal. The GA produces a near-optimal FNN. The near-optimal FNN can be improved using classical derivative-based optimization procedures. The FIS structure found by the GA is optimized with a fitness function based on a response of the actual plant model of the controlled plant. The SC optimizer produces a robust KB that is typically smaller that the KB produced by prior art methods.

3 Claims, 54 Drawing Sheets

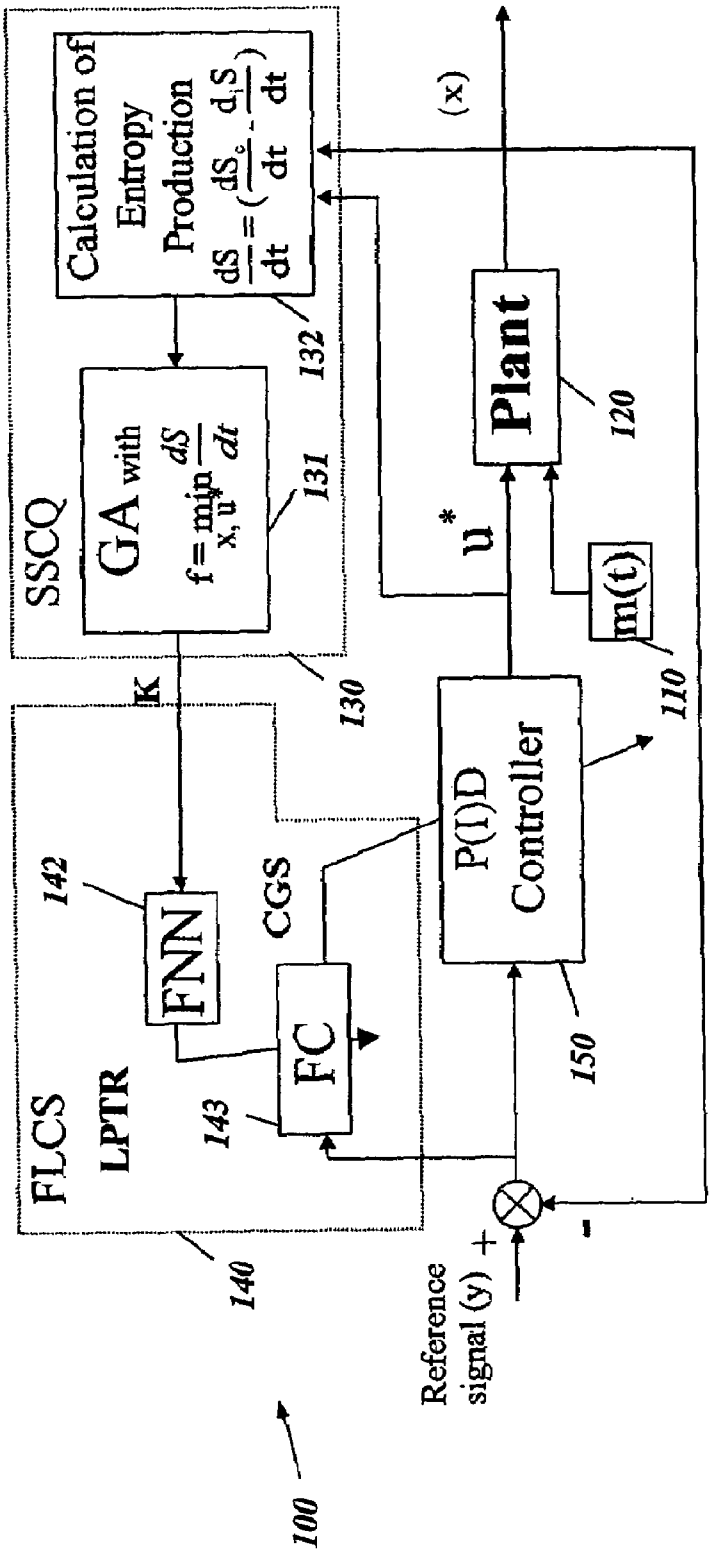
Calculation of Entropy Production
$\frac{dS}{dt}=(\frac{dS_e}{dt}-\frac{d_iS}{dt})$
132
SSCQ
GA with $f=\min_{x,u}\frac{dS}{dt}$
131
130
K
FLCS
LPTR
142
FNN
CGS
143
FC
140
P(I)D Controller
150
110
m(t)
u^*
Plant
120
(x)
Reference signal (y)
+
-
100

Figure 1

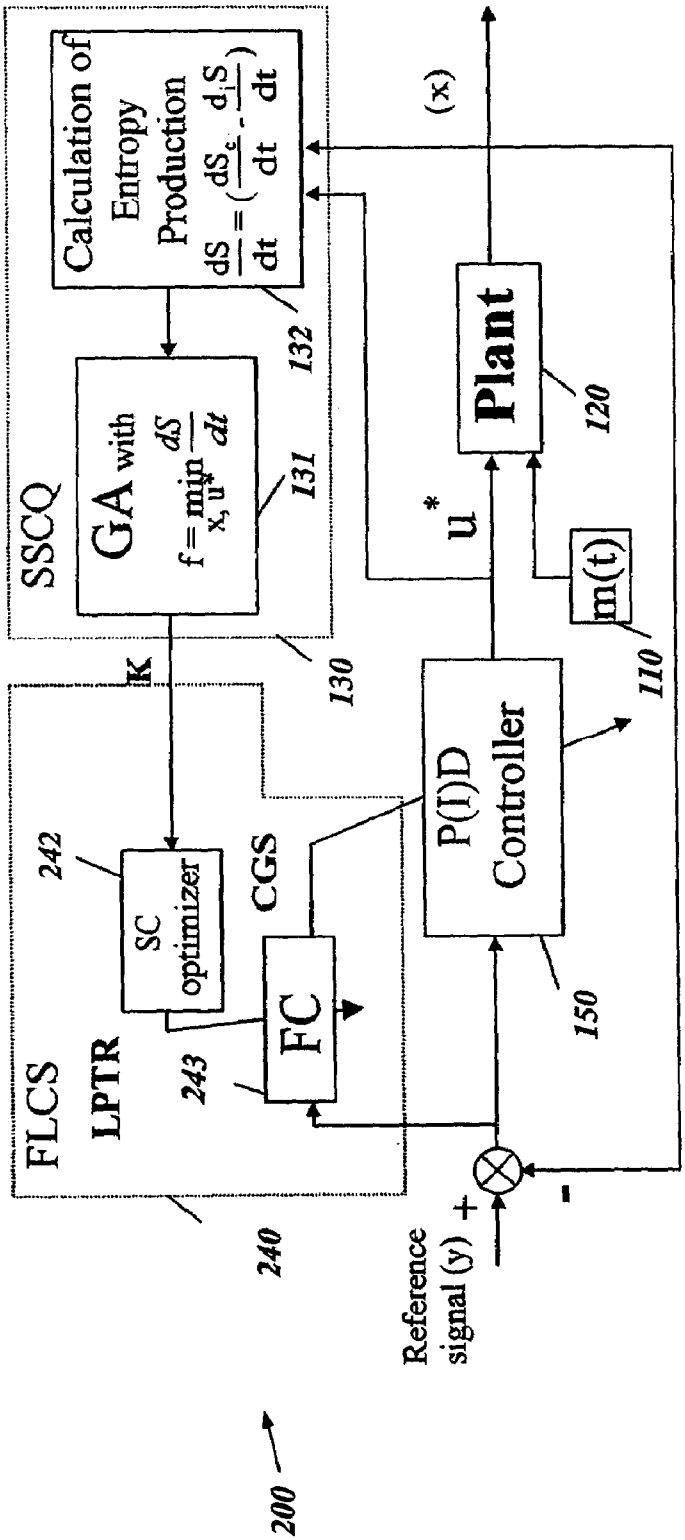
200
240
FLCS
LPTR
242
SC optimizer
243
CGS
FC
K
SSCQ
GA with $f = \min_{x,u^*} \frac{dS}{dt}$
131
Calculation of Entropy Production $\frac{dS}{dt} = (\frac{dS_e}{dt} - \frac{d_iS}{dt})$
132
130
P(I)D Controller
150
110
m(t)
u^*
Plant
120
(x)
Reference signal (y)
+
-

Figure 2

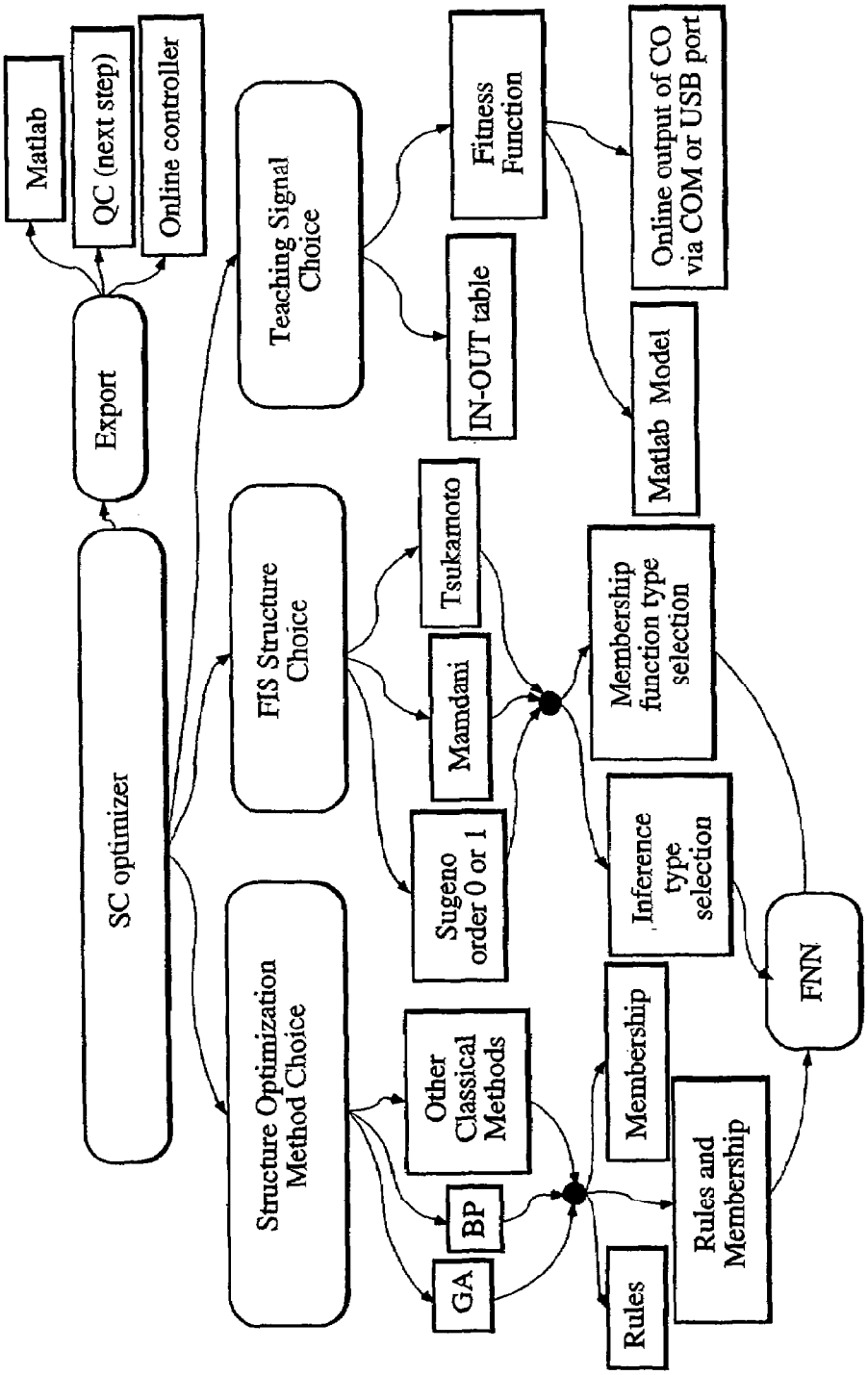
Matlab
QC (next step)
Online controller
Export
SC optimizer
Teaching Signal Choice
Fitness Function
Online output of CO via COM or USB port
IN-OUT table
Matlab Model
FIS Structure Choice
Tsukamoto
Mamdani
Sugeno order 0 or 1
Membership function type selection
Inference type selection
Structure Optimization Method Choice
Other Classical Methods
BP
GA
Membership
Rules
Rules and Membership
FNN

Figure 3

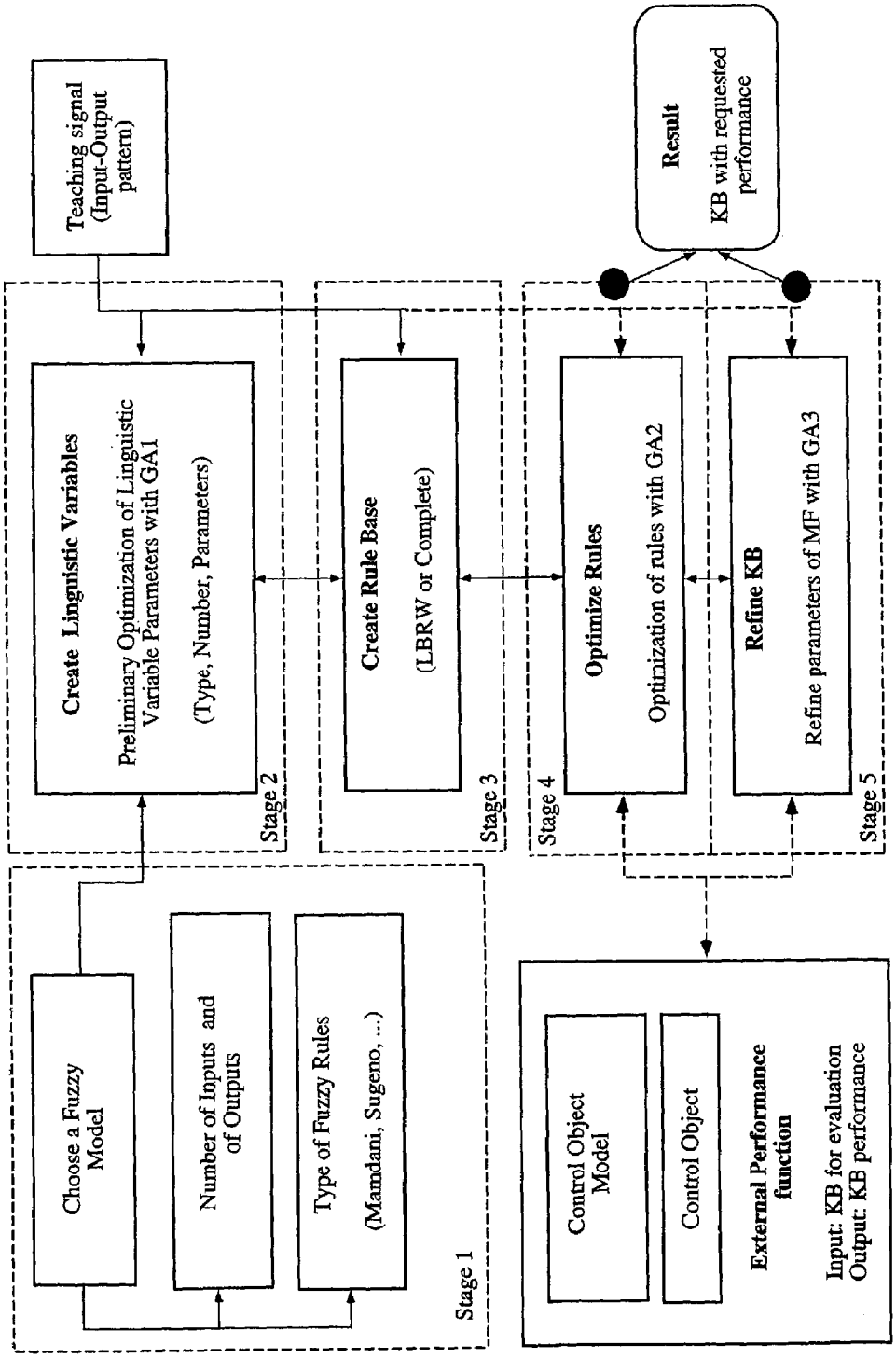
Teaching signal (Input-Output pattern)
Result
KB with requested performance
Create Linguistic Variables
Preliminary Optimization of Linguistic Variable Parameters with GA1
(Type, Number, Parameters)
Stage 2
Create Rule Base
(LBRW or Complete)
Stage 3
Optimize Rules
Optimization of rules with GA2
Stage 4
Refine KB
Refine parameters of MF with GA3
Stage 5
Choose a Fuzzy Model
Number of Inputs and of Outputs
Type of Fuzzy Rules
(Mamdani, Sugeno, ...)
Stage 1
Control Object Model
Control Object
External Performance function
Input: KB for evaluation
Output: KB performance

Figure 4

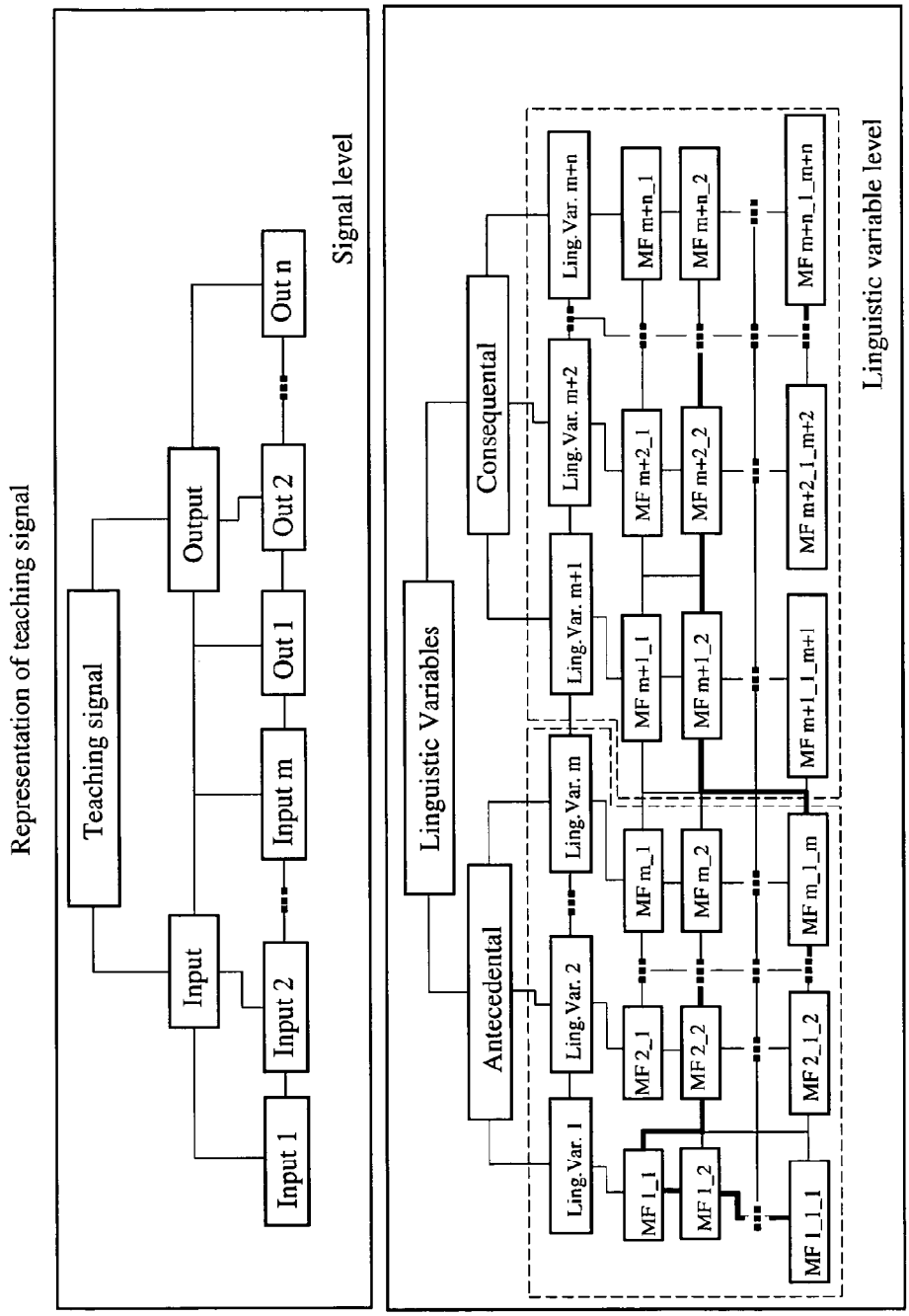
Representation of teaching signal
Teaching signal
Input
Input 1
Input 2
Input m
Output
Out 1
Out 2
Out n
Signal level
Linguistic Variables
Antecedental
Consequental
Ling.Var. 1
Ling.Var. 2
Ling.Var. m
Ling.Var. m+1
Ling.Var. m+2
Ling.Var. m+n
MF 1_1
MF 2_1
MF m_1
MF m+1_1
MF m+2_1
MF m+n_1
MF 1_2
MF 2_2
MF m_2
MF m+1_2
MF m+2_2
MF m+n_2
MF 1_1_1
MF 2_1_2
MF m_1_m
MF m+1_1_m+1
MF m+2_1_m+2
MF m+n_1_m+n
Linguistic variable level

Figure 5

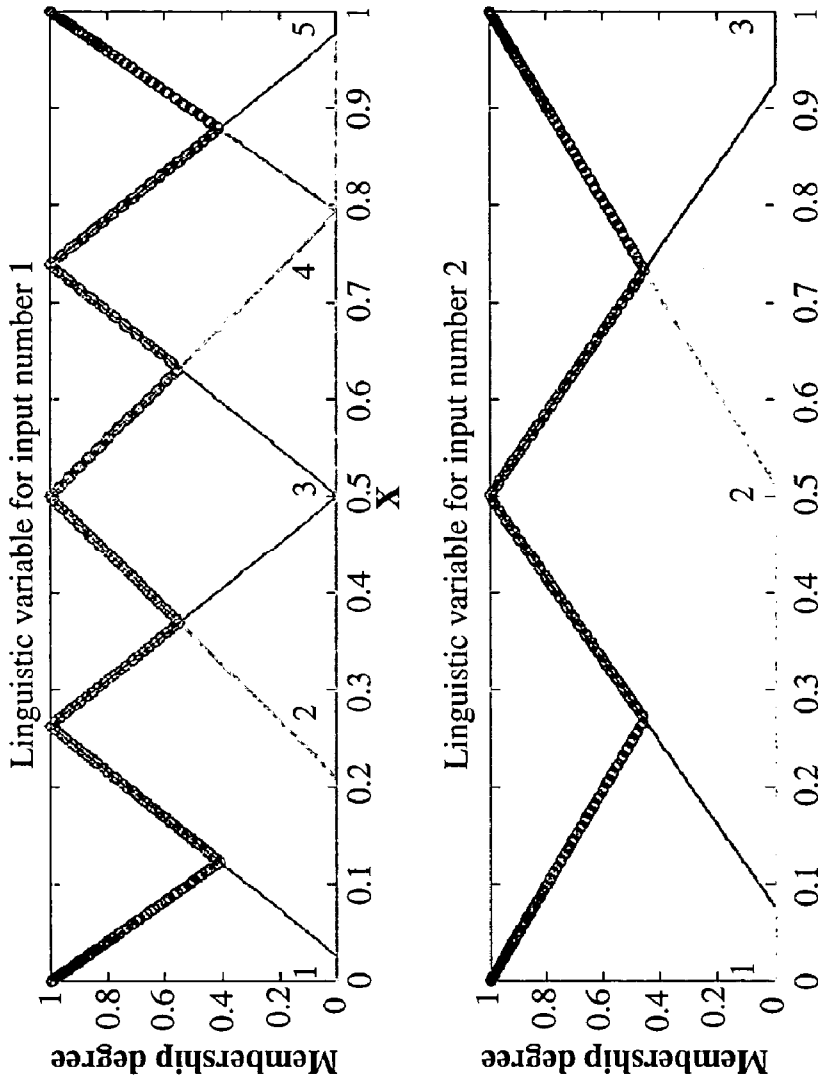
Linguistic variable for input number 1
Membership degree
X
1
2
3
4
5
Linguistic variable for input number 2
Membership degree
X
1
2
3

Figure 6

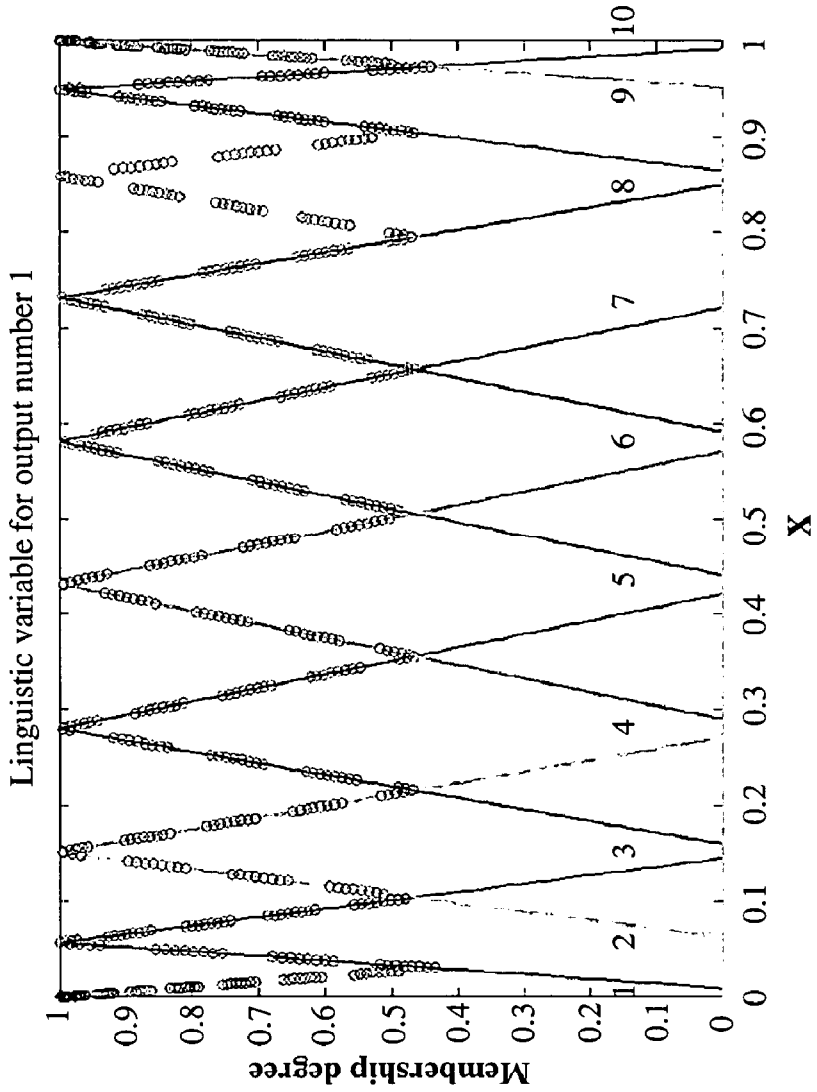
Linguistic variable for output number 1
Membership degree
x
1
2
3
4
5
6
7
8
9
10
0
0.1
0.2
0.3
0.4
0.5
0.6
0.7
0.8
0.9
1

Figure 7

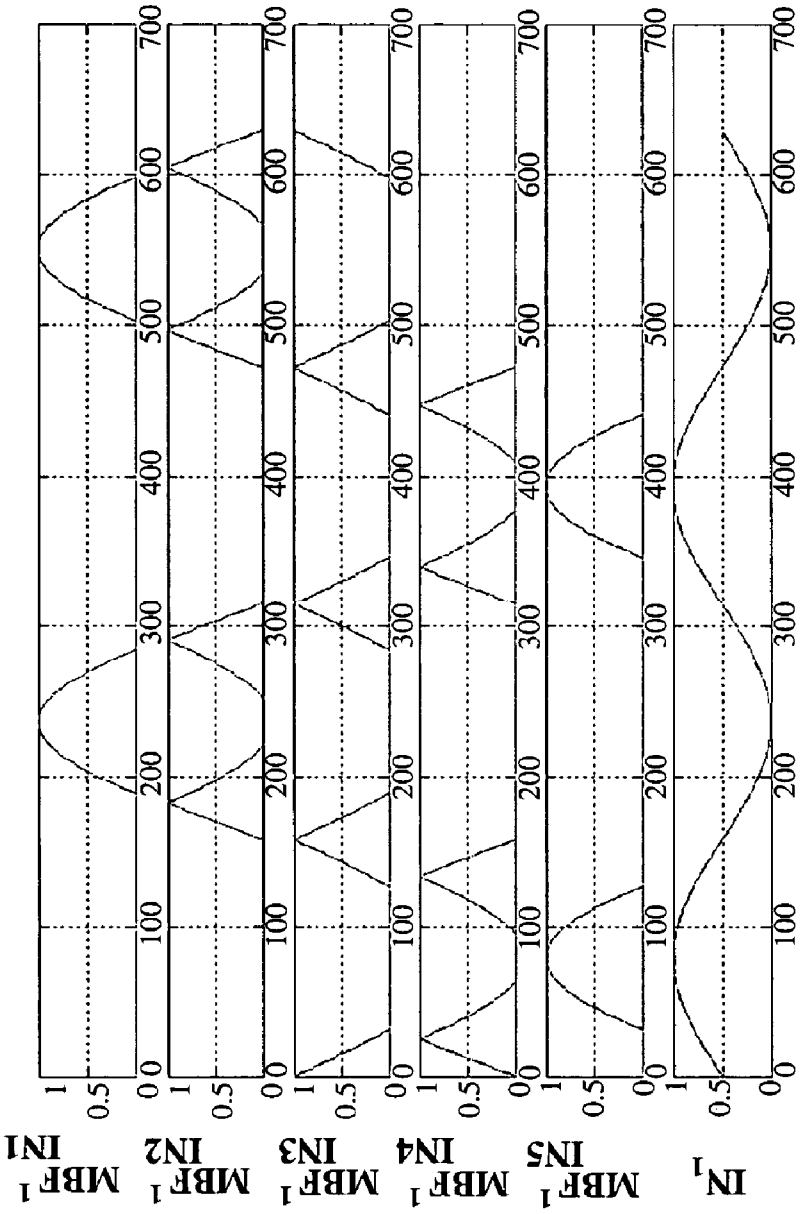
MBF 1 IN1
MBF 1 IN2
MBF 1 IN3
MBF 1 IN4
MBF 1 IN5
IN1
Pattern number

Figure 8

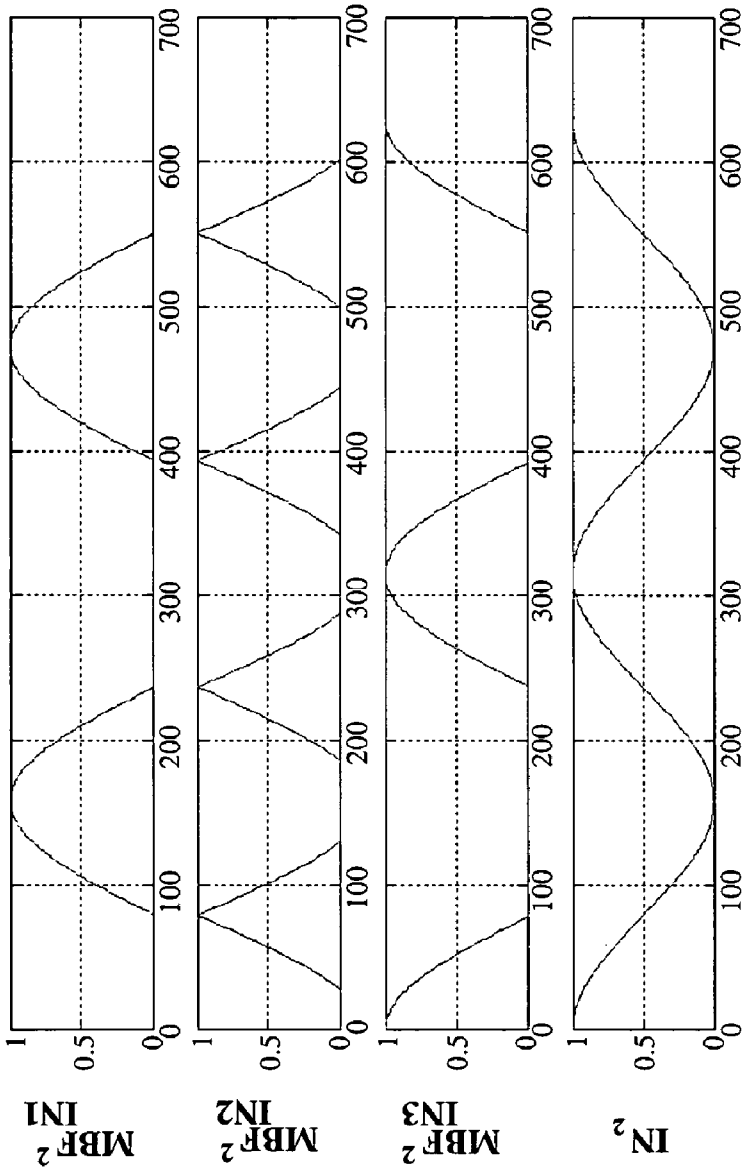
MBF² IN1
MBF² IN2
MBF² IN3
IN₂
0
0.5
1
0
100
200
300
400
500
600
700
Pattern number

Figure 9

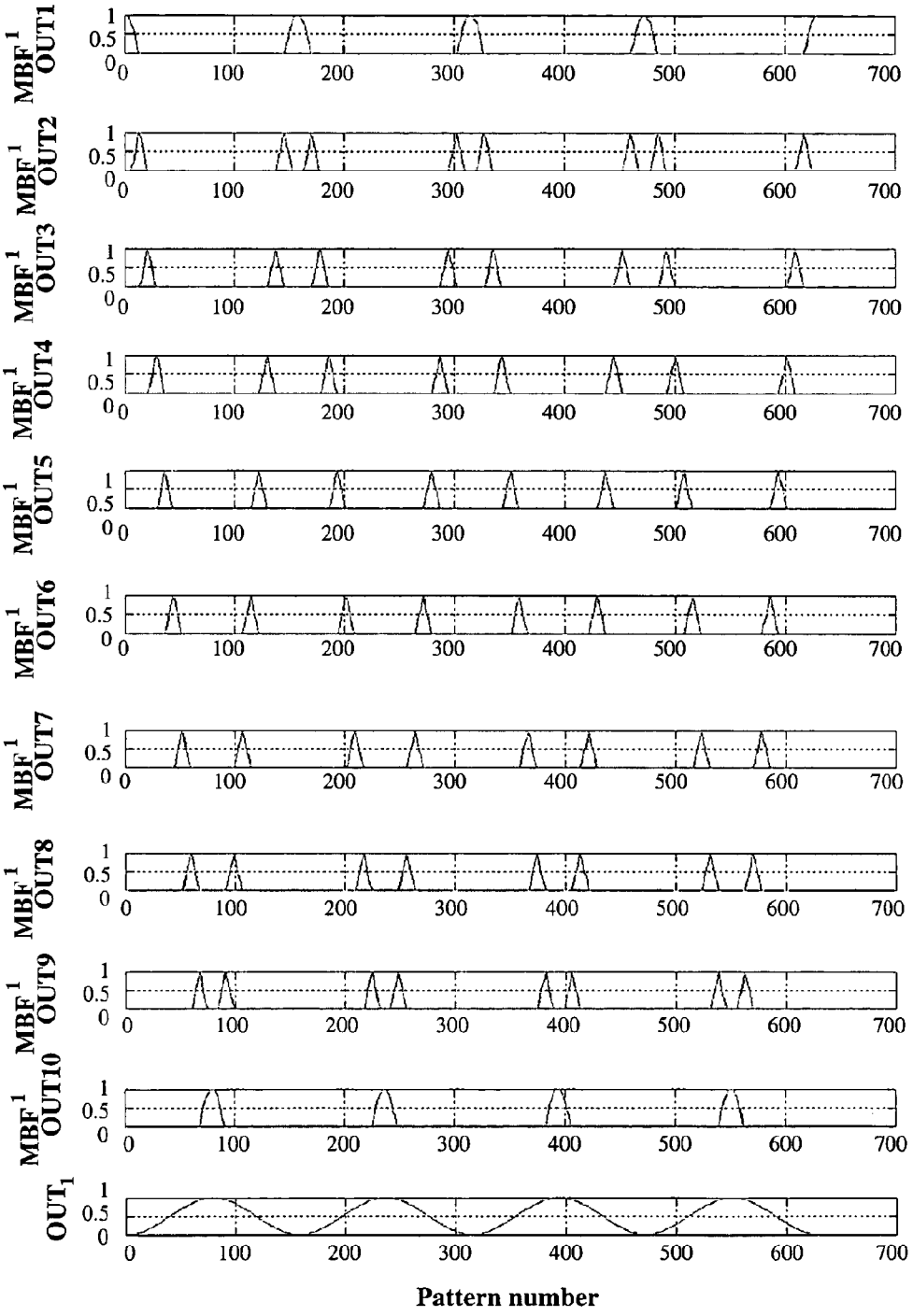
MBF 1 OUT1
MBF 1 OUT2
MBF 1 OUT3
MBF 1 OUT4
MBF 1 OUT5
MBF 1 OUT6
MBF 1 OUT7
MBF 1 OUT8
MBF 1 OUT9
MBF 1 OUT10
OUT1
1
0.5
0
0 100 200 300 400 500 600 700
Pattern number

Figure 10

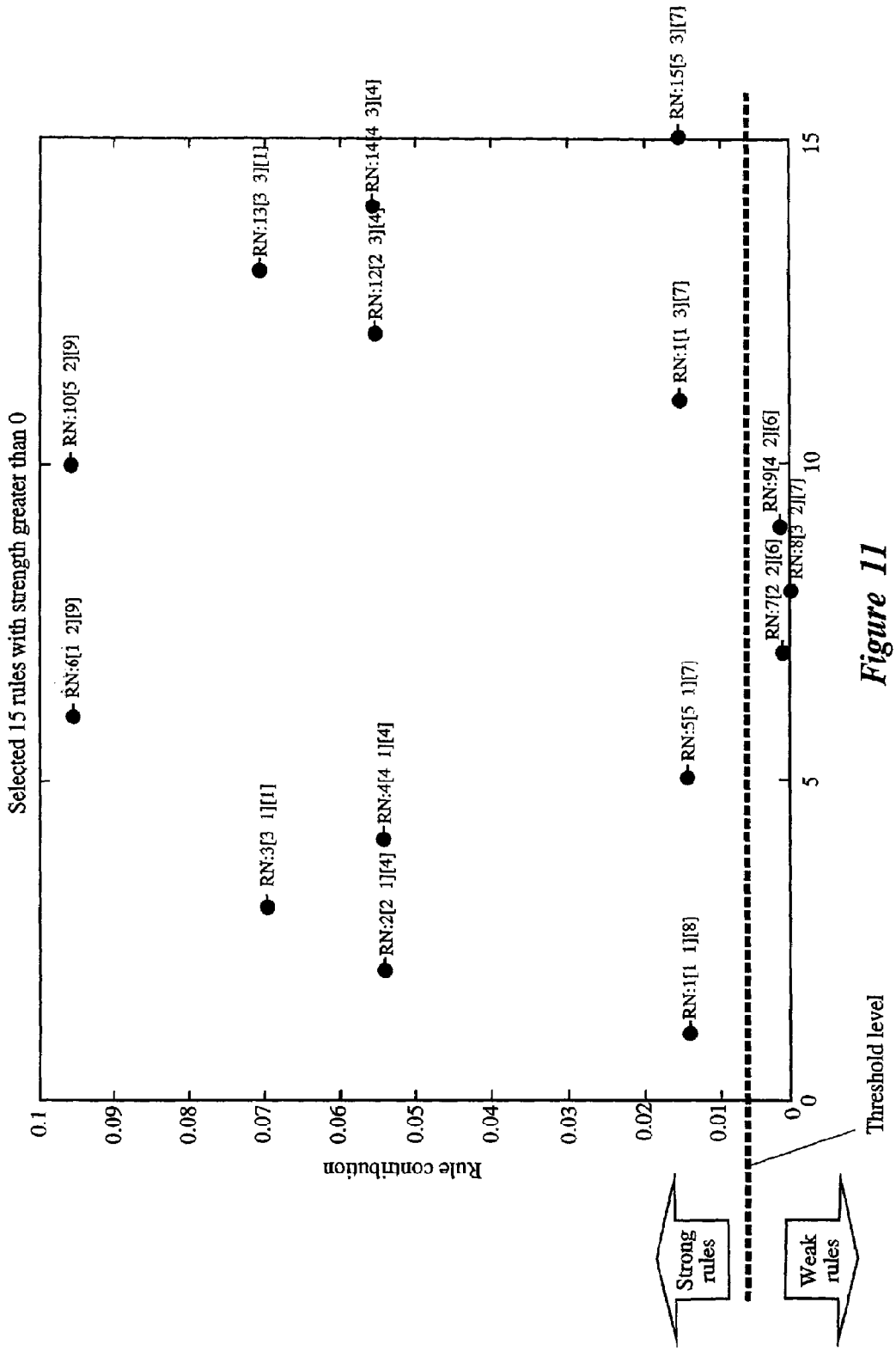
Selected 15 rules with strength greater than 0
Rule contribution
0.1
0.09
0.08
0.07
0.06
0.05
0.04
0.03
0.02
0.01
0
5
10
15
RN:6[1 2][9]
RN:10[5 2][9]
RN:3[3 1][1]
RN:13[3 3][1]
RN:2[2 1][4]
RN:4[4 1][4]
RN:12[2 3][4]
RN:14[4 3][4]
RN:1[1 1][8]
RN:5[5 1][7]
RN:1[1 3][7]
RN:15[5 3][7]
RN:7[2 2][6]
RN:9[4 2][6]
RN:8[3 2][7]
Strong rules
Weak rules
Threshold level

Figure 11

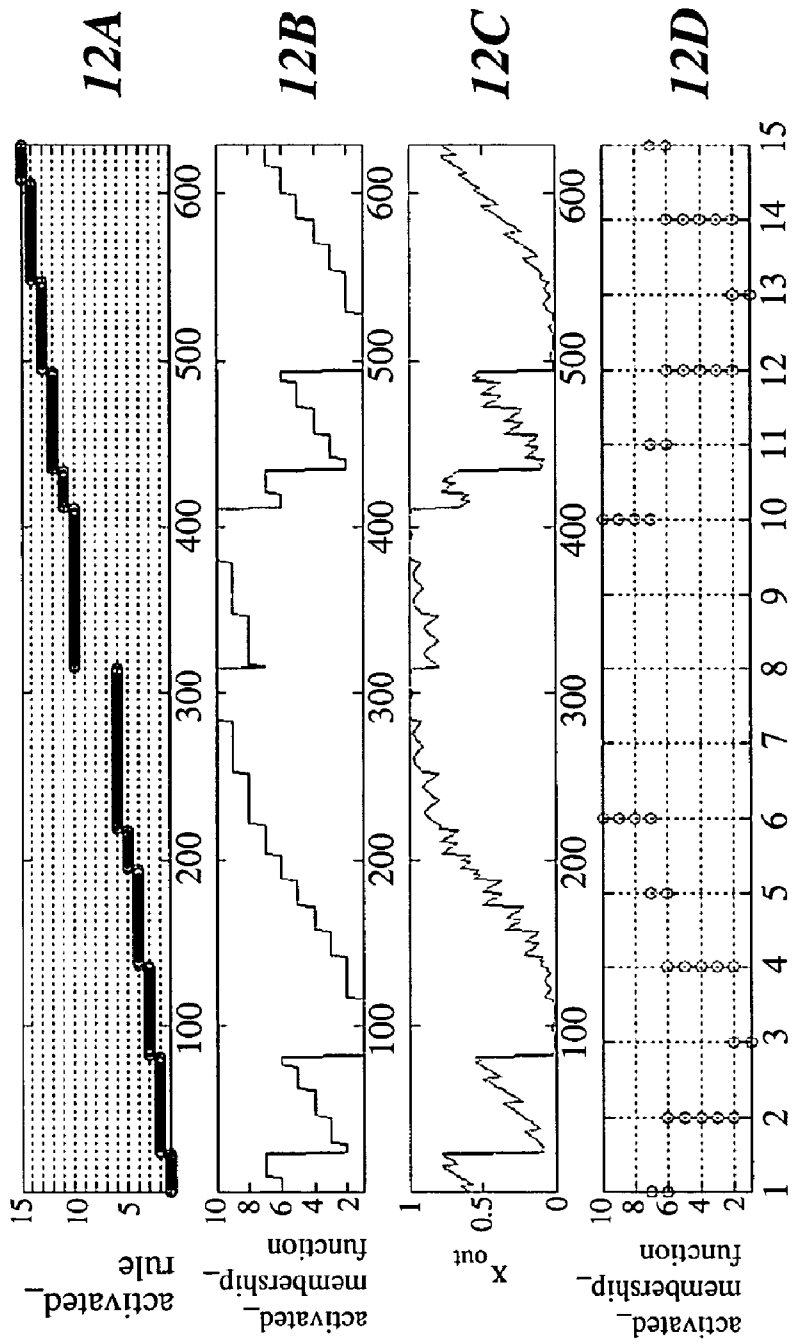
12A
12B
12C
12D
activated_ rule
activated_ membership_ function
x out
activated_ membership_ function
activated_rule

Figure 12

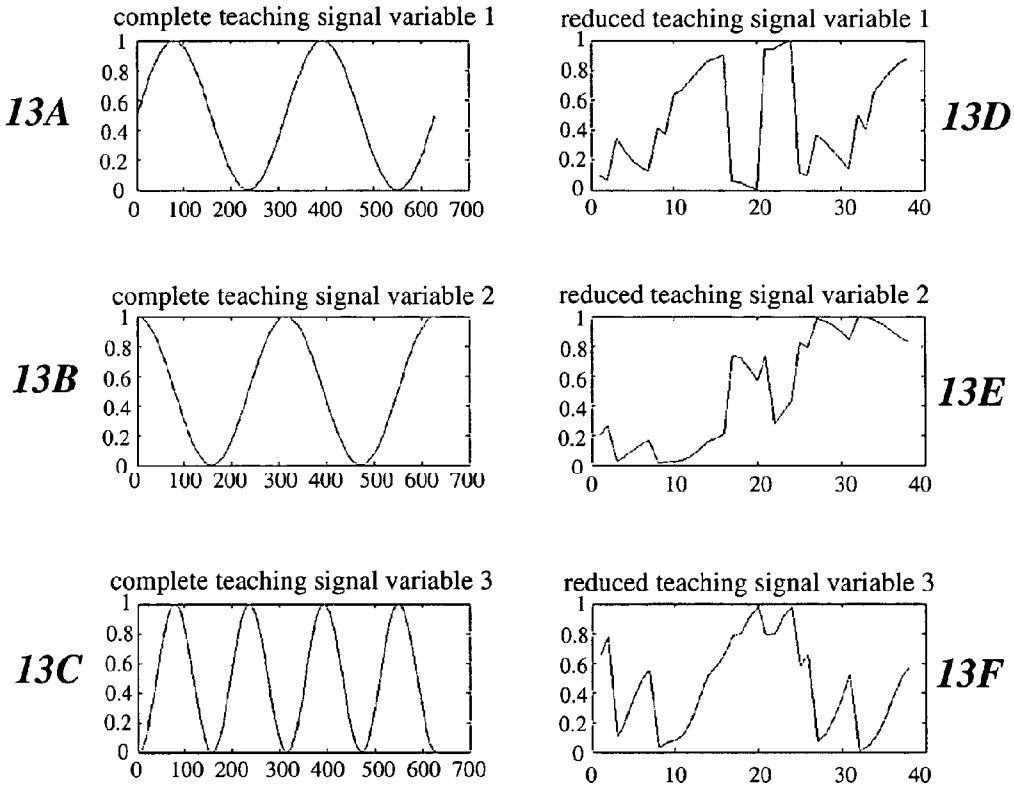
13A
complete teaching signal variable 1
1
0.8
0.6
0.4
0.2
0
0 100 200 300 400 500 600 700
13D
reduced teaching signal variable 1
1
0.8
0.6
0.4
0.2
0
0 10 20 30 40
13B
complete teaching signal variable 2
1
0.8
0.6
0.4
0.2
0
0 100 200 300 400 500 600 700
13E
reduced teaching signal variable 2
1
0.8
0.6
0.4
0.2
0
0 10 20 30 40
13C
complete teaching signal variable 3
1
0.8
0.6
0.4
0.2
0
0 100 200 300 400 500 600 700
13F
reduced teaching signal variable 3
1
0.8
0.6
0.4
0.2
0
0 10 20 30 40

Figure 13

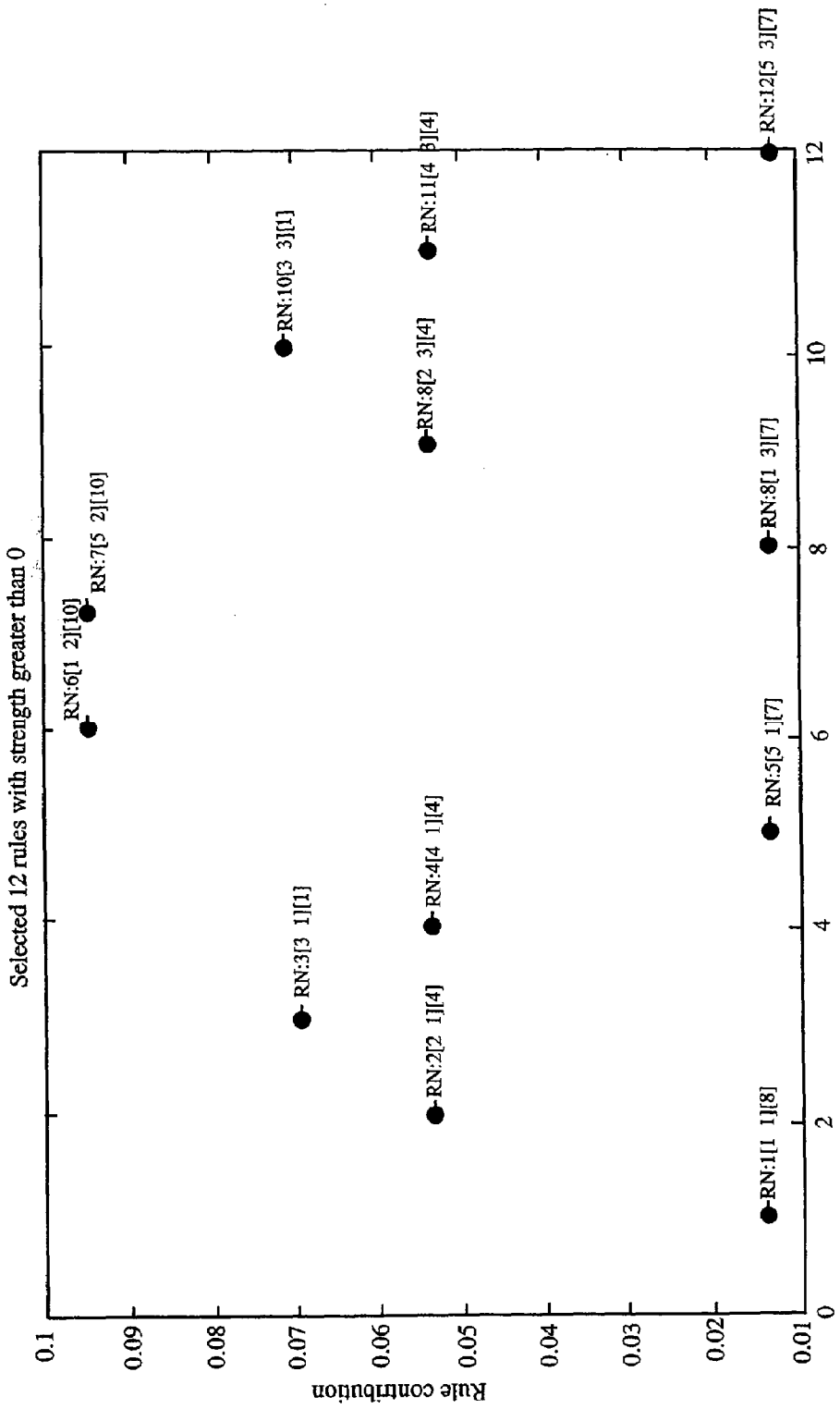
Selected 12 rules with strength greater than 0
Rule contribution
0.1
0.09
0.08
0.07
0.06
0.05
0.04
0.03
0.02
0.01
0
2
4
6
8
10
12
RN:6[1 2][10]
RN:7[5 2][10]
RN:10[3 3][1]
RN:11[4 3][4]
RN:12[5 3][7]
RN:3[3 1][1]
RN:8[2 3][4]
RN:8[1 3][7]
RN:4[4 1][4]
RN:2[2 1][4]
RN:5[5 1][7]
RN:1[1 1][8]

Figure 14

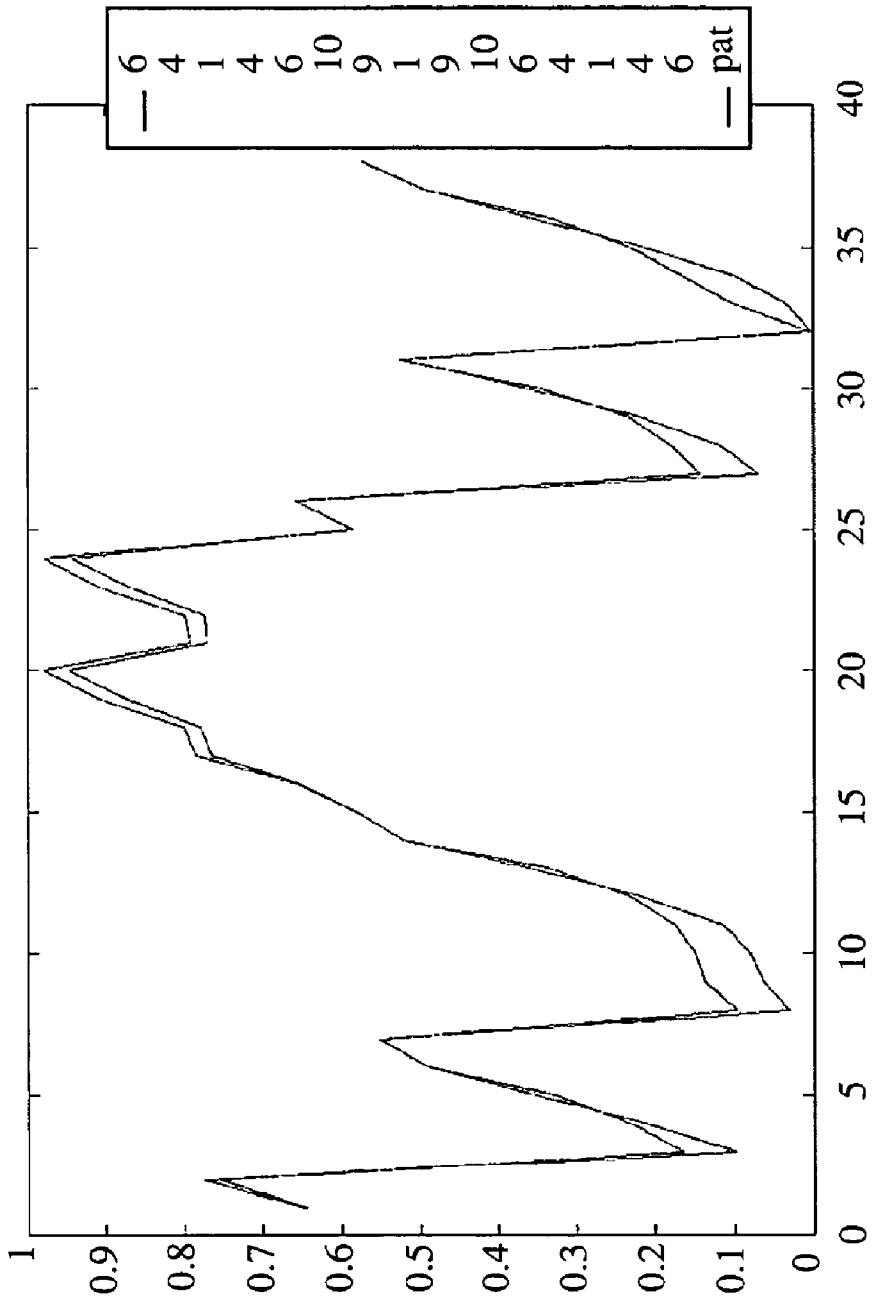
6
4
1
4
6
10
9
1
9
10
6
4
1
4
6
pat
0
5
10
15
20
25
30
35
40
0
0.1
0.2
0.3
0.4
0.5
0.6
0.7
0.8
0.9
1

Figure 15

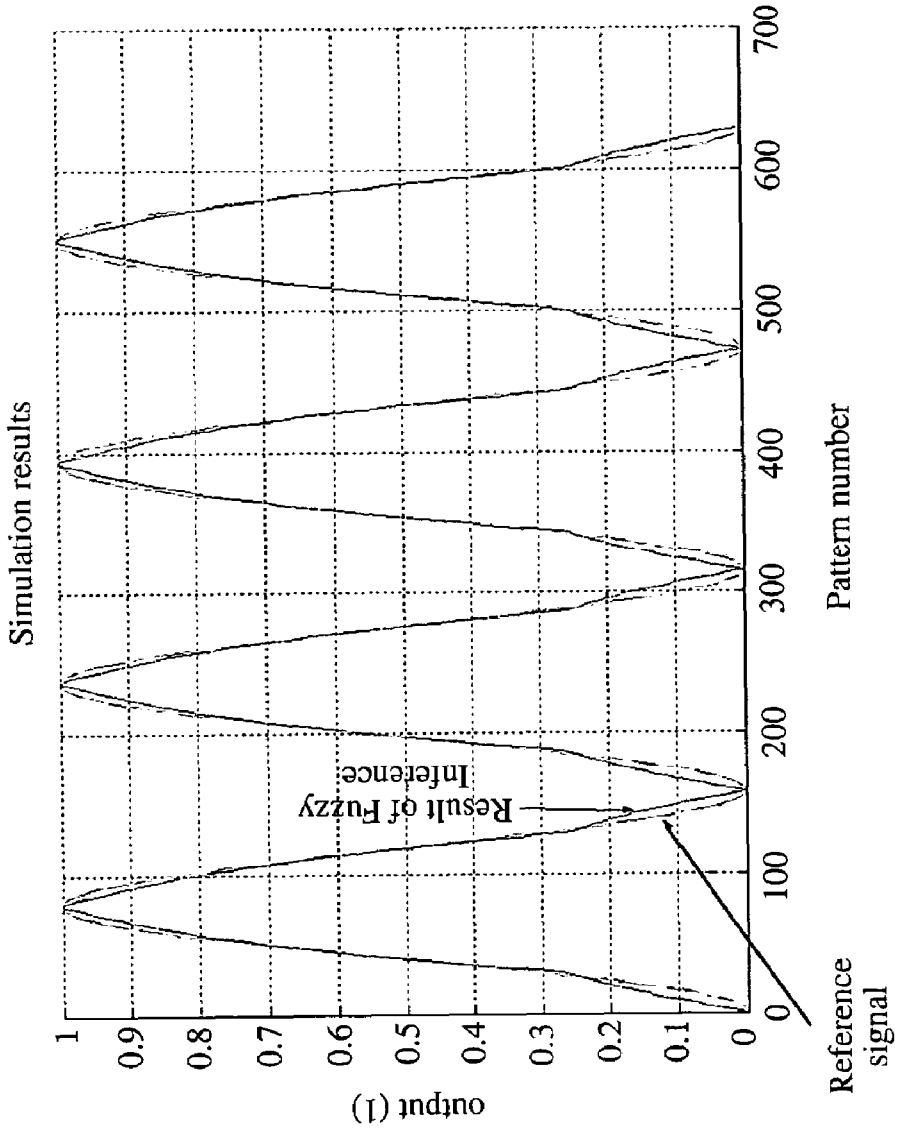
Simulation results
output (1)
1
0.9
0.8
0.7
0.6
0.5
0.4
0.3
0.2
0.1
0
0
100
200
300
400
500
600
700
Pattern number
Reference signal
Result of Fuzzy Inference

Figure 16

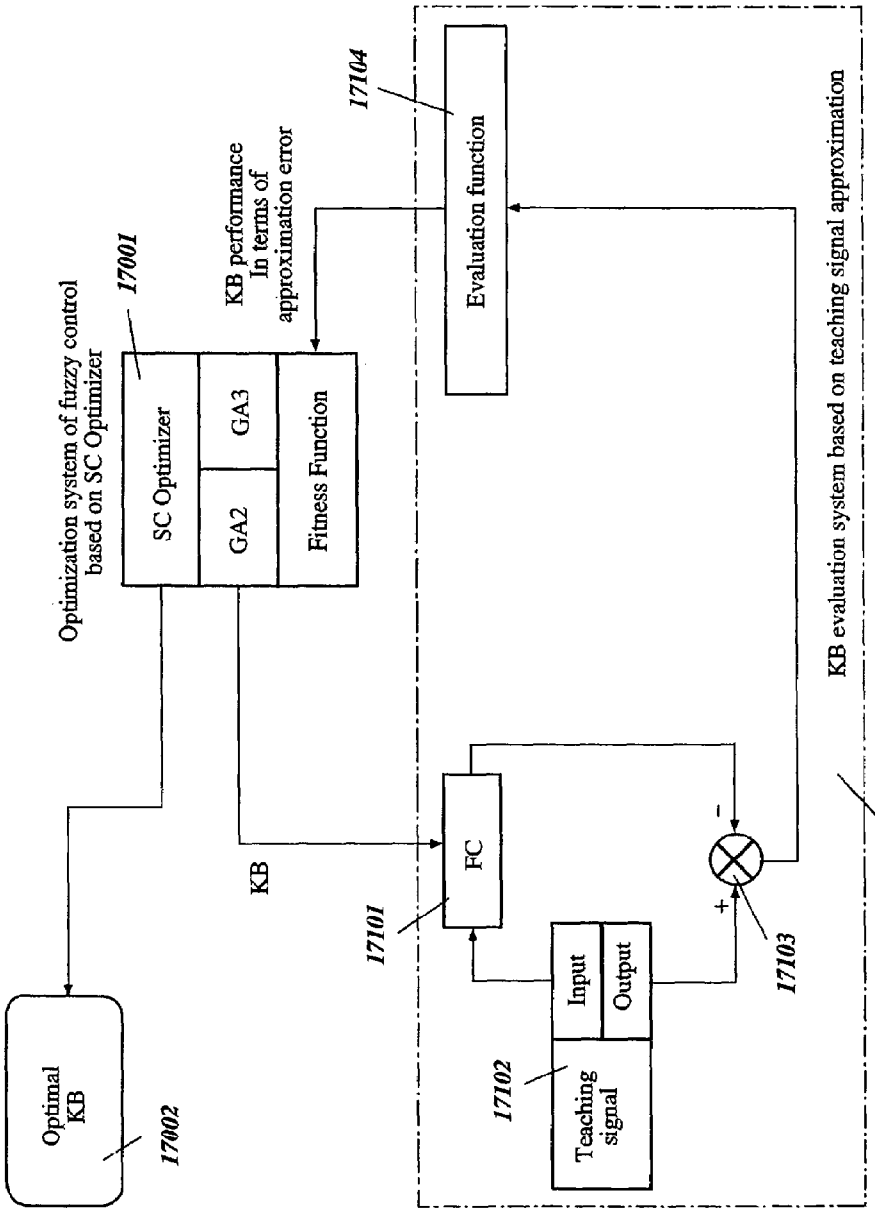
Optimization system of fuzzy control based on SC Optimizer
17001
SC Optimizer
GA3
GA2
Fitness Function
KB performance In terms of approximation error
17104
Evaluation function
KB
FC
17101
Input
Output
Teaching signal
17102
17103
KB evaluation system based on teaching signal approximation
17100
Optimal KB
17002

Figure 17

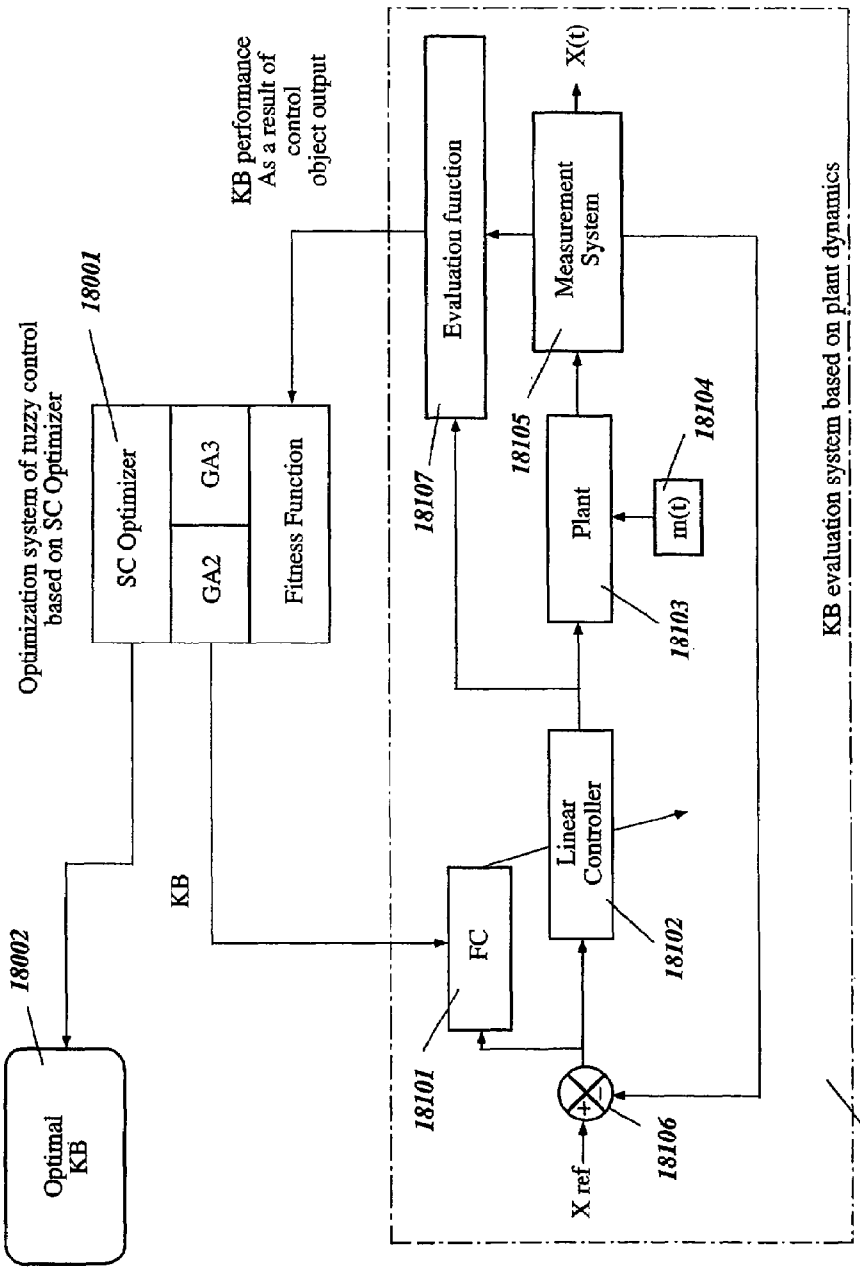
Optimization system of fuzzy control based on SC Optimizer
18001
SC Optimizer
GA3
GA2
Fitness Function
KB performance As a result of control object output
Evaluation function
X(t)
Measurement System
18107
18105
Plant
m(t)
18104
18103
KB evaluation system based on plant dynamics
KB
FC
Linear Controller
18102
18002
Optimal KB
18101
18106
X ref
18100

Figure 18

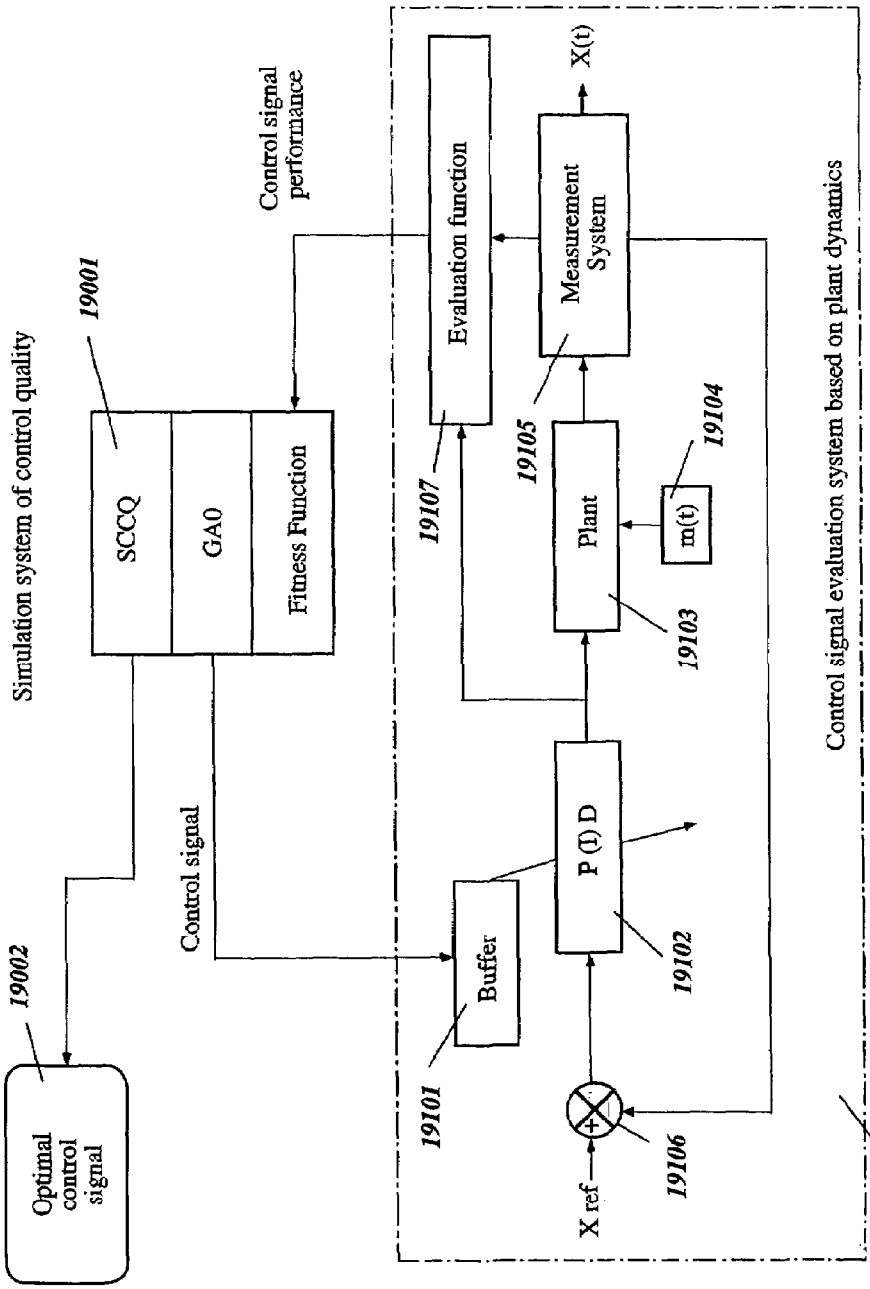
Simulation system of control quality
19001
SCCQ
GA0
Fitness Function
Control signal performance
Evaluation function
19107
X(t)
Measurement System
19105
Plant
19104
m(t)
19103
Control signal
Buffer
19101
P (I) D
19102
Control signal evaluation system based on plant dynamics
19002
Optimal control signal
X ref
19106
19100

Figure 19

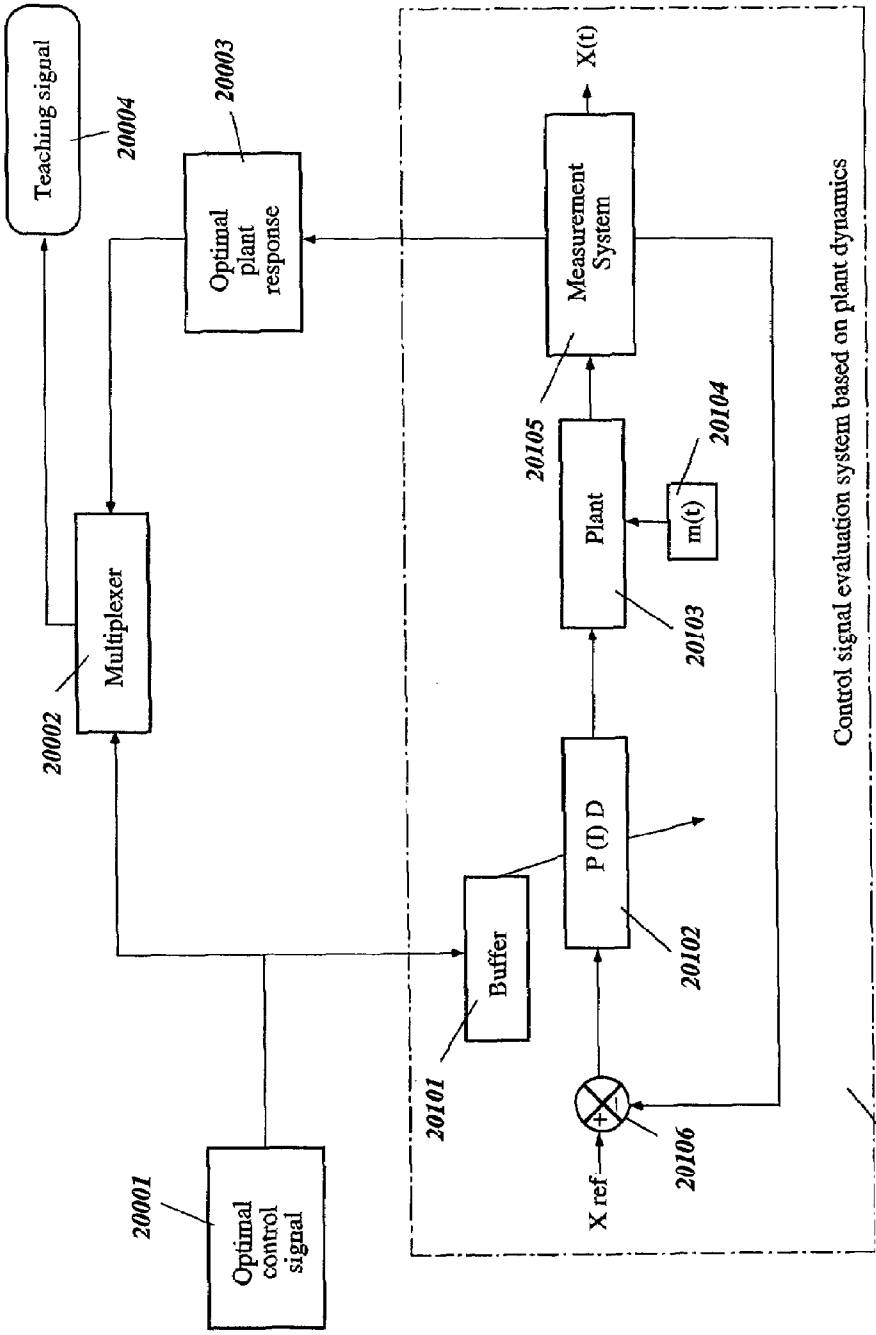
Teaching signal
20004
20003
Optimal plant response
X(t)
Measurement System
Control signal evaluation system based on plant dynamics
Multiplexer
20002
20105
Plant
20104
m(t)
20103
P (I) D
Buffer
20102
20101
X ref
20106
Optimal control signal
20001
20100

Figure 20

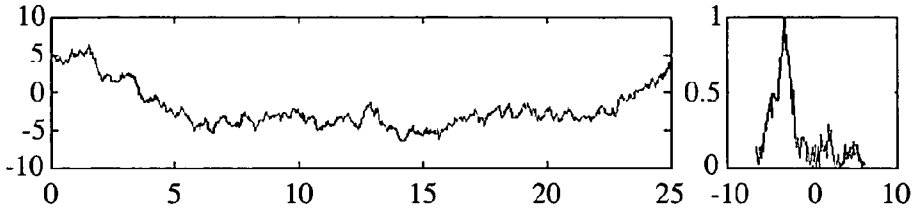

Figure 21

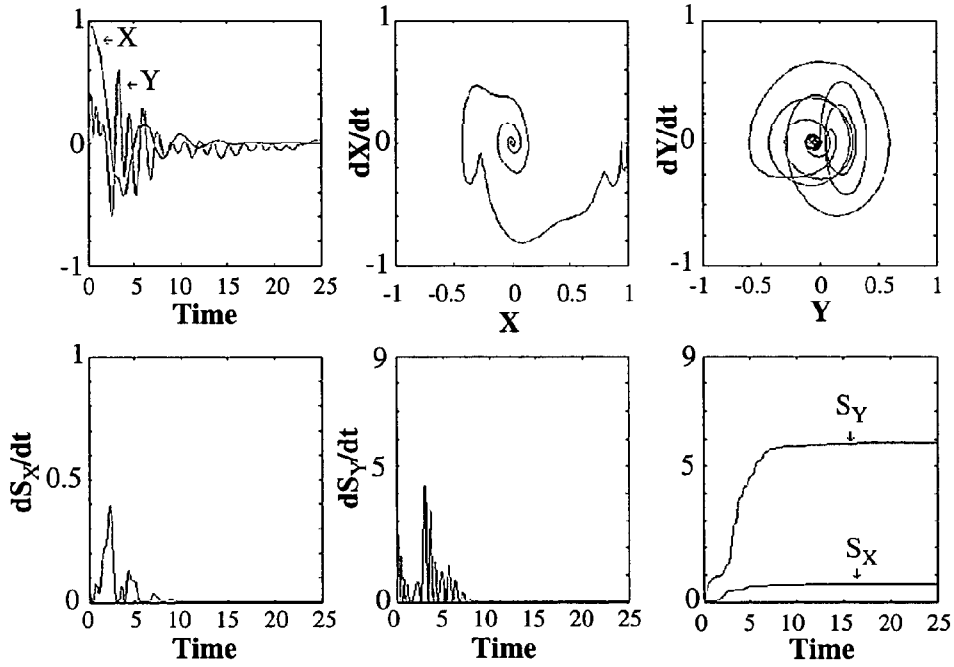

Figure 22

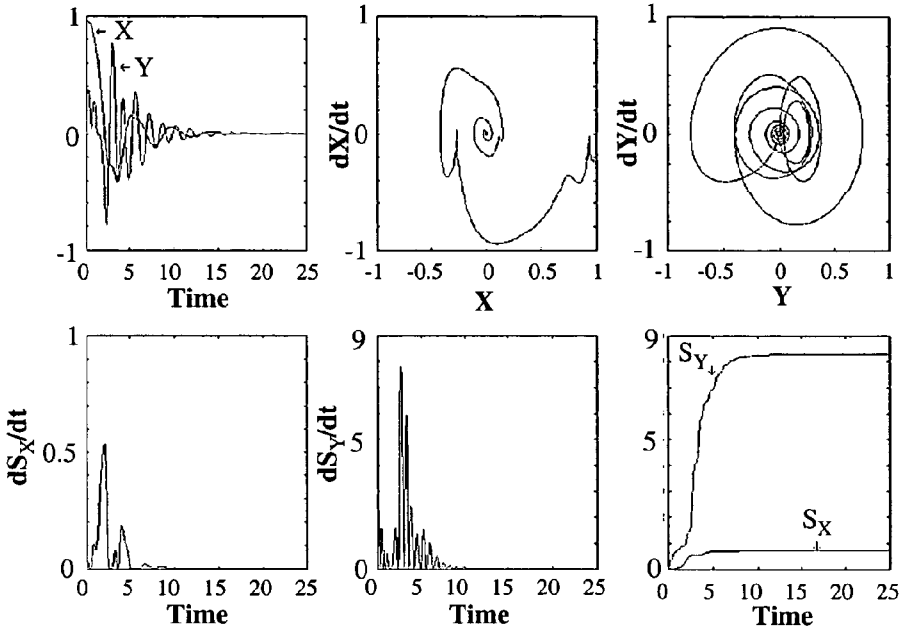

Figure 23

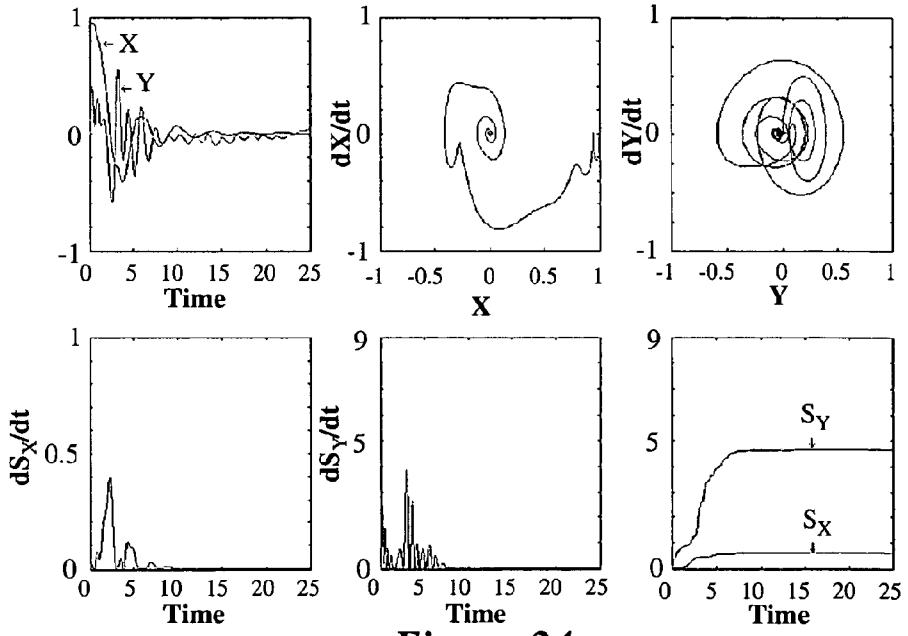

Figure 24

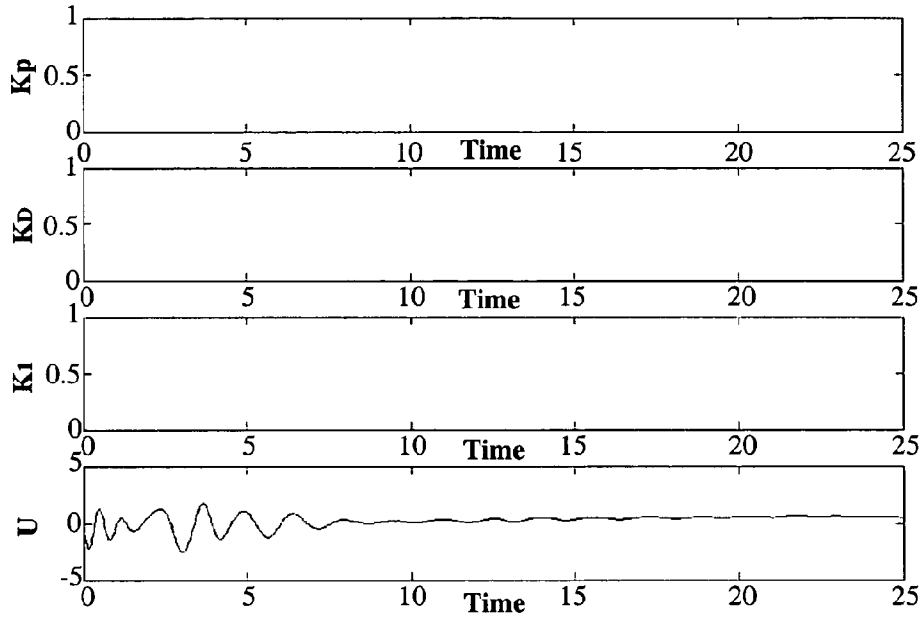

Figure 25

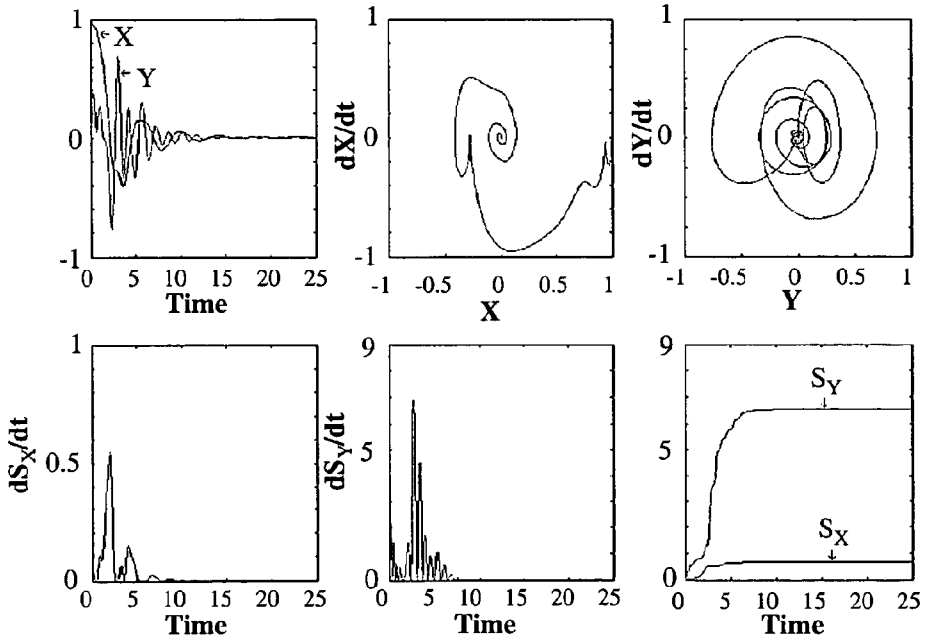

Figure 26

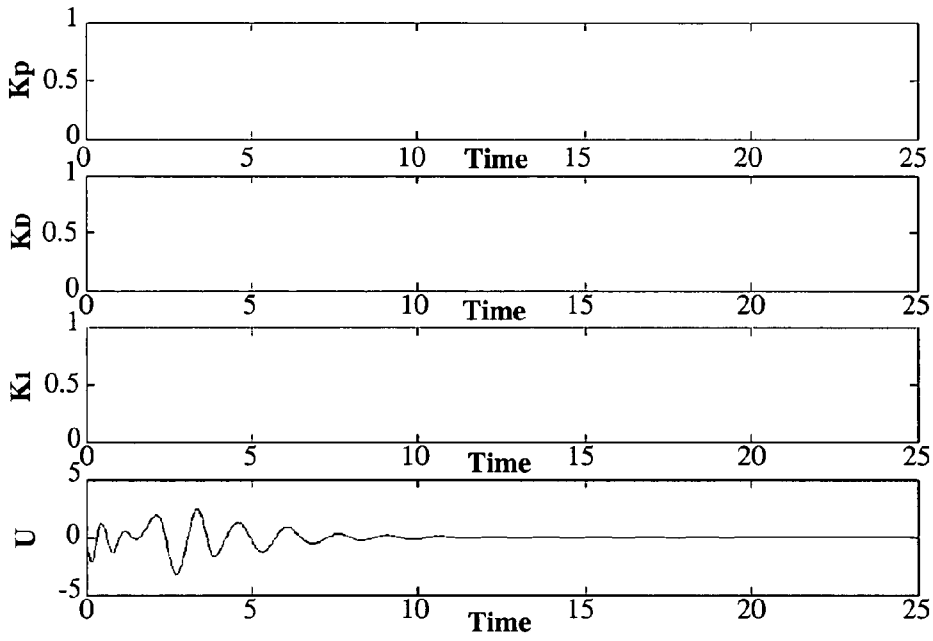

Figure 27

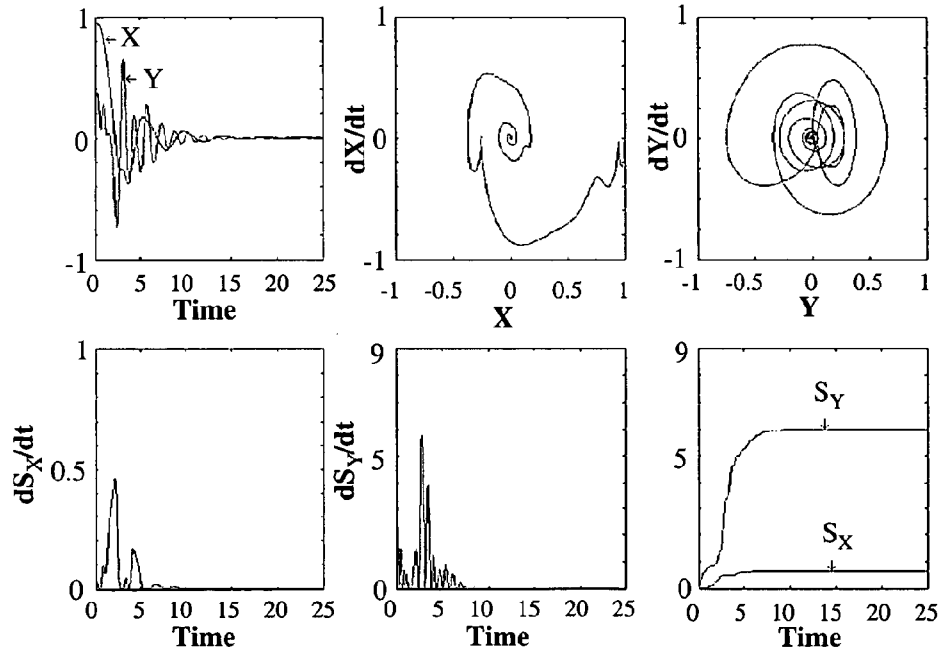

Figure 28

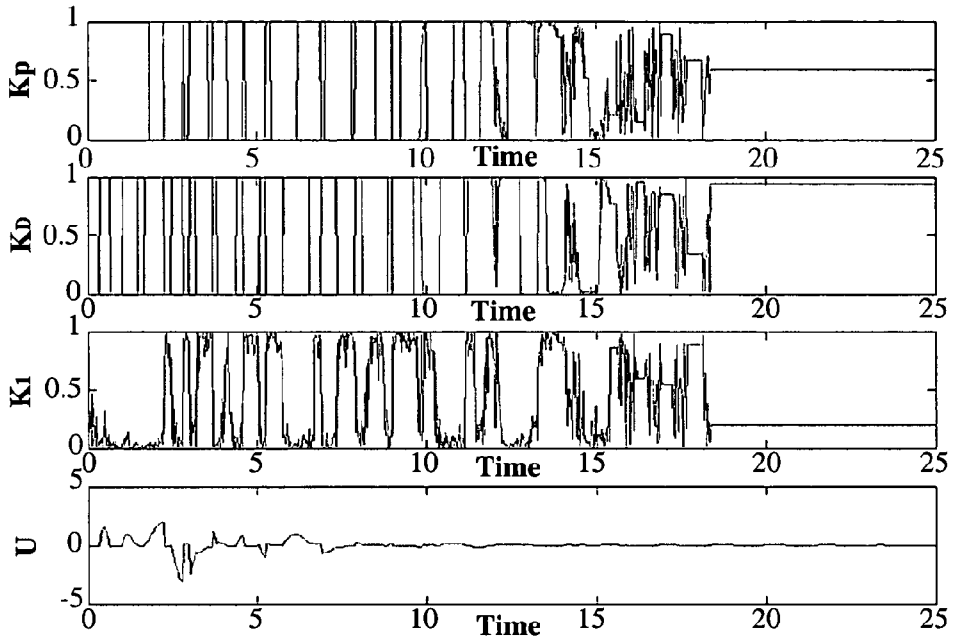

Figure 29

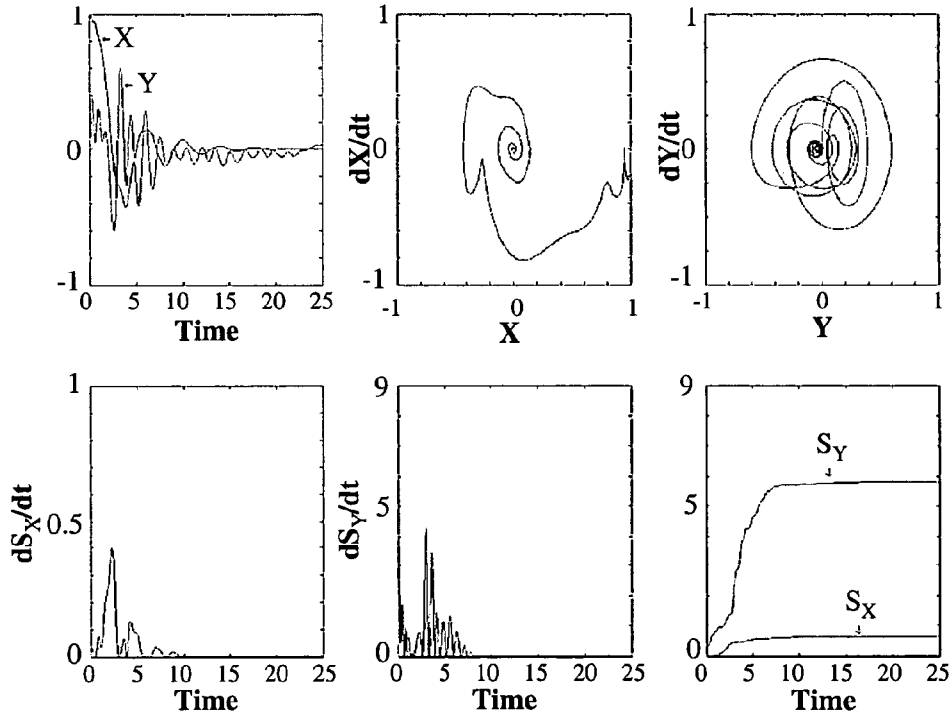

Figure 30

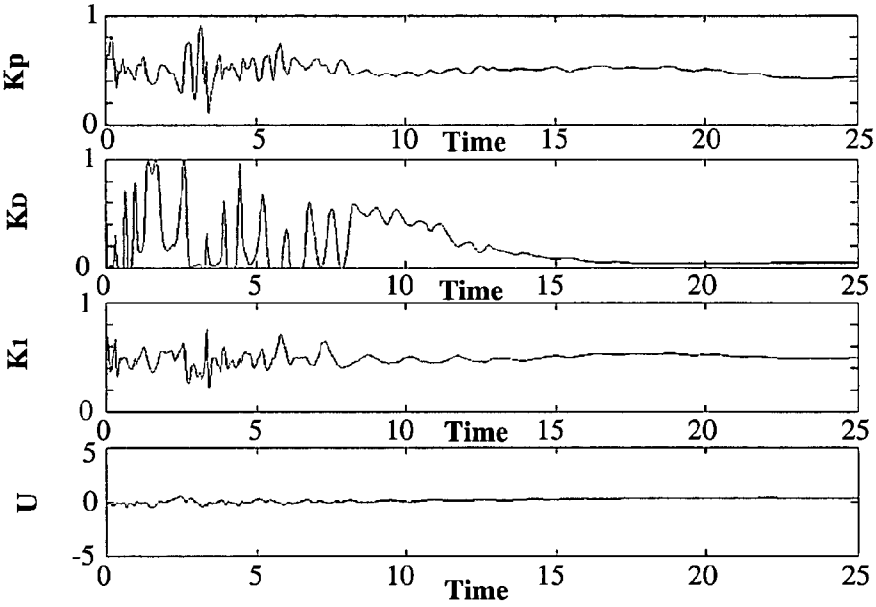

Figure 31

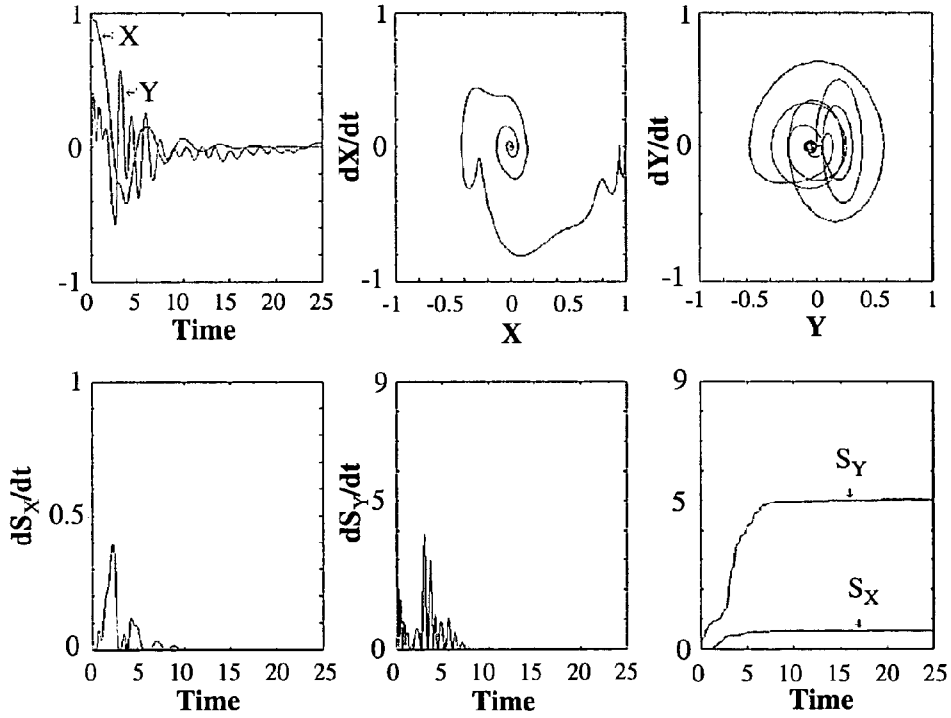

Figure 32

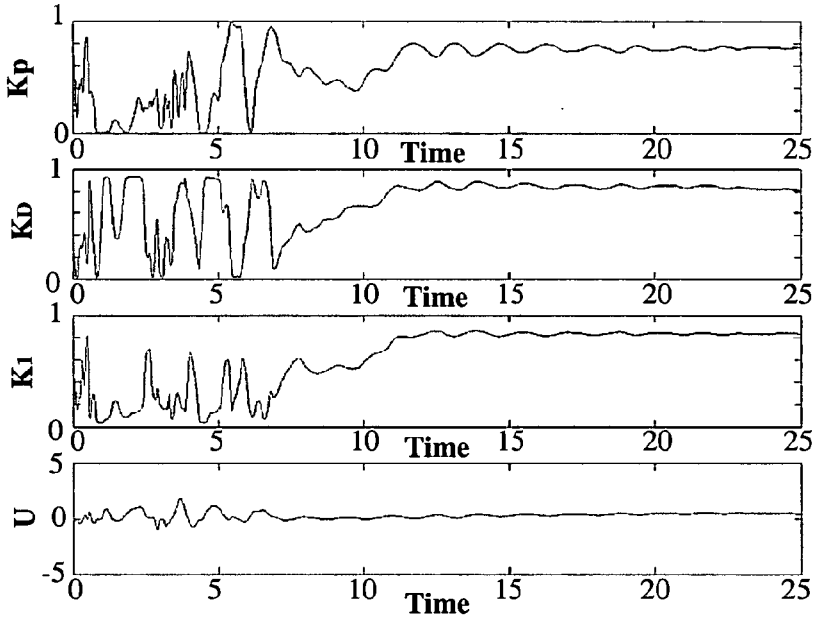

Figure 33

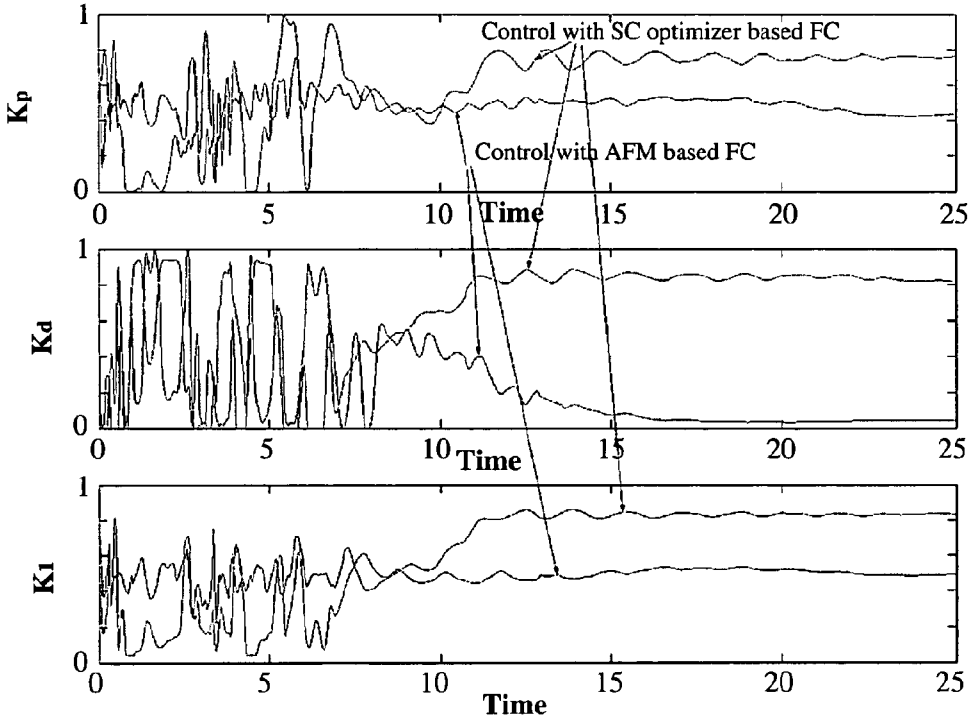

Figure 34

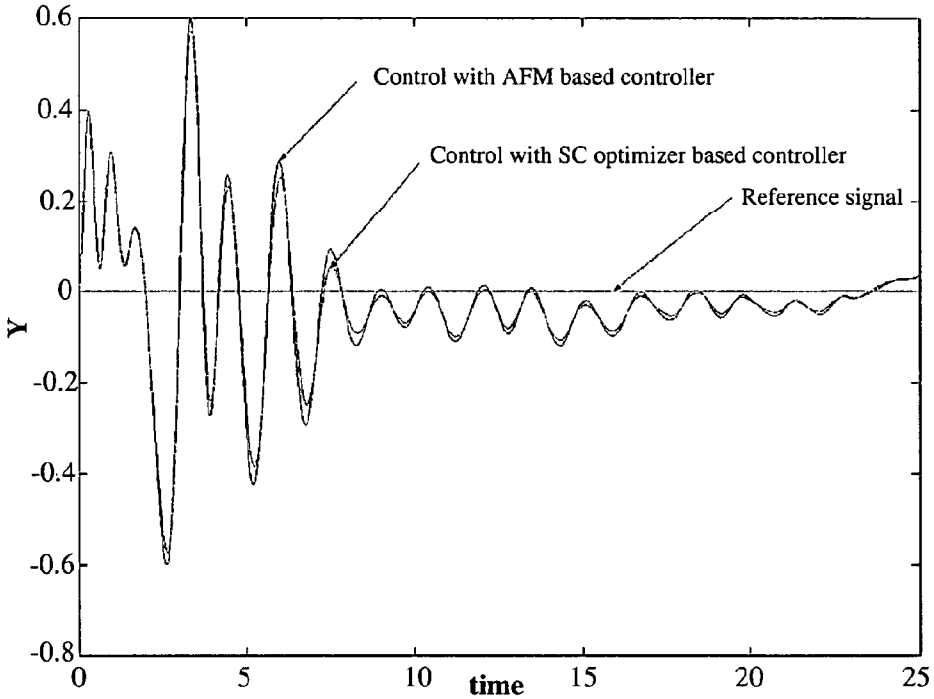

Figure 35

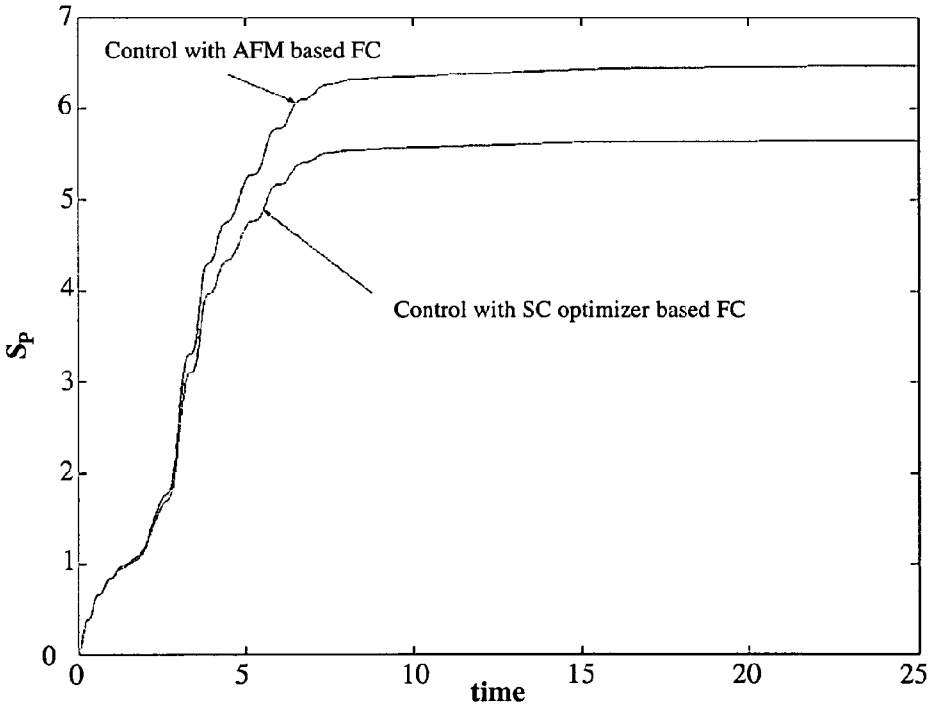

Figure 36

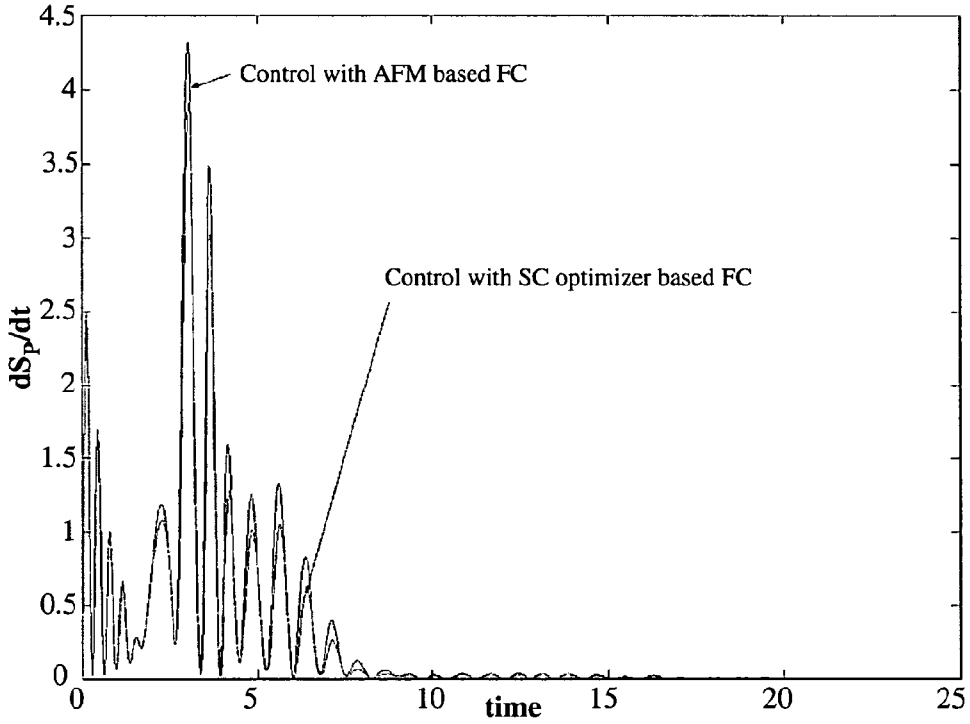
4.5
4
3.5
3
2.5
2
1.5
1
0.5
0
dSp/dt
Control with AFM based FC
Control with SC optimizer based FC
0
5
10
15
20
25
time

Figure 37

$$\begin{cases} \ddot{\theta} + 2\frac{\dot{l}}{l}\dot{\theta} + \frac{g}{l}\sin\theta = 0 \\ \ddot{l} + 2k\dot{l} - l\dot{\theta}^2 - g\cos\theta = \frac{1}{m}\left(k_p \cdot e_l + k_d \cdot \dot{e}_l + k_i \cdot \int e_l dt + \xi(t)\right) \end{cases}$$

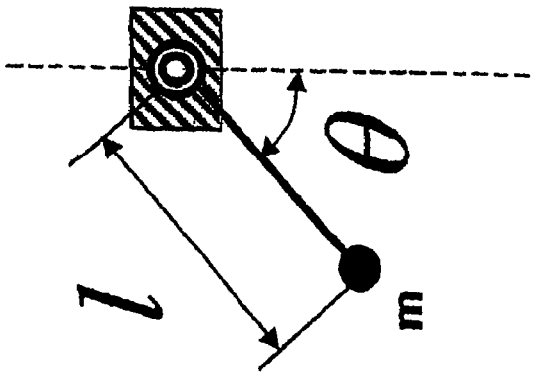

Figure 38

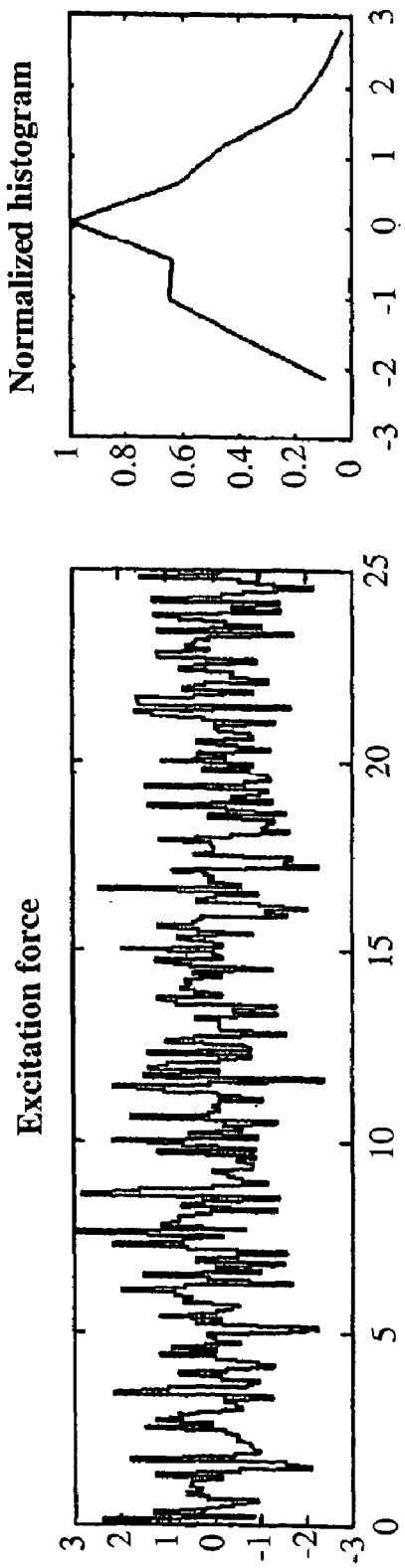
Normalized histogram
1
0.8
0.6
0.4
0.2
0
-3
-2
-1
0
1
2
3
Excitation force
3
2
1
0
-1
-2
-3
0
5
10
15
20
25

Figure 39

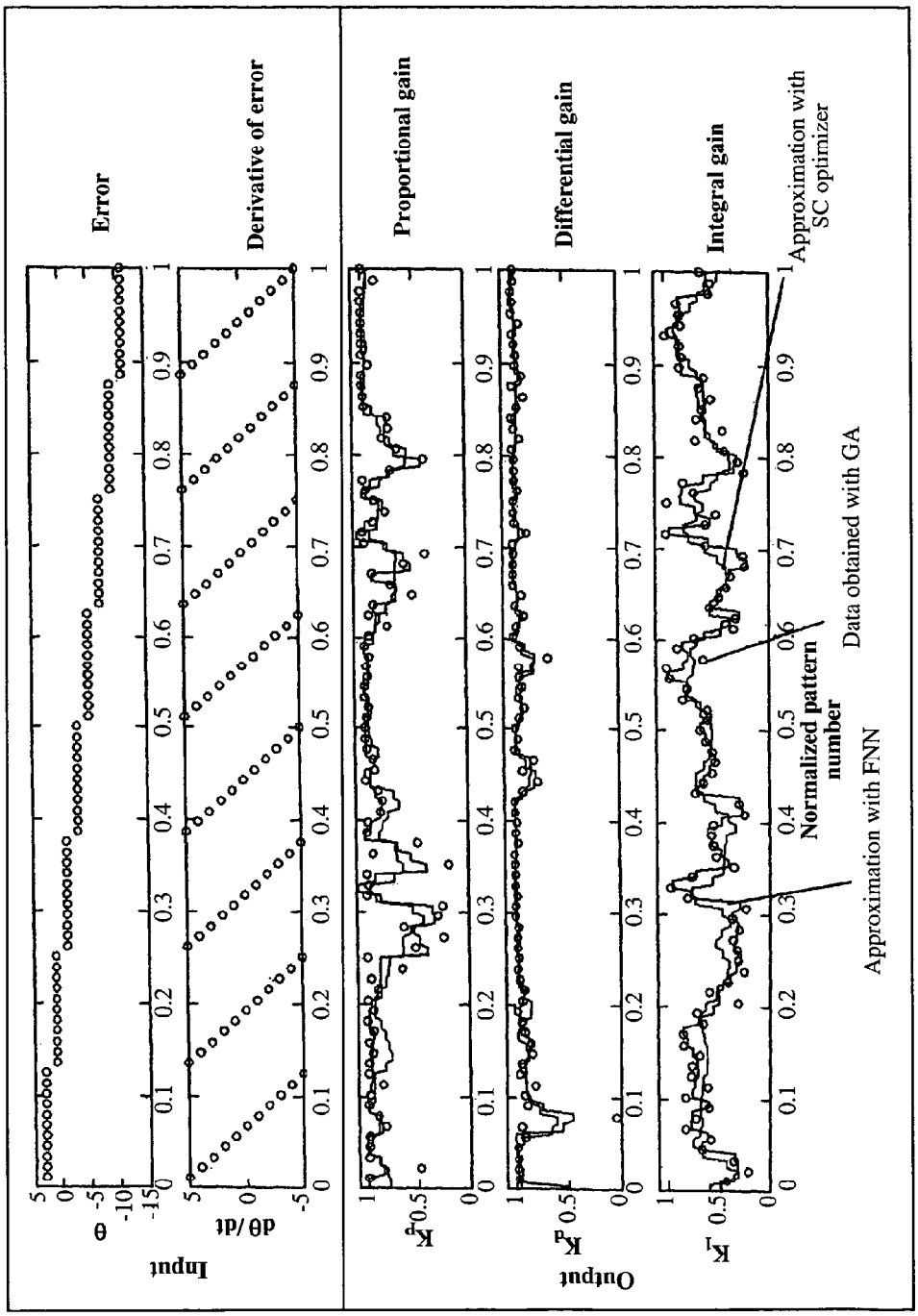
Input
Error
Derivative of error
dθ/dt
θ
Output
Proportional gain
Differential gain
Integral gain
K_P
K_D
K_I
Approximation with SC optimizer
Normalized pattern number
Data obtained with GA
Approximation with FNN

Figure 40

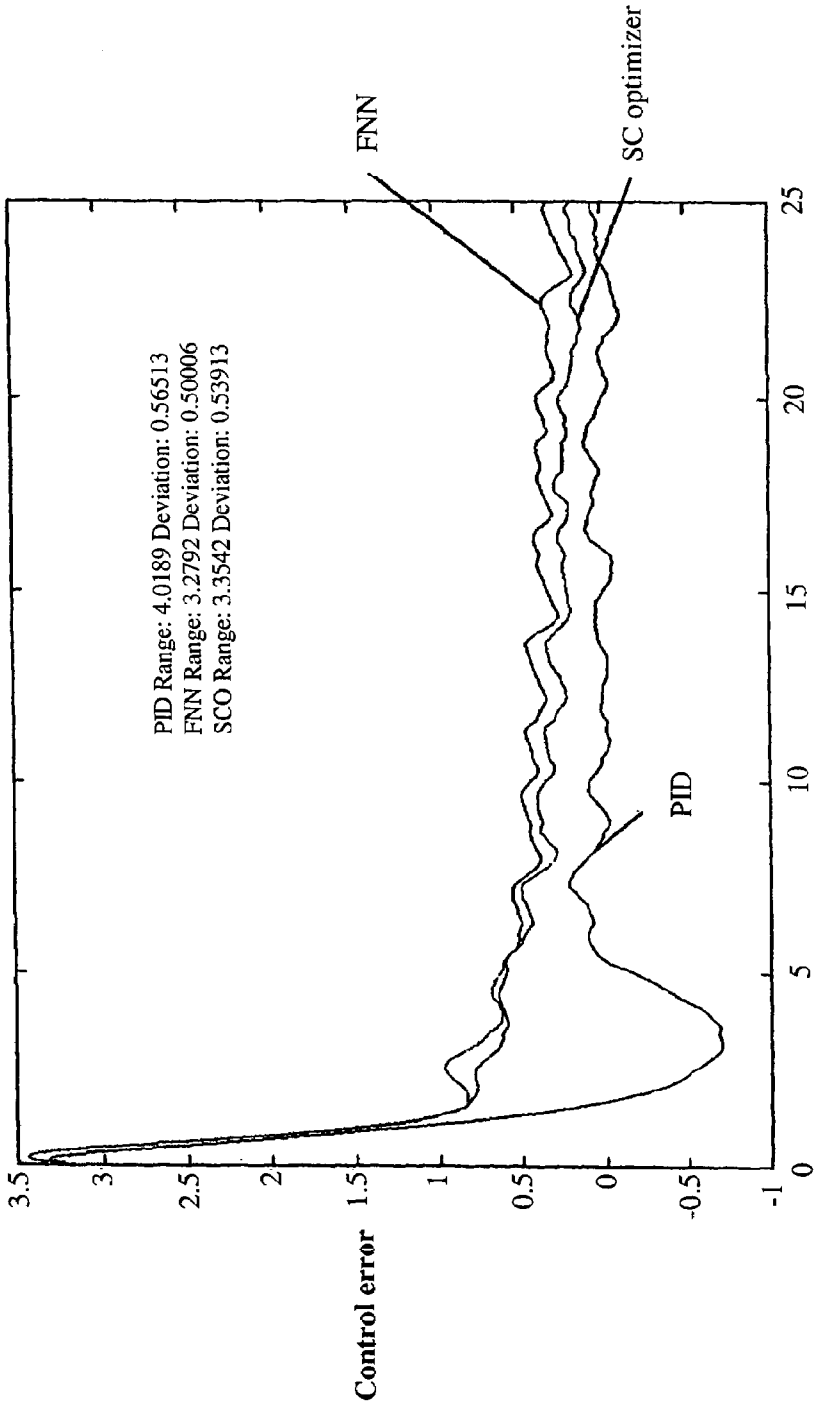
FNN
SC optimizer
PID
PID Range: 4.0189 Deviation: 0.56513
FNN Range: 3.2792 Deviation: 0.50006
SCO Range: 3.3542 Deviation: 0.53913
Control error
3.5
3
2.5
2
1.5
1
0.5
0
-0.5
-1
0
5
10
15
20
25

Figure 41

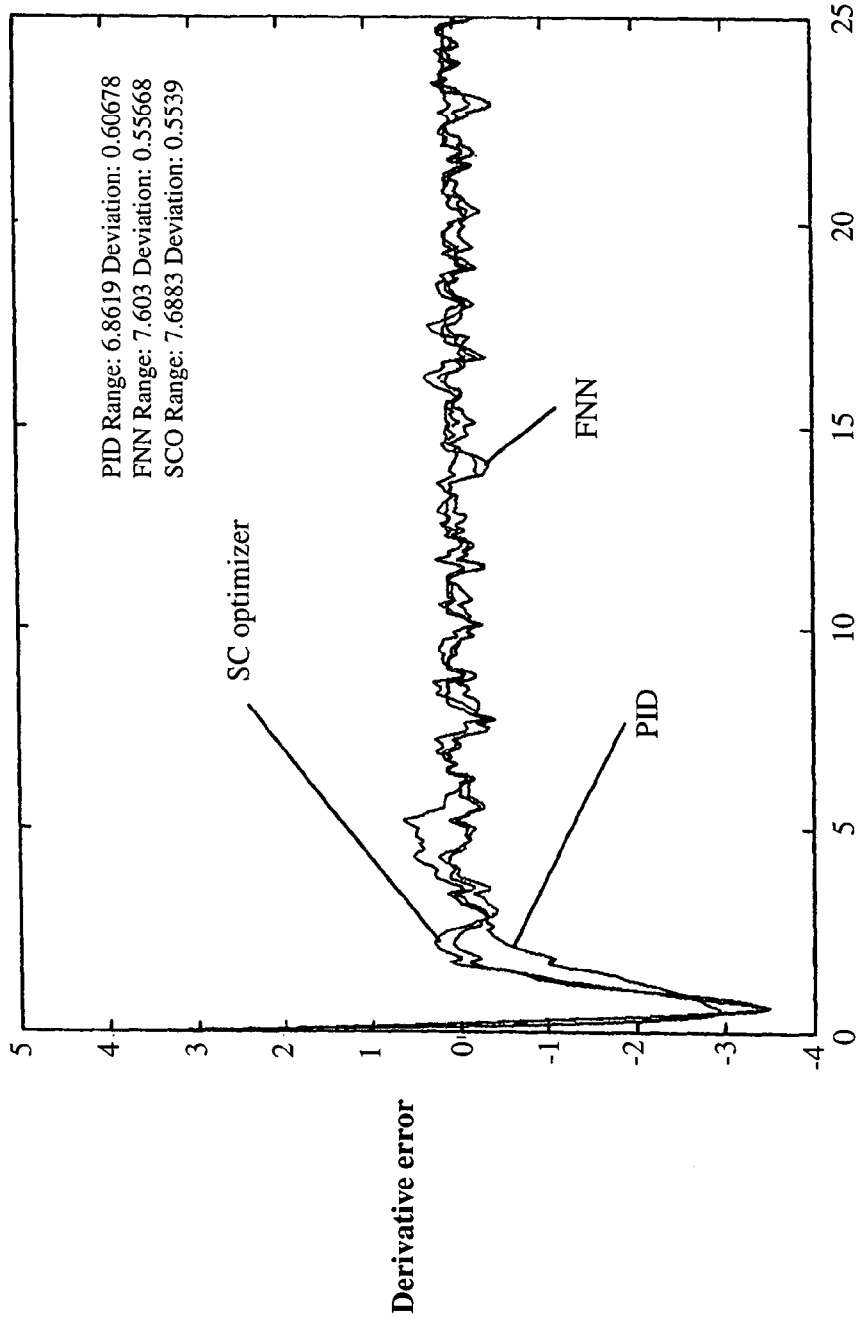
PID Range: 6.8619 Deviation: 0.60678
FNN Range: 7.603 Deviation: 0.55668
SCO Range: 7.6883 Deviation: 0.5539
SC optimizer
FNN
PID
Derivative error
5
4
3
2
1
0
-1
-2
-3
-4
0
5
10
15
20
25

Figure 42

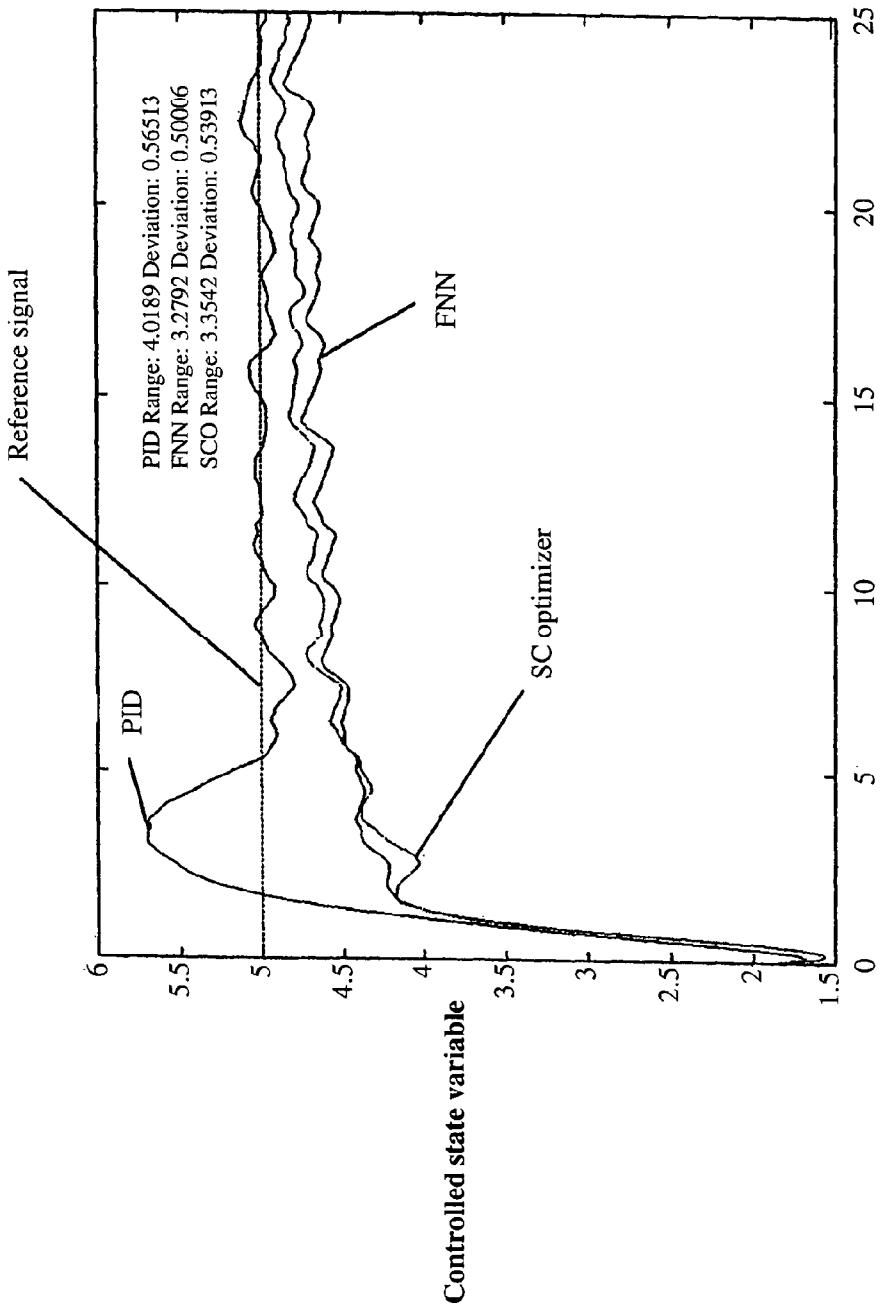
Reference signal
PID Range: 4.0189 Deviation: 0.56513
FNN Range: 3.2792 Deviation: 0.50006
SCO Range: 3.3542 Deviation: 0.53913
PID
FNN
SC optimizer
Controlled state variable
6
5.5
5
4.5
4
3.5
3
2.5
2
1.5
0
5
10
15
20
25

Figure 43

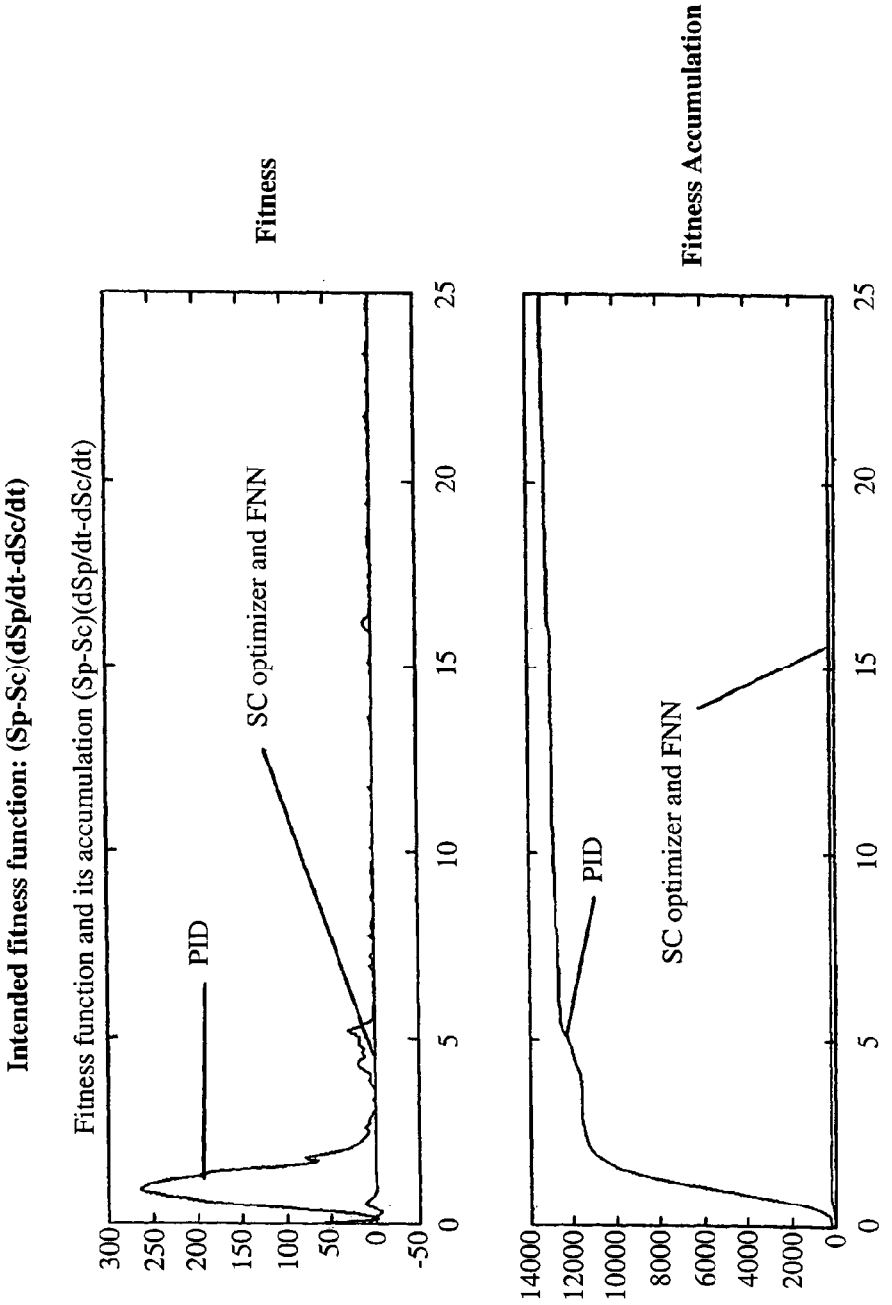
Intended fitness function: (Sp-Sc)(dSp/dt-dSc/dt)
Fitness function and its accumulation (Sp-Sc)(dSp/dt-dSc/dt)
Fitness
PID
SC optimizer and FNN
300
250
200
150
100
50
0
-50
0
5
10
15
20
25
Fitness Accumulation
PID
SC optimizer and FNN
14000
12000
10000
8000
6000
4000
2000
0
0
5
10
15
20
25

Figure 44

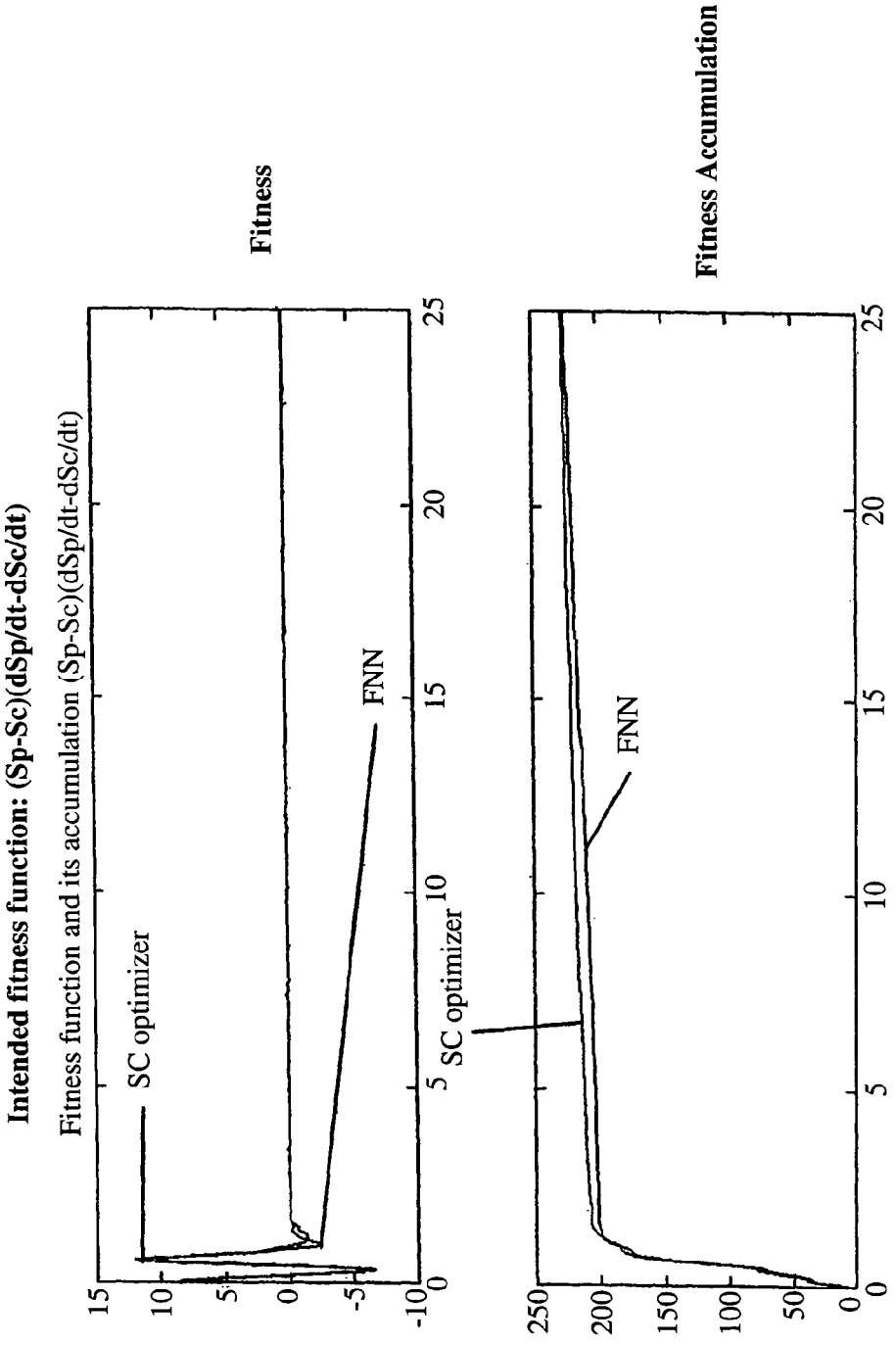
Intended fitness function: (Sp-Sc)(dSp/dt-dSc/dt)
Fitness function and its accumulation (Sp-Sc)(dSp/dt-dSc/dt)
Fitness
SC optimizer
FNN
15
10
5
0
-5
-10
0
5
10
15
20
25
Fitness Accumulation
SC optimizer
FNN
250
200
150
100
50
0
0
5
10
15
20
25

Figure 45

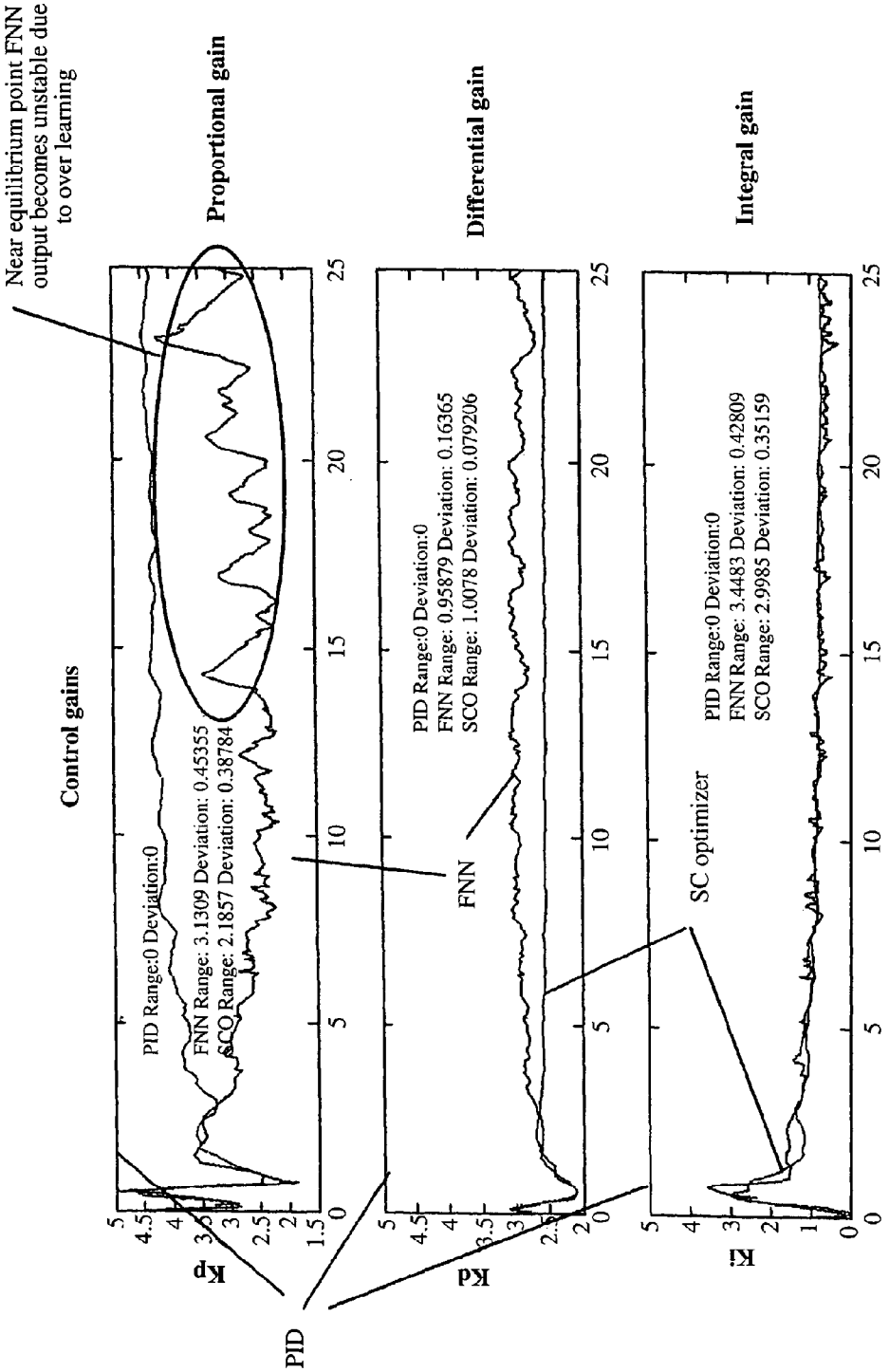
Near equilibrium point FNN output becomes unstable due to over learning
Control gains
Proportional gain
Differential gain
Integral gain
PID Range:0 Deviation:0
FNN Range: 3.1309 Deviation: 0.45355
SCO Range: 2.1857 Deviation: 0.38784
PID Range:0 Deviation:0
FNN Range: 0.95879 Deviation: 0.16365
SCO Range: 1.0078 Deviation: 0.079206
PID Range:0 Deviation:0
FNN Range: 3.4483 Deviation: 0.42809
SCO Range: 2.9985 Deviation: 0.35159
SC optimizer
FNN
PID
Kp
Kd
Ki

Figure 46

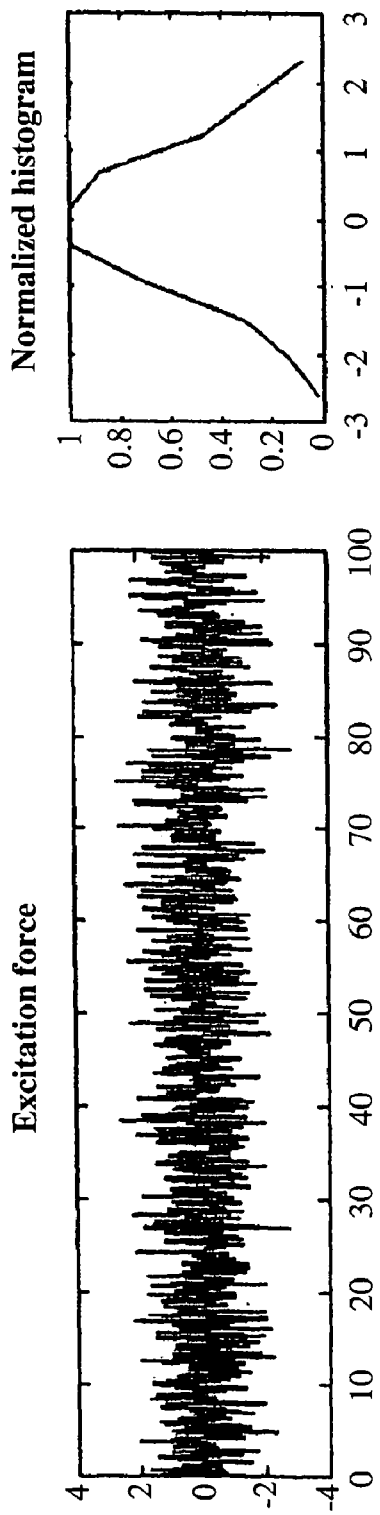
Normalized histogram
1
0.8
0.6
0.4
0.2
0
-3
-2
-1
0
1
2
3
Excitation force
4
2
0
-2
-4
0
10
20
30
40
50
60
70
80
90
100

Figure 47

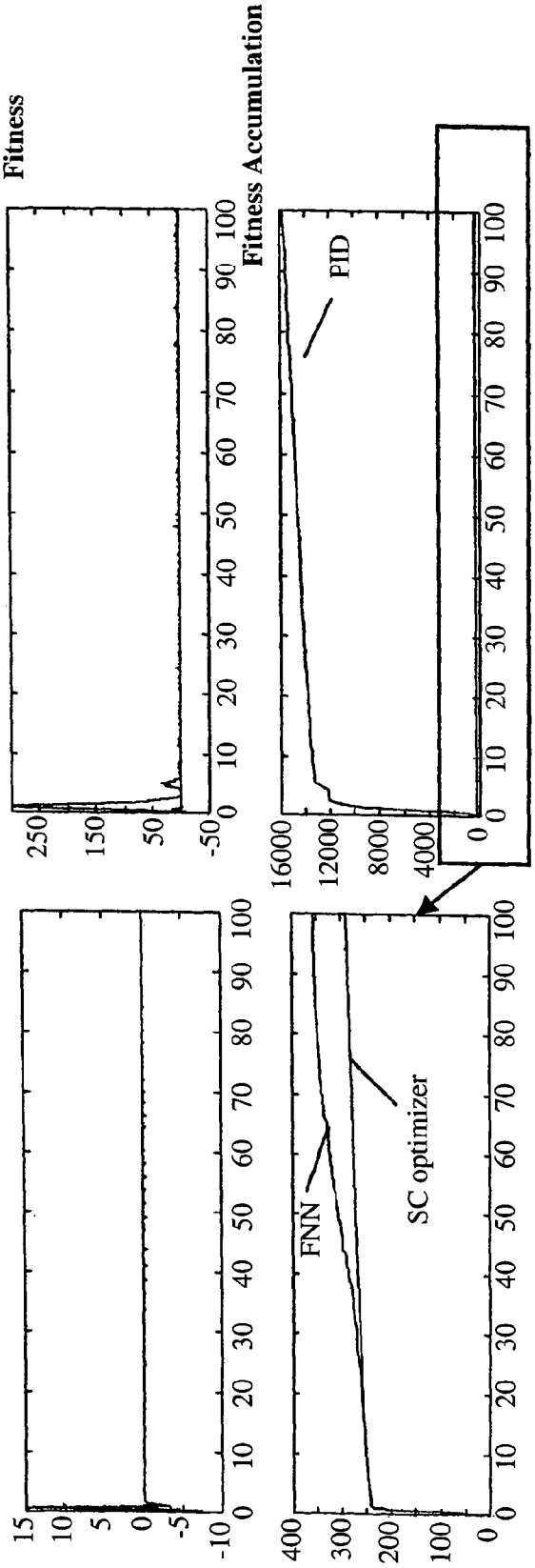

Figure 48

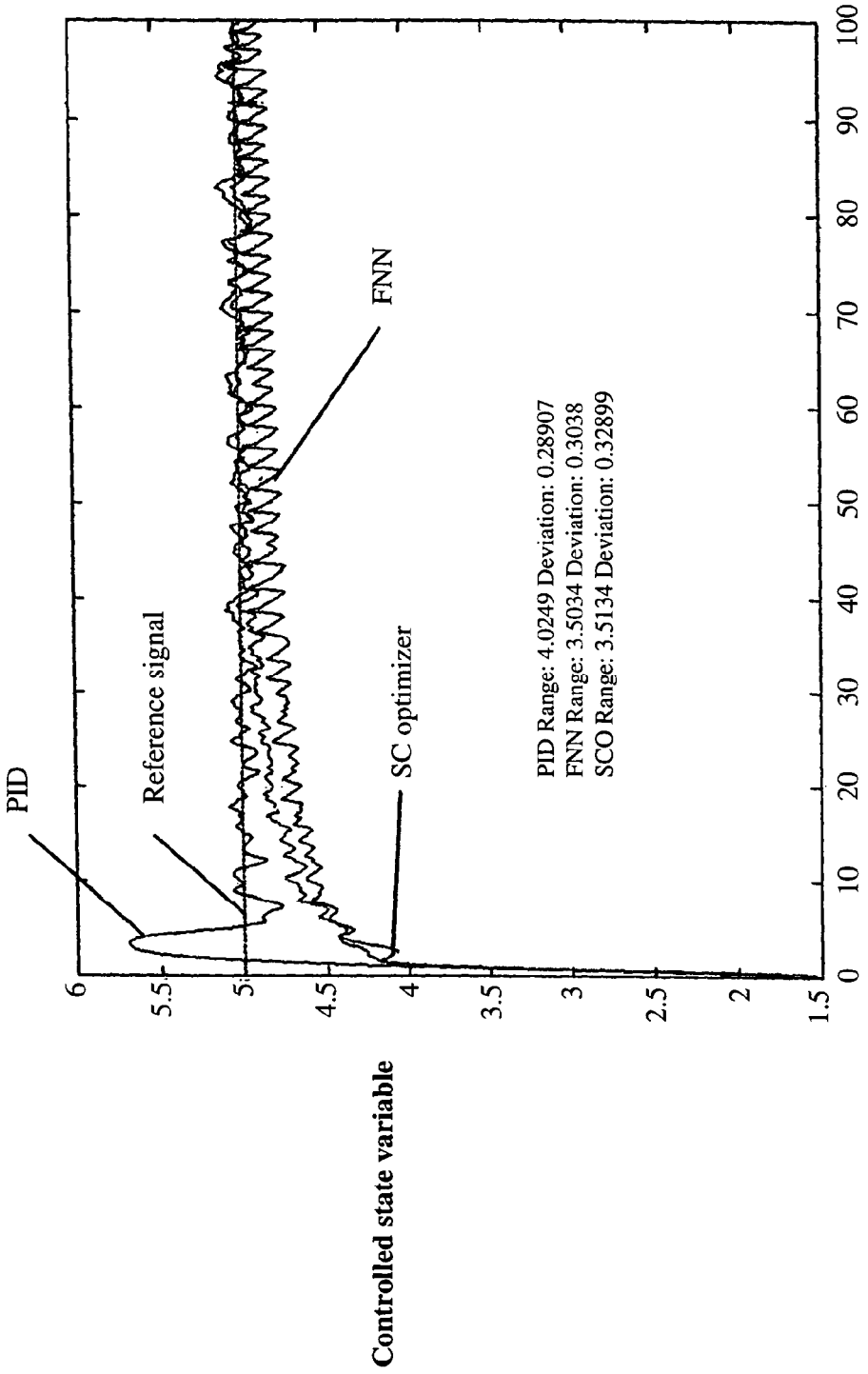
PID
Reference signal
SC optimizer
FNN
PID Range: 4.0249 Deviation: 0.28907
FNN Range: 3.5034 Deviation: 0.3038
SCO Range: 3.5134 Deviation: 0.32899
Controlled state variable
6
5.5
5
4.5
4
3.5
3
2.5
2
1.5
0
10
20
30
40
50
60
70
80
90
100

Figure 49

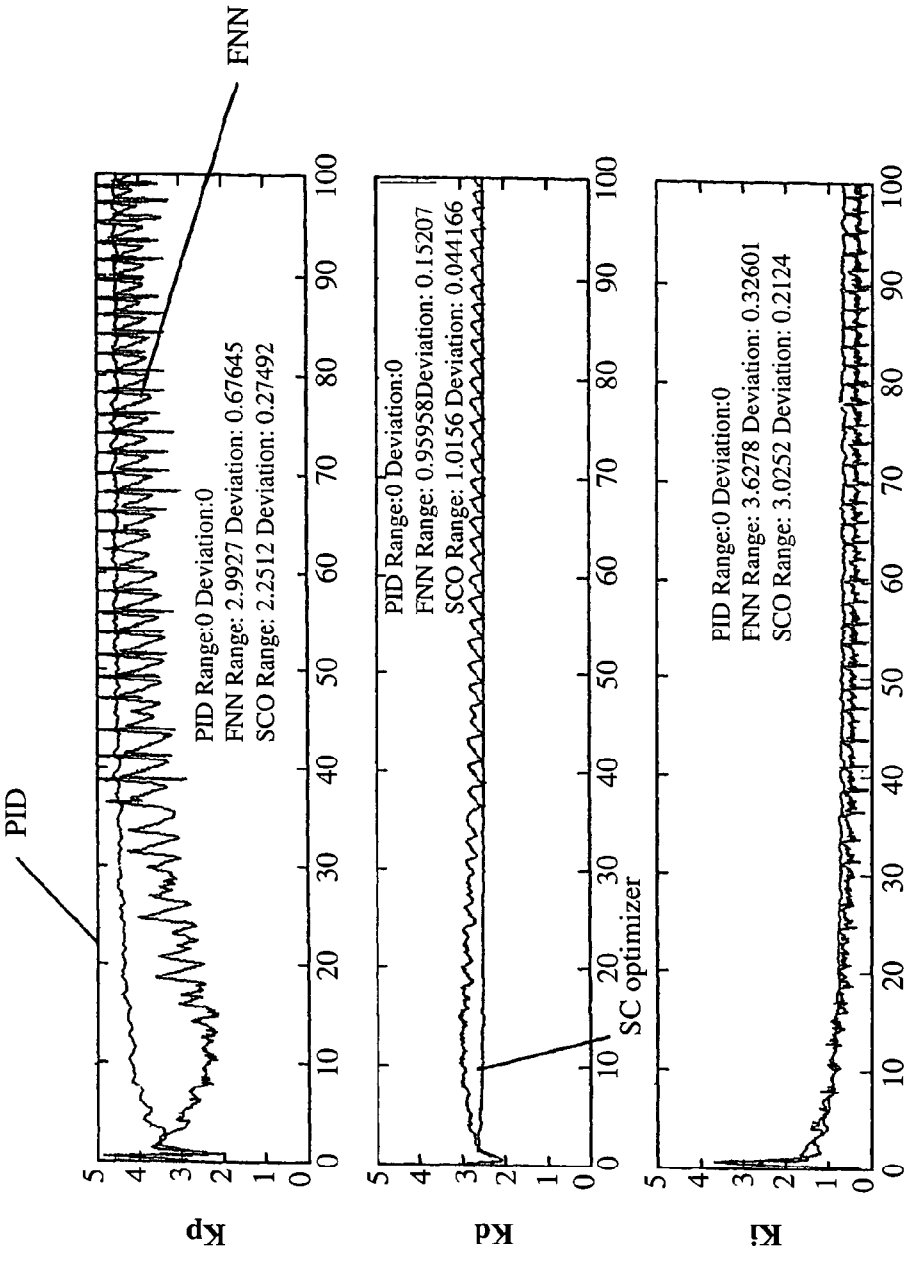
PID
FNN
PID Range:0 Deviation:0
FNN Range: 2.9927 Deviation: 0.67645
SCO Range: 2.2512 Deviation: 0.27492
Kp
PID Range:0 Deviation:0
FNN Range: 0.95958Deviation: 0.15207
SCO Range: 1.0156 Deviation: 0.044166
SC optimizer
Kd
PID Range:0 Deviation:0
FNN Range: 3.6278 Deviation: 0.32601
SCO Range: 3.0252 Deviation: 0.2124
Ki

Figure 50

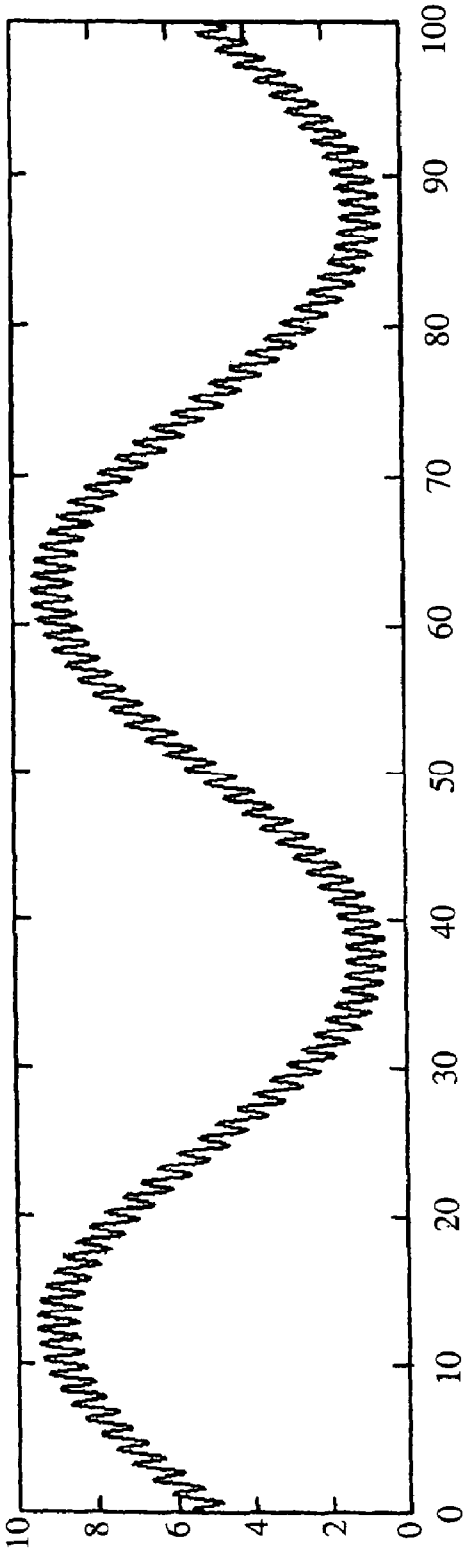

$$Rs(t) = 5 + 4\sin\left(\frac{2\pi}{50}t\right) + 0.5\sin(2\pi t)$$

Figure 51

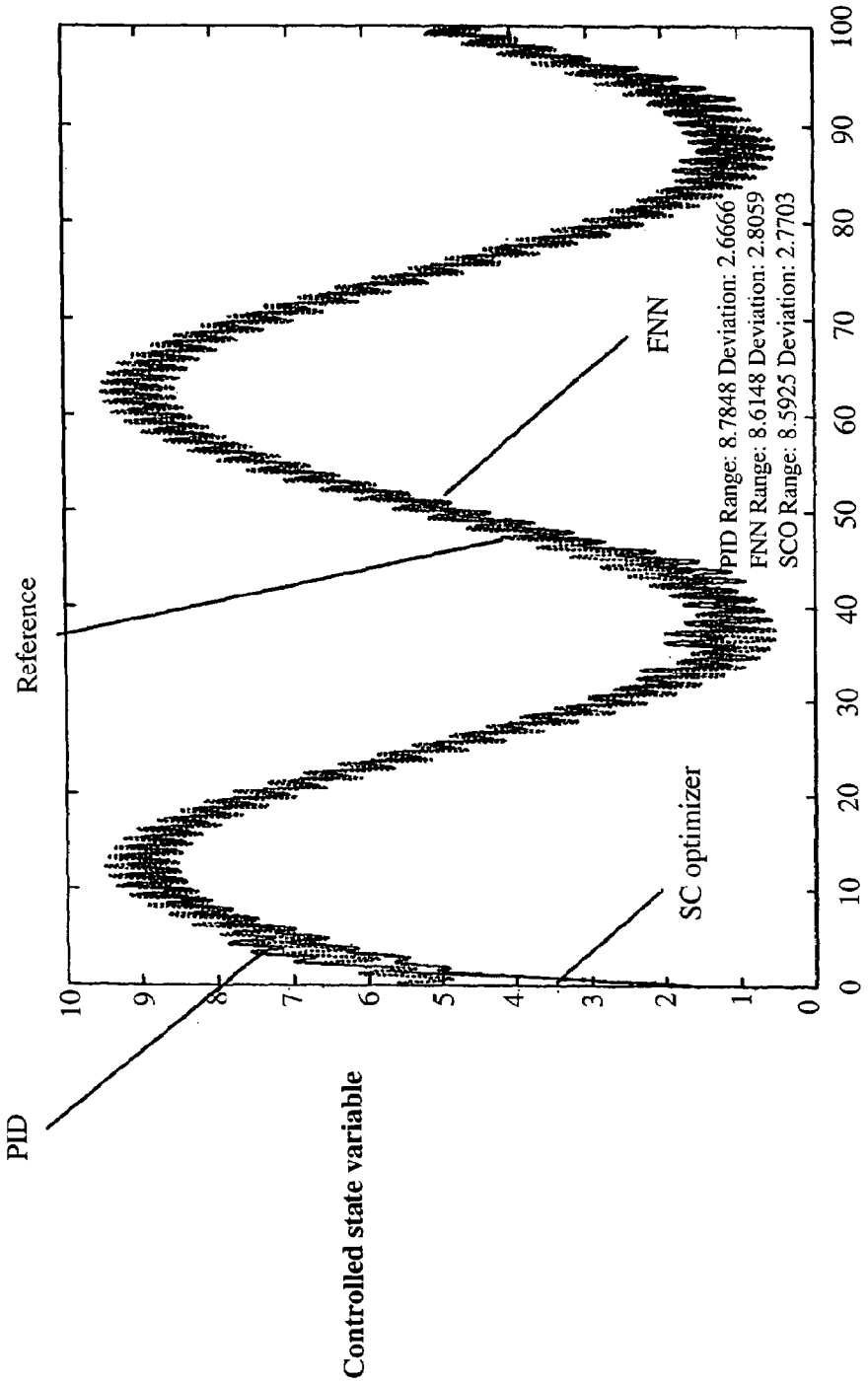
Reference
PID
FNN
SC optimizer
PID Range: 8.7848 Deviation: 2.6666
FNN Range: 8.6148 Deviation: 2.8059
SCO Range: 8.5925 Deviation: 2.7703
Controlled state variable
0
1
2
3
4
5
6
7
8
9
10
0
10
20
30
40
50
60
70
80
90
100

Figure 52

Intended fitness function: (Sp-Sc)(dSp/dt-dSc/dt)

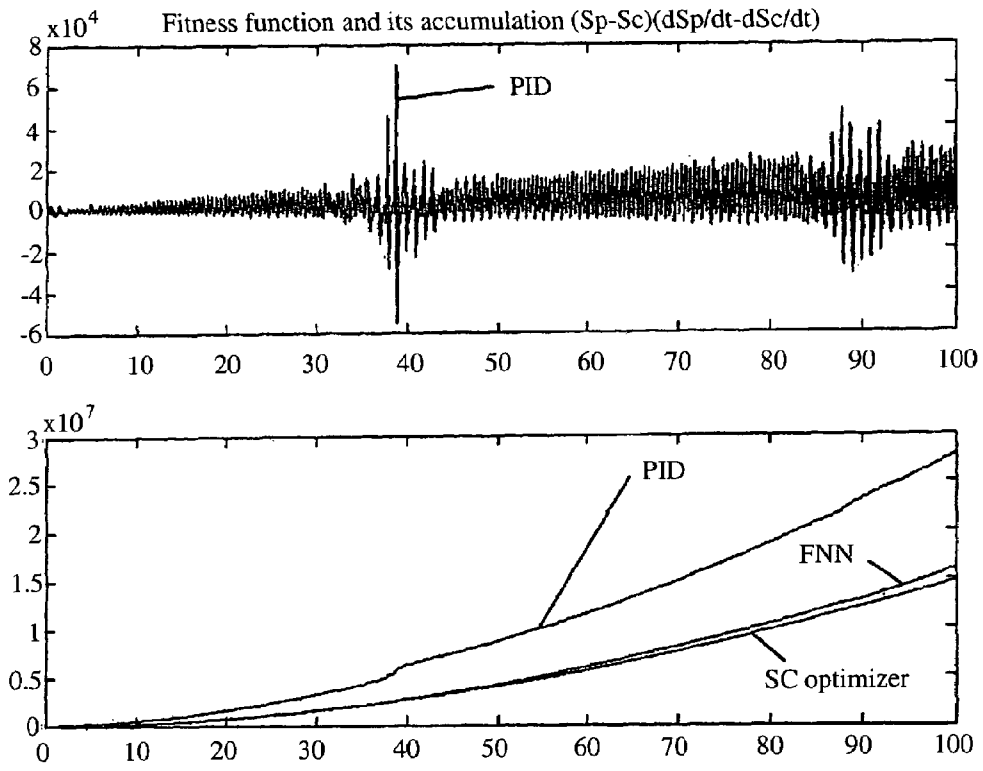

Figure 53

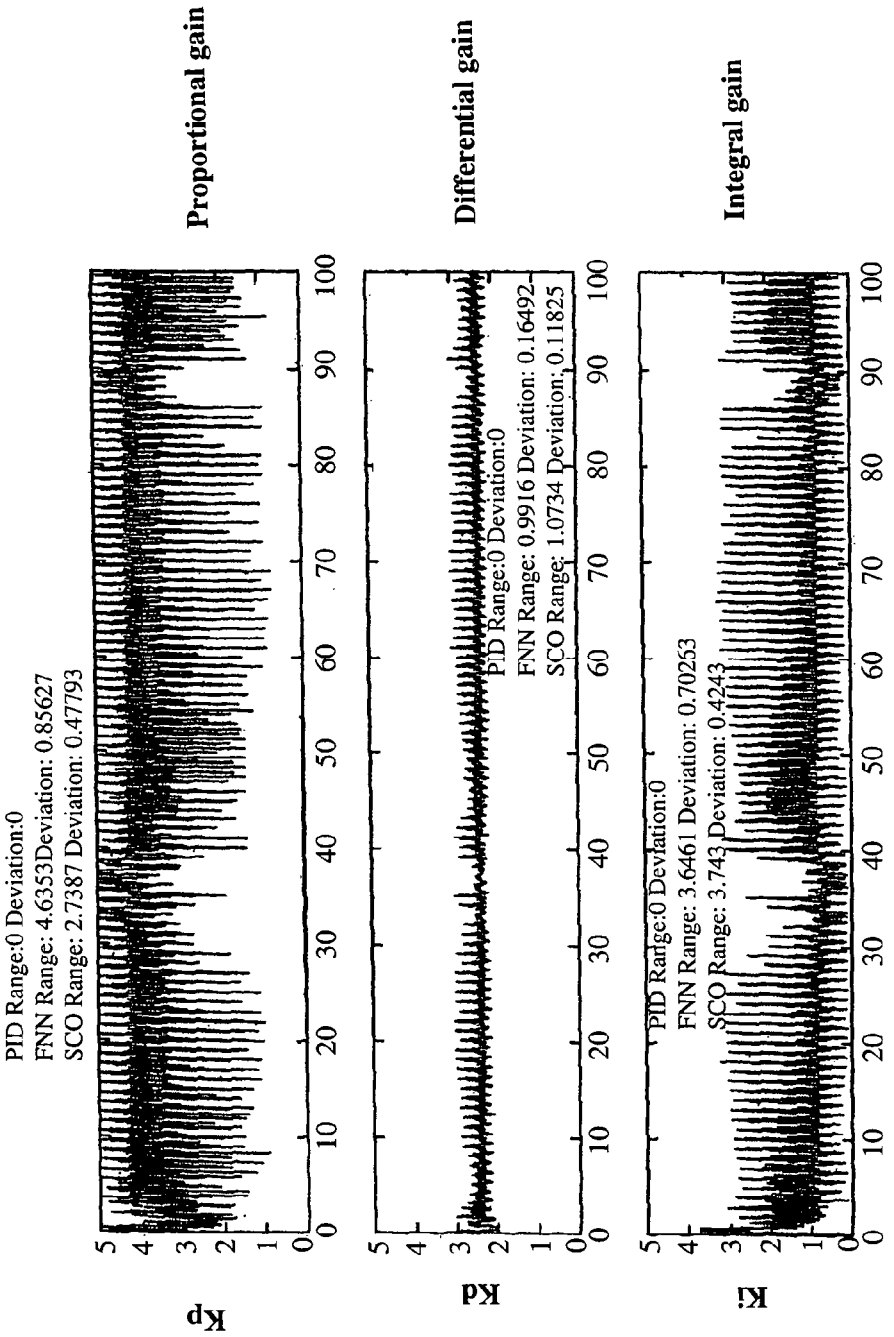
Proportional gain
PID Range:0 Deviation:0
FNN Range: 4.6353Deviation: 0.85627
SCO Range: 2.7387 Deviation: 0.47793
Kp
Differential gain
PID Range:0 Deviation:0
FNN Range: 0.9916 Deviation: 0.16492
SCO Range: 1.0734 Deviation: 0.11825
Kd
Integral gain
PID Rarge:0 Deviation:0
FNN Range: 3.6461 Deviation: 0.70253
SCO Range: 3.743 Deviation: 0.4243
Ki

Figure 54

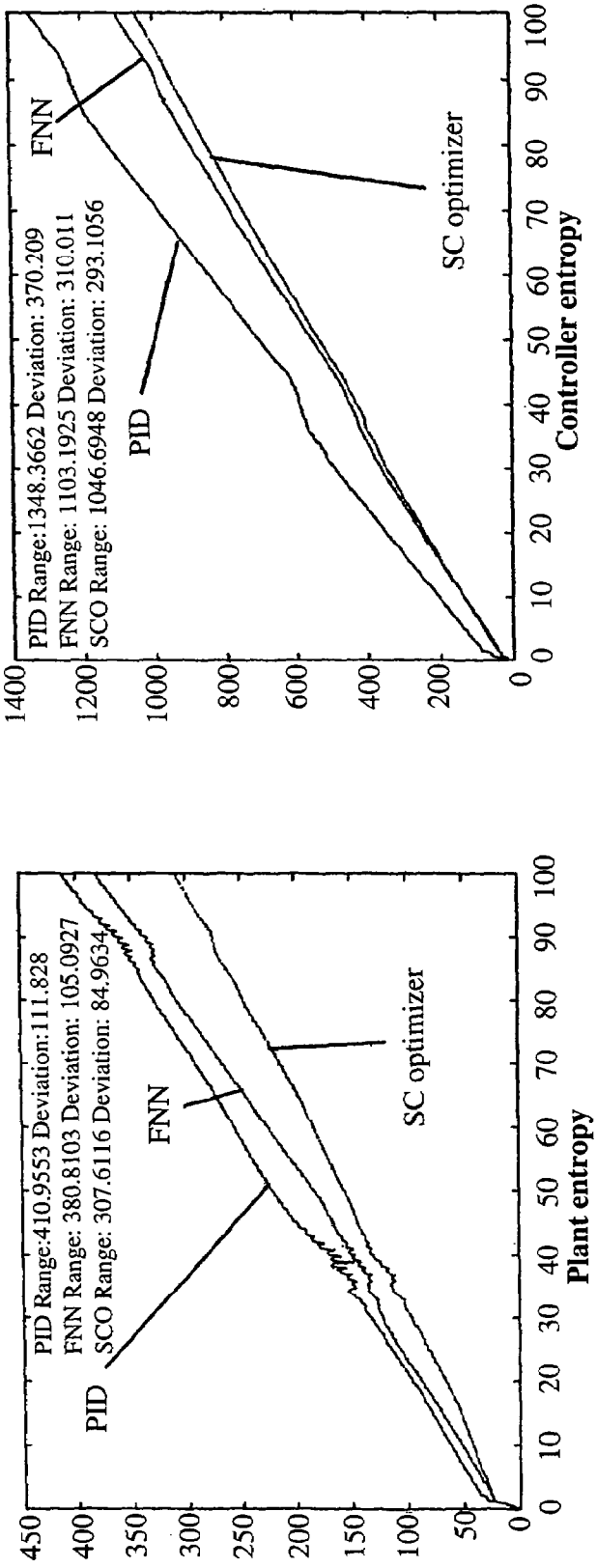
PID Range:1348.3662 Deviation: 370.209
FNN Range: 1103.1925 Deviation: 310.011
SCO Range: 1046.6948 Deviation: 293.1056
PID
FNN
SC optimizer
Controller entropy
PID Range:410.9553 Deviation:111.828
FNN Range: 380.8103 Deviation: 105.0927
SCO Range: 307.6116 Deviation: 84.9634
PID
FNN
SC optimizer
Plant entropy

Figure 55

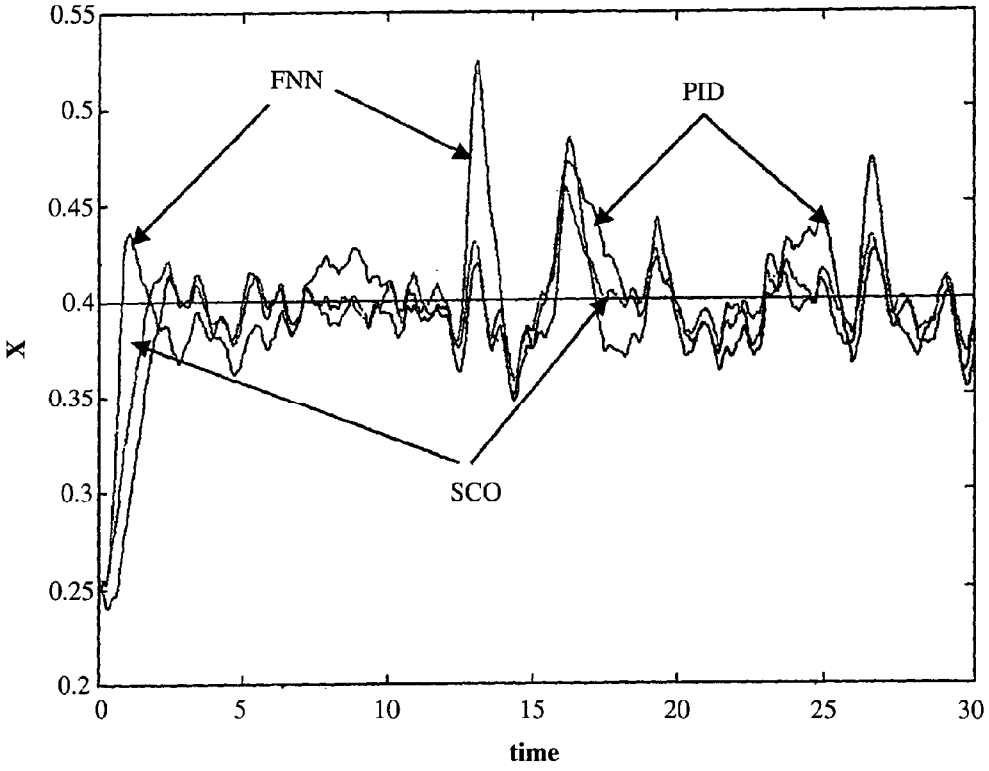

Figure 56

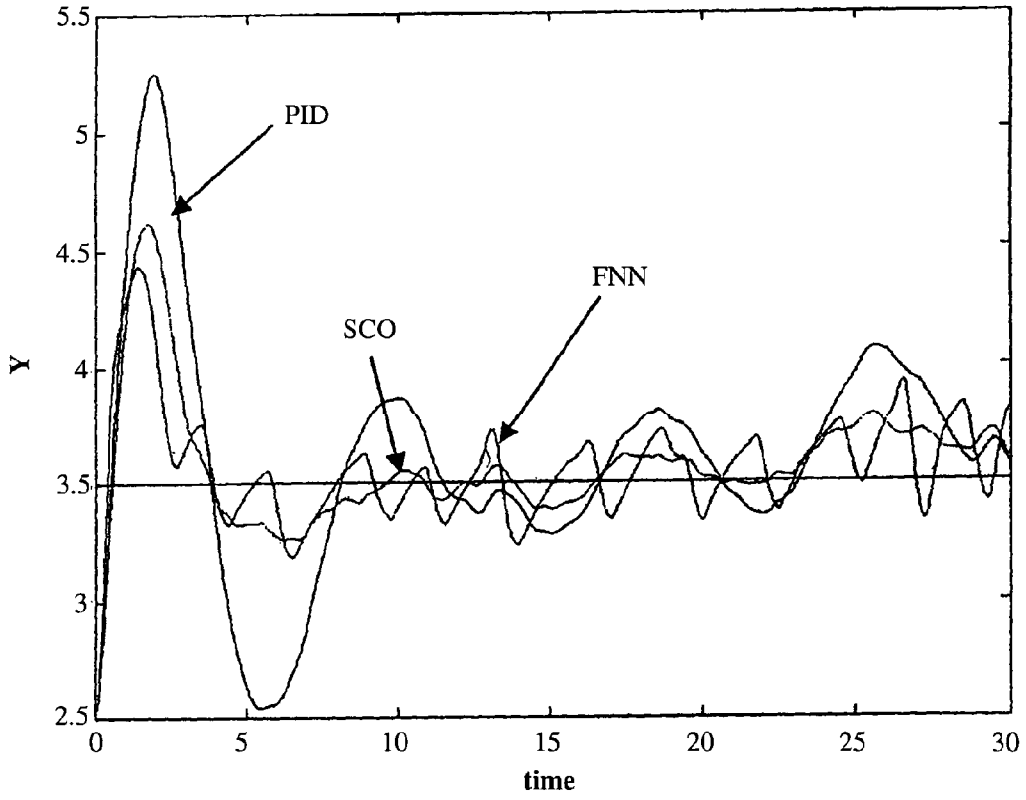

Figure 57

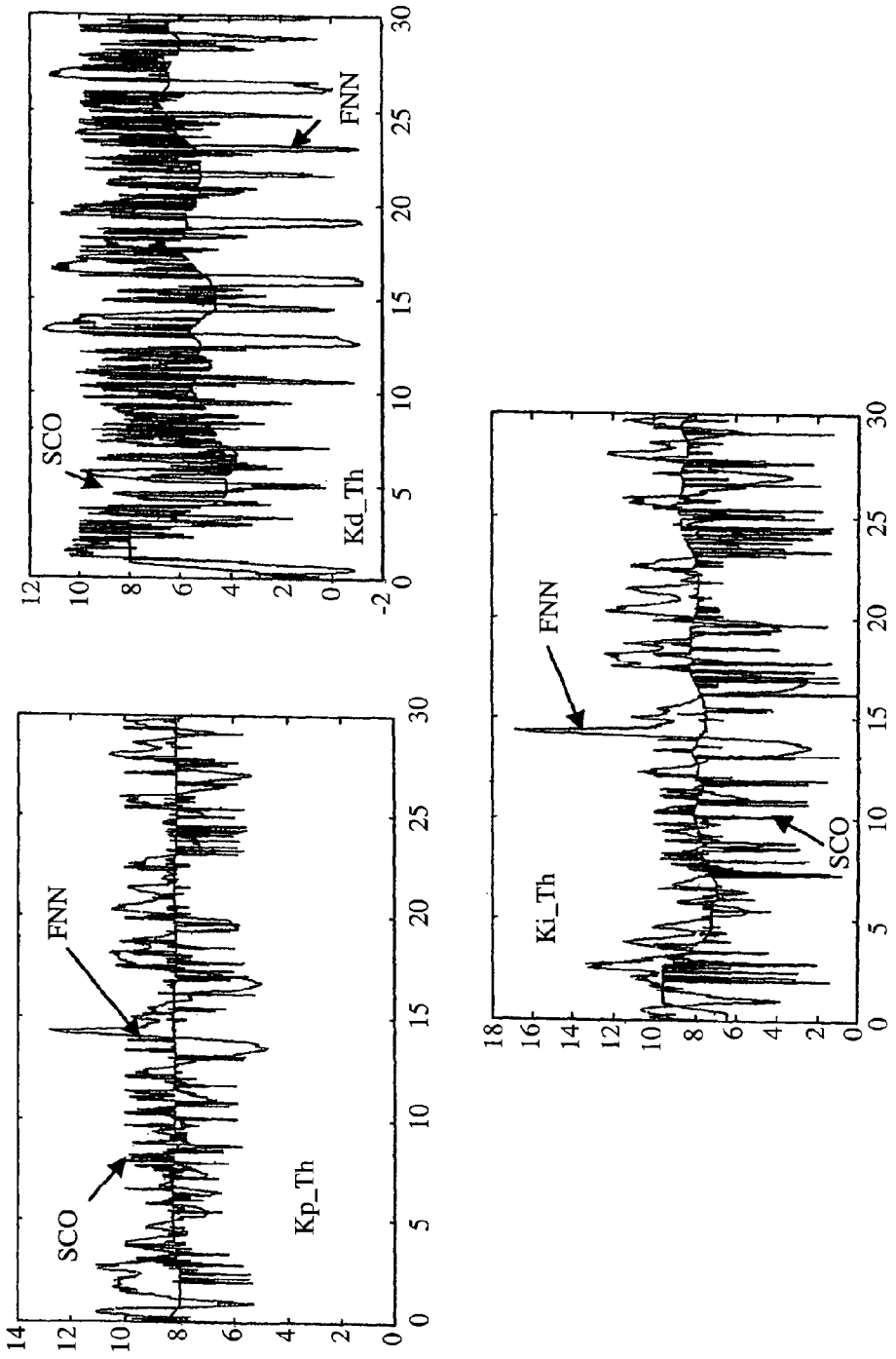

Figure 58

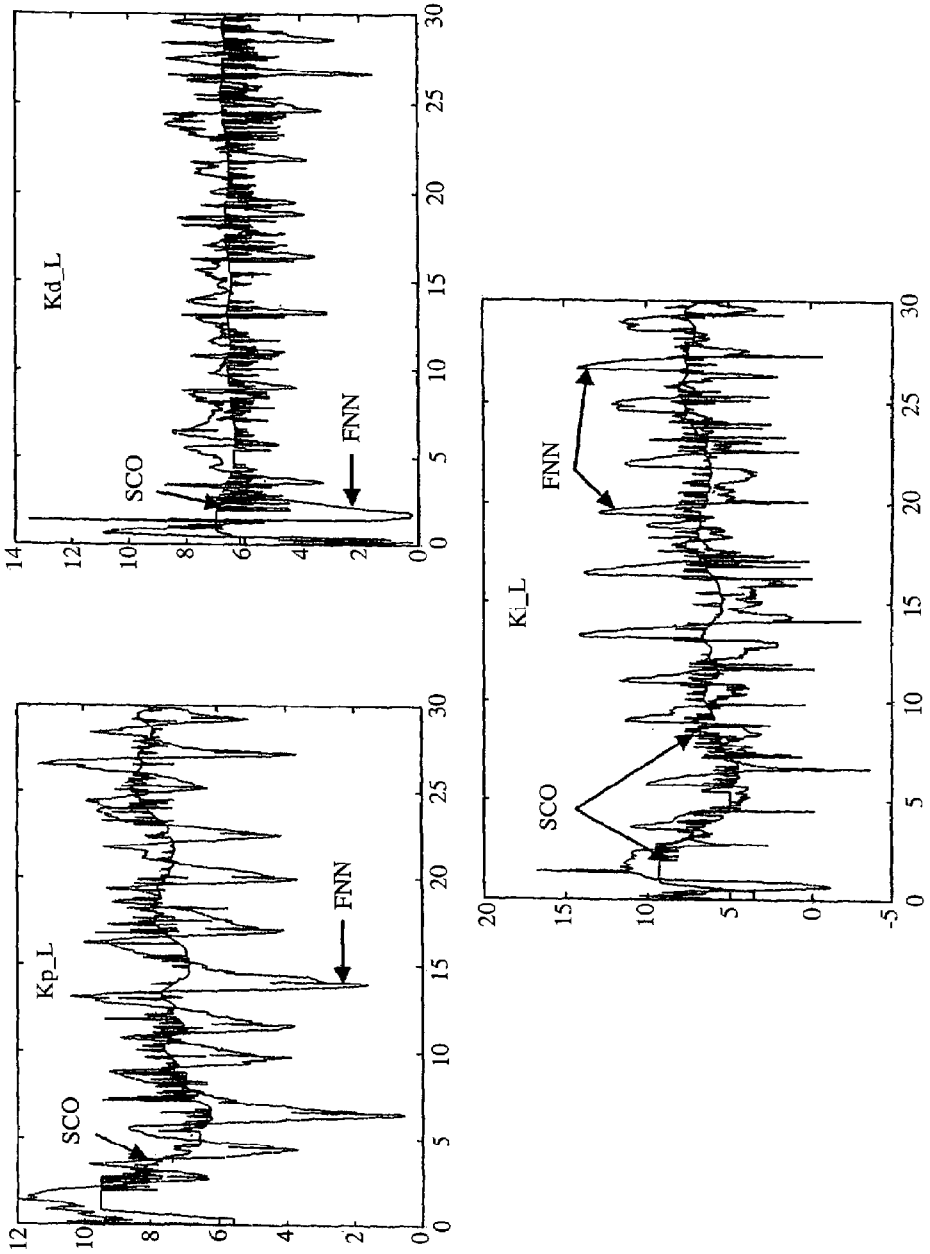

Figure 59

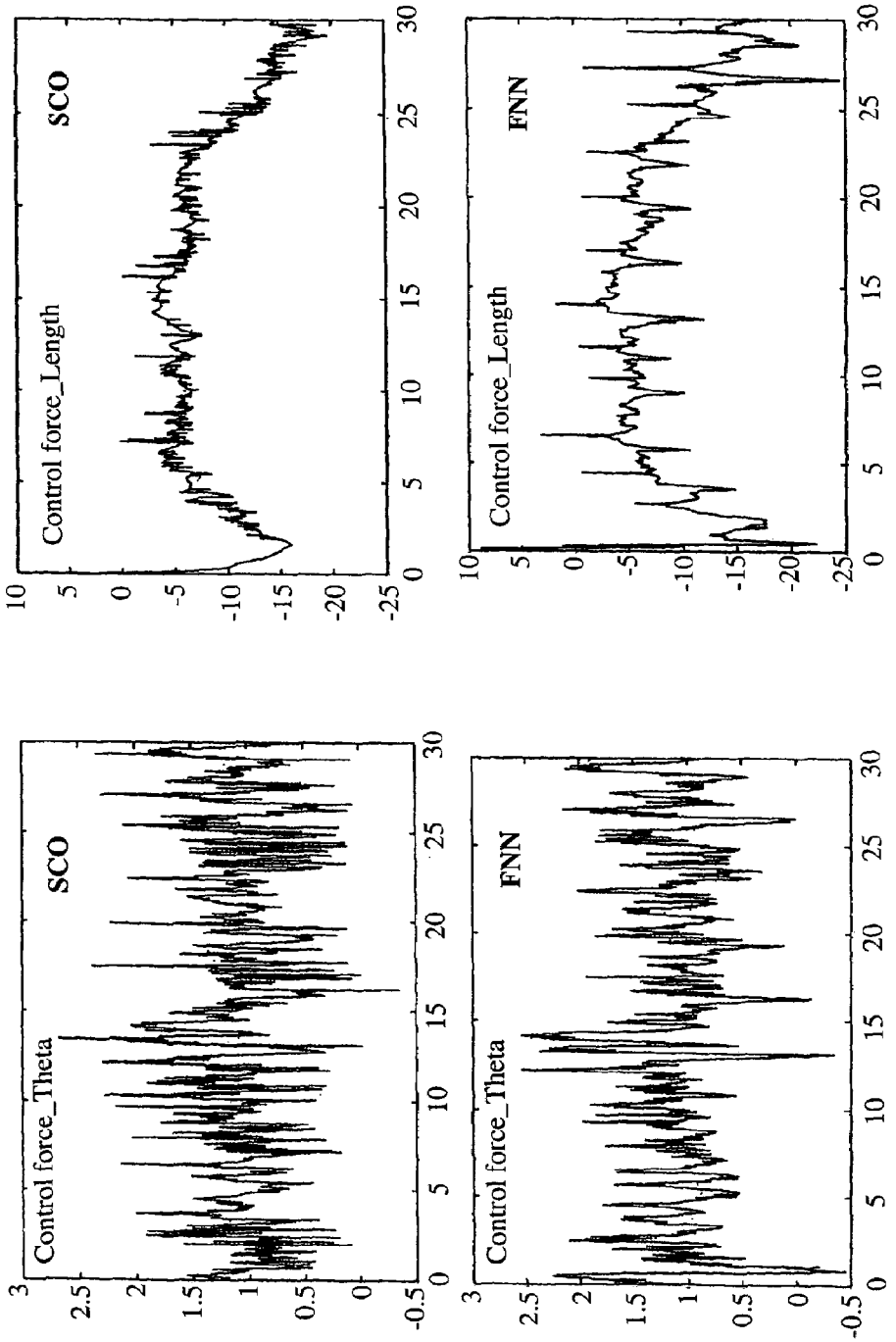
SCO
Control force_Length
FNN
Control force_Length
SCO
Control force_Theta
FNN
Control force_Theta

Figure 60

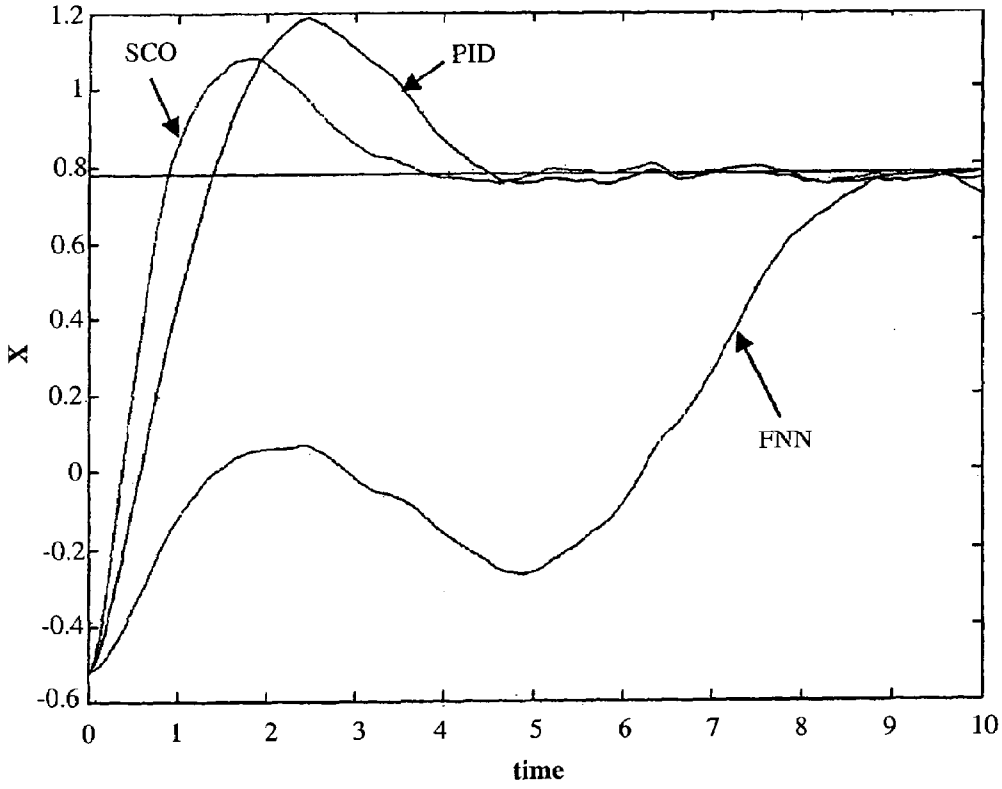

Figure 61

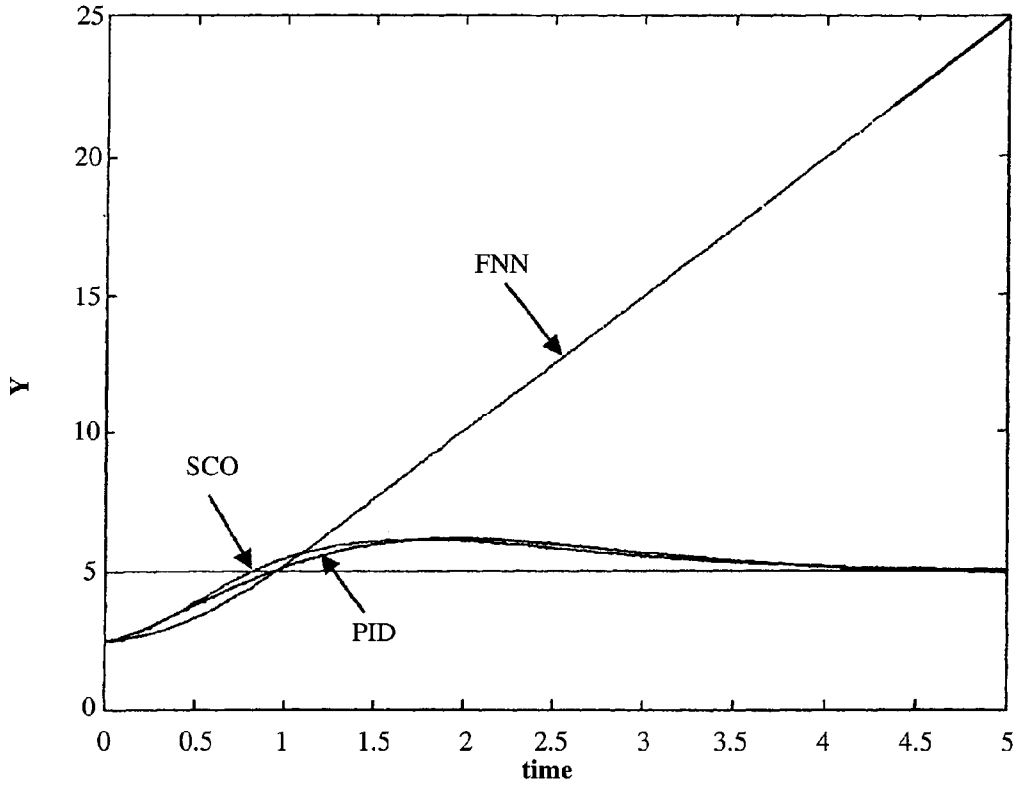

Figure 62

SOFT COMPUTING OPTIMIZER OF INTELLIGENT CONTROL SYSTEM STRUCTURES

REFERENCE TO RELATED APPLICATIONS

This present application claims priority benefit of U.S. Provisional Application No. 60/490,397, filed Jul. 25, 2003, titled "SOFT COMPUTING OPTIMIZER OF INTELLIGENT CONTROL SYSTEM STRUCTURES," the entire contents of which is hereby incorporated by reference.

BACKGROUND

1. Field of the Invention

The present invention relates generally to control systems, and more particularly to the design method of intelligent control system structures based on soft computing optimization.

2. Description of the Related Art

Feedback control systems are widely used to maintain the output of a dynamic system at a desired value in spite of external disturbances that would displace it from the desired value. For example, a household space-heating furnace, controlled by a thermostat, is an example of a feedback control system. The thermostat continuously measures the air temperature inside the house, and when the temperature falls below a desired minimum temperature the thermostat turns the furnace on. When the interior temperature reaches the desired minimum temperature, the thermostat turns the furnace off. The thermostat-furnace system maintains the household temperature at a substantially constant value in spite of external disturbances such as a drop in the outside temperature. Similar types of feedback controls are used in many applications.

A central component in a feedback control system is a controlled object, a machine or a process that can be defined as a "plant", whose output variable is to be controlled. In the above example, the "plant" is the house, the output variable is the interior air temperature in the house and the disturbance is the flow of heat (dispersion) through the walls of the house. The plant is controlled by a control system. In the above example, the control system is the thermostat in combination with the furnace. The thermostat-furnace system uses simple on-off feedback control proportional feedback control, integral feedback control, and derivative feedback control. A feedback control based on a sum of proportional, plus integral, plus derivative feedbacks, is often referred as a P(I)D control.

A P(I)D control system is a linear control system that is based on a dynamic model of the plant. In classical control systems, a linear dynamic model is obtained in the form of dynamic equations, usually ordinary differential equations. The plant is assumed to be relatively linear, time invariant, and stable. However, many real-world plants are time varying, highly non-linear, and unstable. For example, the dynamic model may contain parameters (e.g., masses, inductance, aerodynamics coefficients, etc.), which are either only approximately known or depend on a changing environment. If the parameter variation is small and the dynamic model is stable, then the P(I)D controller may be satisfactory. However, if the parameter variation is large or if the dynamic model is unstable, then it is common to add Adaptive or Intelligent (AI) control functions to the P(I)D control system.

AI control systems use an optimizer, typically a nonlinear optimizer, to program the operation of the P(I)D controller and thereby improve the overall operation of the control system.

Classical advanced control theory is based on the assumption that all controlled "plants" can be approximated as linear systems near equilibrium points. Unfortunately, this assumption is rarely true in the real world. Most plants are highly nonlinear, and often do not have simple control algorithms. In order to meet these needs for a nonlinear control, systems have been developed that use Soft Computing (SC) concepts such Fuzzy Neural Networks (FNN), Fuzzy Controllers (FC), and the like. By these techniques, the control system evolves (changes) in time to adapt itself to changes that may occur in the controlled "plant" and/or in the operating environment.

Control systems based on SC typically use a Knowledge Base (KB) to contain the knowledge of the FC system. The KB typically has many rules that describe how the SC determines control parameters during operation. Thus, the performance of an SC controller depends on the quality of the KB and the knowledge represented by the KB. Increasing the number of rules in the KB generally increases (very often with redundancy) the knowledge represented by the KB but at a cost of more storage and more computational complexity. Thus, design of a SC system typically involves tradeoffs regarding the size of the KB, the number of rules, the types of rules. etc. Unfortunately, the prior art methods for selecting KB parameters such as the number and types of rules are based on ad hoc procedures using intuition and trial-and-error approaches.

SUMMARY

The present invention solves these and other problems by providing a SC optimizer for designing a KB to be used in a SC system such as a SC control system. In one embodiment, the SC optimizer includes a fuzzy inference engine. In one embodiment, the fuzzy inference engine includes a Fuzzy Neural Network (FNN). In one embodiment, the SC Optimizer provides Fuzzy Inference System (FIS) structure selection, FIS structure optimization method selection, and Teaching signal selection.

In one embodiment, the user makes the selection of fuzzy model, including one or more of: the number of input and/or output variables; the type of fuzzy inference model (e.g., Mamdani, Sugeno, Tsukamoto, etc.); and the preliminary type of membership functions.

In one embodiment, a Genetic Algorithm (GA) is used to optimize linguistic variable parameters and the input-output training patterns. In one embodiment, a GA is used to optimize the rule base, using the fuzzy model, optimal linguistic variable parameters, and a teaching signal.

One embodiment, includes fine tuning of the FNN. The GA produces a near-optimal FNN. In one embodiment, the near-optimal FNN can be improved using classical derivative-based optimization procedures.

One embodiment, includes optimization of the FIS structure by using a GA with a fitness function based on a response of the actual plant model.

One embodiment, includes optimization of the FIS structure by a GA with a fitness function based on a response of the actual plant.

The result is a specification of an FIS structure that specifies parameters of the optimal FC according to desired requirements.

BRIEF DESCRIPTION OF THE FIGURES

FIG. **1** is a block diagram of the general structure of a self-organizing intelligent control system based on SC

FIG. **2** is a block diagram of the general structure of a self-organizing intelligent control system based on SC with a SC optimizer.

FIG. **3** shows information flow in the SC optimizer.

FIG. **4** is a flowchart of the SC optimizer.

FIG. **5** shows information levels of the teaching signal and the linguistic variables.

FIG. **6** shows inputs for linguistic variables **1** and **2**.

FIG. **7** shows outputs for linguistic variable **1**.

FIG. **8** shows the activation history of the membership functions presented in FIGS. **6** and **7**.

FIG. **9** shows the activation history of the membership functions presented in FIGS. **6** and **7**.

FIG. **10** shows the activation history of the membership functions presented in FIGS. **6** and **7**.

FIG. **11** is a diagram showing rule strength versus rule number for 15 rules

FIG. **12**A shows the ordered history of the activations of the rules, where the Y-axis corresponds to the rule index, and the X-axis corresponds to the pattern number (t).

FIG. **12**B shows the output membership functions, activated in the same points of the teaching signal, corresponding to the activated rules of FIG. **12**A.

FIG. **12**C shows the corresponding output teaching signal.

FIG. **12**D shows the relation between rule index, and the index of the output membership functions it may activate.

FIG. **13**A shows an example of a first complete teaching signal variable.

FIG. **13**B shows an example of a second complete teaching signal variable.

FIG. **13**C shows an example of a third complete teaching signal variable.

FIG. **13**D shows an example of a first reduced teaching signal variable.

FIG. **13**E shows an example of a second reduced teaching signal variable.

FIG. **13**F shows an example of a third reduced teaching signal variable.

FIG. **14** is a diagram showing rule strength versus rule number for 15 selected rules after second GA optimization.

FIG. **15** shows approximation results using a reduced teaching signal corresponding to the rules from FIG. **14**.

FIG. **16** shows the complete teaching signal corresponding to the rules from FIG. **14**.

FIG. **17** shows embodiment with KB evaluation based on approximation error.

FIG. **18** shows embodiment with KB evaluation based on plant dynamics.

FIG. **19** shows optimal control signal acquisition.

FIG. **20** shows teaching signal acquisition form an optimal control signal.

FIG. **21** shows the stochastic excitation as a left subplot showing time history, and a right subplot showing the normalized histogram.

FIG. **22** shows the free oscillations under stochastic excitation.

FIG. **23** shows the free oscillations without excitation.

FIG. **24** shows the P(I)D control under stochastic excitation.

FIG. **25** shows the P(I)D gains and control force, obtained with P(I)D control under stochastic excitation.

FIG. **26** shows the P(I)D control without excitations.

FIG. **27** shows the P(I)D gains and control force, obtained with P(I)D control without excitation.

FIG. **28** shows the output of plant controlled by P(I)D controller with gains scheduled with SSCQ with minimum of plant entropy production.

FIG. **29** shows the P(I)D gains adjusted with SSCQ with minimum of plant entropy production, and corresponding control force.

FIG. **30** shows the output of plant with P(I)D gains adjusted with FC obtained using AFM, and as a teaching signals the results of SSCQ with minimum of plant entropy production.

FIG. **31** shows the control gains and control force obtained with AFM.

FIG. **32** shows the output of plant with P(I)D gains adjusted with FC obtained using SC optimizer, and as a teaching signals the results of SSCQ with minimum of plant entropy production.

FIG. **33** shows the control gains and control force obtained with SC optimizer.

FIG. **34** shows a comparison of the control gains obtained with SC optimizer and with AFM.

FIG. **35** shows a comparison of the plant controlled variable obtained with SC optimizer and with AFM controller.

FIG. **36** shows the plant entropy obtained with AFM based FC and with SC optimizer based FC.

FIG. **37** shows the plant entropy production obtained with AFM based FC and with SC optimizer based FC.

FIG. **38** shows the swing dynamic system.

FIG. **39** shows the stochastic excitation used for teaching signal acquisition.

FIG. **40** shows the teaching signal obtained with GA and Approximated with FNN and with SC optimizer.

FIG. **41** shows the control error obtained with different controllers, simulation conditions are the same as was set for teaching signal acquisition.

FIG. **42** shows the control error derivative obtained with different controllers, simulation conditions are the same as was set for teaching signal acquisition.

FIG. **43** shows the controlled state variable dynamics obtained with different controllers, simulation conditions are the same as was set for teaching signal acquisition.

FIG. **44** shows the intended fitness function of the control obtained with different controllers, simulation conditions are the same as was set for teaching signal acquisition.

FIG. **45** shows the intended fitness function of the control obtained with different controllers, simulation conditions are the same as was set for teaching signal. Comparison only between FNN and SC optimizer based control.

FIG. **46** shows the control gains obtained with different controllers, simulation conditions are the same as was set for teaching signal. P(I)D was set up to the constant gains [5 5 5].

FIG. **47** shows the stochastic excitation used for check of the robustness of the obtained KB.

FIG. **48** shows the different realization of the stochastic excitation from the same distribution as for teaching signal.

FIG. **49** shows the controlled variable for a new excitation signal.

FIG. **50** shows the coefficient gains for the new excitation signal.

FIG. **51** shows the different reference signal.

FIG. **52** shows the simulation results.

FIG. **53** shows the fitness functions.

FIG. **54** shows the coefficient gains.

FIG. **55** shows the plant and controller entropy.

FIG. **56** shows swing motion under fuzzy control with two P(I)D controllers. Motion along Theta-axis under Gaussian stochastic excitation Comparison of P(I)D,FNN and SCO control.

FIG. **57** shows Swing motion under fuzzy control with two P(I)D controllers. Motion along L-axis under non-Gaussian (Rayleigh) stochastic excitation Comparison of P(I)D, FNN and SCO control.

FIG. **58** shows Swing motion under fuzzy control with two P(I)D controllers, Motion along Theta-axis under Gaussian stochastic excitation SCO and FNN Control law comparison, control along Theta-axis.

FIG. **59** shows Swing motion under fuzzy control with two P(I)D controllers, Motion along Length-axis under Gaussian stochastic excitation SCO and FNN Control law comparison, Control along Length-axis.

FIG. **60** shows Swing motion under fuzzy control with two P(I)D controllers. SCO and FNN Control force (Theta-axis and Length-axis) comparison.

FIG. **61** shows Swing motion under fuzzy control with two P(I)D controllers, investigation of robustness, Motion along Theta-axis under Gaussian stochastic excitation, comparison of P(I)D, FNN and SCO control.

FIG. **62** shows swing motion under fuzzy control with two P(I)D controllers, investigation of robustness, motion along Length-axis under non-Gaussian (Rayleigh) stochastic excitation, comparison of P(I)D, FNN and SCO control.

DETAILED DESCRIPTION

FIG. **1** shows a self-organizing control system **100** for controlling a plant based on Soft Computing (SC). The control system **100** includes a plant **120**, a Simulation System of Control Quality (SSCQ) **130**, Fuzzy Logic Classifier System (FLCS) **140** and a P(I)D controller **150**. The SSCQ **130** includes a module **132** for calculating a fitness function, such as, in one embodiment, entropy production from of the plant **120**, and a control signal output from the P(I)D controller **150**. The SSCQ **130** also includes a Genetic Algorithm (GA) **131**. In one embodiment, a fitness function of the GA **131** is configured to reduce entropy production. The FLCS **140** includes a FNN **142** to program a FC **143**. An output of the FC **143** is a coefficient gain schedule for the P(I)D controller **150**. The P(I)D controller **150** controls the plant **120**.

Using a set of inputs, a fitness function **132** in a GA **131** works in a manner similar to an evolutionary process to arrive at a solution which is, hopefully, optimal. The GA **131** generates sets of "chromosomes" (that is, possible solutions) and then sorts the chromosomes by evaluating each solution using the fitness function **132**. The fitness function **132** determines where each solution ranks on a fitness scale. Chromosomes (solutions) which are more fit, are those which correspond to solutions that rate high on the fitness scale. Chromosomes which are less fit, are those which correspond to solutions that rate low on the fitness scale.

Chromosomes that are more fit are kept (survive) and chromosomes that are less fit are discarded (die). New chromosomes are created to replace the discarded chromosomes. The new chromosomes are created by crossing pieces of existing chromosomes and by introducing mutations.

A P(I)D controller **150** has a substantially linear transfer function and thus is based upon a linearized equation of motion for the controlled "plant" **120**. Prior art GA used to program P(I)D controllers typically use simple fitness functions and thus do not solve the problem of poor controllability typically seen in linearization models. As is the case with most optimizers, the success or failure of the optimization often ultimately depends on the selection of the performance (fitness) function **132**.

Evaluating the motion characteristics of a nonlinear plant is often difficult, in part due to the lack of a general analysis method. Conventionally, when controlling a plant with nonlinear motion characteristics, it is common to find certain equilibrium points of the plant and the motion characteristics of the plant are linearized in a vicinity near an equilibrium point. Control is then based on evaluating the pseudo (linearized) motion characteristics near the equilibrium point. This technique is scarcely, if at all, effective for plants described by models that are unstable or dissipative.

Computation of optimal control based on SC includes the GA **131** as the first step of global search for optimal solution on a fixed space of positive solutions. The GA searches for a set of control weights for the plant. Firstly the weight vector $K=\{k_1, \ldots, k_n\}$ is used by a conventional proportional-integral-differential (P(I)D) controller **150** in the generation of a signal $\delta(K)$ which is applied to the plant. The entropy $S(\delta(K))$ associated to the behavior of the plant on this signal is assumed as a fitness function to minimize. The GA is repeated several times at regular time intervals in order to produce a set of weight vectors. The vectors generated by the GA **131** are then provided to a FNN **142** and the output of the FNN **142** to a Fuzzy Controller (FC) **143**. The output of the FC **143** is a collection of gain schedules for the P(I)D-controller **150** that controls the plant.

FIG. **2** shows the self-organizing control system of FIG. **1**, where the FLCS **140** is replaced by an FLCS **240**. The FLCS **240** includes a SC optimizer **242** configured to program an optimal FC **243**.

The SSCQ **130** finds teaching patterns (input-output pairs) for optimal control by using the GA **131** based on a mathematical model of controlled plant **120** and physical criteria of minimum of entropy production rate. The FLCS **240** produces an approximation of the optimal control produces by the SSCQ **130** by programming the optimal FC **243**.

The SSCQ **130** provides acquisition of a robust teaching signal for optimal control. The output of SSCQ **130** is the robust teaching signal, which contains the necessary information about the optimal behavior of the plant **120** and corresponding behavior of the control system **200**.

The SC optimizer **242** produces an approximation of the teaching signal by building a Fuzzy Inference System (FIS). The output of the SC optimizer **242** includes a Knowledge Base (KB) for the optimal FC **243**.

The optimal FC operates using an optimal KB from the FC **243** including, but not limited to, the number of input-output membership functions, the shapes and parameters of the membership functions, and a set of optimal fuzzy rules based on the membership functions.

In one embodiment the optimal FC **243** is obtained using a FNN trained using a training method, such as, for example, the error back propagation algorithm. The error back propagation algorithm is based on application of the gradient descent method to the structure of the FNN. The error is calculated as a difference between the desired output of the FNN and an actual output of the FNN. Then the error is "back propagated" through the layers of the FNN, and the parameters of each neuron of each layer are modified towards the direction of the minimum of the propagated error. The back propagation algorithm has a few disadvantages. First, in order to apply the back propagation approach

it is necessary to know the complete structure of the FNN prior to the optimization. The back propagation algorithm can not be applied to a network with an unknown number of layers or an unknown number nodes. Second, the back propagation process cannot modify the types of the membership functions. Finally, the back propagation algorithm very often finds only a local optimum close to the initial state rather then the desired global minimum. This occurs because the initial coefficients for the back propagation algorithm are usually generated randomly. The error back propagation algorithm is used, in a commercially available Adaptive Fuzzy Modeler (AFM). The AFM permits creation of Sugeno 0 order FIS from digital input-output data using the error back propagation algorithm. The algorithm of the AFM has two steps. In the first AFM step, a user specifies the parameters of a future FNN. Parameters include the number of inputs and number of outputs and the number of fuzzy sets for each input/output. Then AFM "optimizes" the rule base, using a so-called "let the best rule win" (LBRW) technique. During this phase, the membership functions are fixed as uniformly distributed among the universe of discourse, and the AFM calculates the firing strength of the each rule, eliminating the rules with zero firing strength, and adjusting centers of the consequents of the rules with nonzero firing strength. It is possible during optimization of the rule base to specify the learning rate parameter. The AFM also includes an option to build the rule base manually. In this case, user can specify the centroids of the input fuzzy sets, and then the system builds the rule base according to the specified centroids.

In the second AFM step, the AFM builds the membership functions. The user can specify the shape factors of the input membership functions. Shape factor supported by the AFM include: Gaussian; Isosceles Triangular; and Scalene Triangular. The user must also specify the type of fuzzy AND operation in the Sugeno model, either as a product or a minimum.

After specification of the membership function shape and Sugeno inference method, AFM starts optimization of the membership function shapes. The user can also specify optional parameters to control optimization rate such as a target error and the number of iterations.

AFM inherits the limitations and weaknesses of the back propagation algorithm described above. The user must specify the types of membership functions, the number of membership functions for each linguistic variable and so on. AFM uses rule number optimization before membership functions optimization, and as a result, the system becomes very often unstable during the membership function optimization phase.

The Structure of an Intelligent Control System Including SC-Optimizer

In FIG. **2** the SC optimizer **242** creates a FIS using the teaching signal from the SSCQ **130**. The SC optimizer **242** provides GA based FNN learning including rule extraction and KB optimization. The SC optimizer **242** can use as a teaching signal either an output from the SSCQ **130** and/or output from the plant **120** (or a model of the plant **120**).

In one embodiment, the SC optimizer **242** includes (as shown in FIG. **3**) a fuzzy inference engine in the form of a FNN. The SC optimizer also allows FIS structure selection using models, such as, for example, Sugeno FIS order 0 and 1, Mamdani FIS, Tsukamoto FIS, etc. The SC optimizer **242** also allows selection of the FIS structure optimization method including optimization of linguistic variables, and/or optimization of the rule base. The SC optimizer **242** also allows selection of the teaching signal source, including: the teaching signal as a look up table of input-output patterns; the teaching signal as a fitness function calculated as a dynamic system response; the teaching signal as a fitness function is calculated as a result of control of a real plant; etc.

In one embodiment, output from the SC optimizer **242** can be exported to other programs or systems for simulation or actual control of a plant **130**. For example, output from the FC optimizer **242** can be exported to a simulation program for simulation of plant dynamic responses, to an online controller (to use in control of a real plant), etc.

The Structure of the SC Optimizer

FIG. **4** is a high-level flowchart **400** for the SC optimizer **242**. By way of explanation, and not by way of limitation, the operation of the flowchart divides operation in to four stages, shown as Stages 1, 2, 3, 4, and 5.

In Stage 1, the user selects a fuzzy model by selecting one or parameters such as, for example, the number of input and output variables, the type of fuzzy inference model (Mamdani, Sugeno, Tsukamoto, etc.), and the source of the teaching signal.

In Stage 2, a first GA (GA1) optimizes linguistic variable parameters, using the information obtained in Stage 1 about the general system configuration, and the input-output training patterns, obtained from the training signal as an input-output table. In one embodiment, the teaching signal is obtained using structure presented in FIGS. **19** and **20**.

In Stage 3 precedent part of the rule base is created and rules are ranked according to their firing strength. Rules with high firing strength are kept, whereas weak rules with small firing strength are eliminated.

In Stage 4, a second GA (GA2) optimizes a rule base, using the fuzzy model obtained in Stage 1, optimal linguistic variable parameters obtained in Stage 2, selected set of rules obtained in Stage 3 and the teaching signal.

In Stage 5, the structure of FNN is further optimized. In order to reach the optimal structure, the classical derivative-based optimization procedures can be used, with a combination of initial conditions for back propagation, obtained from previous optimization stages. The result of Stage 5 is a specification of fuzzy inference structure that is optimal for the plant **120**. Stage 5 is optional and can be bypassed. If Stage 5 is bypassed, then the FIS structure obtained with the GAs of Stages 2 and 4 is used.

In one embodiment Stage 5 can be realized as a GA which further optimizes the structure of the linguistic variables, using set of rules obtained in the Stage 3 and 4. In this case only parameters of the membership functions is modified in order to reduce approximation error.

In one embodiment of Stage 4 and Stage 5, selected components of the KB are optimized. In one embodiment, if KB has more than one output signals, the consequent part of the rules may be optimized independently for each output in Stage 4. In one embodiment if KB has more than one input, membership functions of selected inputs are optimized in Stage 5.

In one embodiment, while Stage 4 and Stage 5 the actual plant response in form of the fitness function can be used as performance criteria of FIS structure while GA optimization.

In one embodiment, the SC optimizer **242** uses a GA approach to solve optimization problems related with choosing the number of membership functions, the types and parameters of the membership functions, optimization of fuzzy rules and refinement of KB.

GA optimizers are often computationally expensive because each chromosome created during genetic operations is evaluated according to a fitness function. For example a GA with a population size of 100 chromosomes evolved 100 generations, may require up to 10000 calculations of the fitness function. Usually this number is smaller, since it is possible to keep track of chromosomes and avoid re-evaluation. Nevertheless, the total number of calculations is typically much greater than the number of evaluations required by some sophisticated classical optimization algorithm. This computational complexity is a payback for the robustness obtained when a GA is used. The large number of evaluations acts as a practical constraint on applications using a GA. This practical constraint on the GA makes it worthwhile to develop simpler fitness functions by dividing the extraction of the KB of the FIS into several simpler tasks, such as: define the number and shape of membership functions; select optimal rules; fix optimal rules structure; and refine the KB structure. Each of these tasks is discussed in more detail below. In some sense SC optimizer **242** uses divide and conquer type of algorithm applied to the KB optimization problem.

Definition of the Numbers and of Shapes of the Membership Functions with GA

In one embodiment the teaching signal, representing one or more input signals and one or more output signals, can be presented as shown in the FIG. **5**. The teaching signal is divided into input and output parts. Each of the parts is divided into one or more signals. Thus, in each time point of the teaching signal there is a correspondence between the input and output parts, indicated as a horizontal line in FIG. **5**.

Each component of the teaching signal (input or output) is assigned to a corresponding linguistic variable, in order to explain the signal characteristics using linguistic terms. Each linguistic variable is described by some unknown number of membership functions, like "Large", "Medium", "Small", etc. FIG. **5** shows various relationships between the membership functions and their parameters.

"Vertical relations" represent the explicitness of the linguistic representation of the concrete signal, e.g. how the membership functions is related to the concrete linguistic variable. Increasing the number of vertical relations will increase the number of membership functions, and as a result will increase the correspondence between possible states of the original signal, and its linguistic representation. An infinite number of vertical relations would provide an exact correspondence between signal and its linguistic representation, because to each possible value of the signal would be assigned a membership function, but in this case the situations as "over learning" may occur. Smaller number of vertical relations will increase the robustness, since some small variations of the signal will not affect much the linguistic representation. The balance between robustness and precision is a very important moment in design of the intelligent systems, and usually this task is solved by Human expert.

"Horizontal relations" represent the relationships between different linguistic variables. Selected horizontal relations can be used to form components of the linguistic rules.

To define the "horizontal" and "vertical" relations mathematically, consider a teaching signal:

[x(t),y(t)],

Where:

t=1, . . . , N—time stamps;

N—number of samples in the teaching signal;

$x(t)=(x_1(t), \ldots, x_m(t))$—input components;

$y(t)=(y_1(t), \ldots y_n(t))$—output components.

Define the linguistic variables for each of the components. A linguistic variable is usually defined as a quintuple: (x,T(x),U,G,M), where x is the name of the variable, T(x) is a term set of the x, that is the set of the names of the linguistic values of x, with a fuzzy set defined in U as a value, G is a syntax rule for the generation of the names of the values of the x and M is a semantic rule for the association of each value with its meaning. In the present case, x is associated with the signal name from x or y, term set T(x) is defined using vertical relations, U is a signal range. In some cases one can use normalized teaching signals, then the range of U is [0,1]. The syntax rule G in the linguistic variable optimization can be omitted, and replaced by indexing of the corresponding variables and their fuzzy sets.

Semantic rule M varies depending on the structure of the FIS, and on the choice of the fuzzy model. For the representation of all signals in the system, it is necessary to define m+n linguistic variables:

Let[X,Y], $X=(X_1, \ldots, X_m)$, $Y=(Y_1, \ldots, Y_n)$ be the set of the linguistic variables associated with the input and output signals correspondingly. Then for each linguistic variable one can define a certain number of fuzzy sets to represent the variable:

$$X_1: \left\{\mu_{x_1}^1, \ldots, \mu_{x_1}^{l_{x_1}}\right\}, \ldots, X_m: \left\{\mu_{X_m}^1, \ldots, \mu_{X_m}^{i_{x_m}}\right\};$$

$$Y_1: \left\{\mu_{Y_1}^1, \ldots, \mu_{Y_1}^{l_{Y_1}}\right\}, \ldots, Y_n: \left\{\mu_{Y_n}^1, \ldots, \mu_{Y_n}^{l_{Y_n}}\right\}$$

Where

$\mu_{X_i}^{j_i}$, i=1, . . . , m, $j_i=1, \ldots, l_{X_i}$ are membership functions of the i th component of the input variable; and

$\mu_{Y_i}^{j_i}$, i=1, . . . , n, $j_i=1, \ldots, l_{Y_i}$ are membership functions of the i th component of the output variable.

Usually, at this stage of the definition of the KB, the parameters of the fuzzy sets are unknown, and it may be difficult to judge how many membership functions are necessary to describe a signal. In this case, the number of membership functions $l_{X_i} \in [1, L_{MAX}]$, i=1, . . . , m can be considered as one of the parameters for the GA (GA1) search, where L_{MAX} is the maximum number of membership functions allowed. In one embodiment, L_{MAX} is specified by the user prior to the optimization, based on considerations such as the computational capacity of the available hardware system.

Knowing the number of membership functions, it is possible to introduce a constraint on the possibility of activation of each fuzzy set, denoted as $p_{X_i}^j$.

One of the possible constraints can be introduced as:

$$p_{X_i}^{j\,\prime} \geq \frac{1}{l_{X_i}}, i = 1, \ldots, m; j = 1, \ldots, l_{X_i}$$

This constraint will cluster the signal into the regions with equal probability, which is equal to division of the signal's histogram into curvilinear trapezoids of the same surface area. Supports of the fuzzy sets in this case are equal or greater to the base of the corresponding trapezoid. How much greater the support of the fuzzy set should be, can be defined from an overlap parameter. For example, the overlap parameter takes zero, when there is no overlap between two attached trapezoids. If it is greater than zero then there is some overlap. The areas with higher probability will have in

this case "sharper" membership functions. Thus, the overlap parameter is another candidate for the GA1 search. The fuzzy sets obtained in this case will have uniform possibility of activation.

Modal values of the fuzzy sets can be selected as points of the highest possibility, if the membership function has unsymmetrical shape, and as a middle of the corresponding trapezoid base in the case of symmetric shape. Thus one can set the type of the membership functions for each signal as a third parameter for the GA1.

The relation between the possibility of the fuzzy set and its membership function shape can also be found. The possibility of activation of each membership function is calculated as follows:

$$p^j_{X_i} = p(x_i \mid x_i = \mu^j_{X_i}) = \frac{1}{N}\sum_{t=1}^{N} \mu^j_{X_i}(x_i(t)) \tag{1.1}$$

Mutual possibility of activation of different membership functions can be defined as:

$$p^{(j,l)}_{X_i|X_k} = p\left(x_i \mid_{x_i=\mu^j_{X_i}, x_k=\mu^l_{X_k}}\right) = \frac{1}{N}\sum_{t=1}^{N}\left[\mu^j_{X_i}(x_i(t)) * \mu^l_{X_k}(x_k(t))\right] \tag{1.2}$$

where * denotes selected T-norm (Fuzzy AND) operation; $j=1, \ldots, l_{X_i}$, $l=1, \ldots, l_{X_k}$ are indexes of the corresponding membership functions.

In fuzzy logic literature, T-norm, denoted as * is a two-place function from [0,1]×[0,1] to [0,1]. It represents a fuzzy intersection operation and can be interpreted as minimum operation, or algebraic product, or bounded product or drastic product. S-conorm, denoted by +, is a two-place function, from [0,1]×[0,1] to [0,1]. It represents a fuzzy union operation and can be interpreted as algebraic sum, or bounded sum and drastic sum. Typical T-norm and S-conorm operators are presented in the Table 1.

TABLE 1

T-norms (fuzzy intersection)	S-conorms (fuzzy union)
min(x, y) – minimum operation	max(x, y) – maximum operation
xy – algebraic product	x + y – xy – algebraic sum
x * y = max[0, x + y – 1] – bounded product	x + y = min[1, x + y] – bounded sum
$x*y = \begin{cases} x, \text{ if } y = 1 \\ y, \text{ if } x = 1 \\ 0, \text{ if } x, y < 1 \end{cases}$ – drastic product	$x+y = \begin{cases} x, \text{ if } y = 0 \\ y, \text{ if } x = 0 \\ 0, \text{ if } x, y > 0 \end{cases}$ – drastic sum

If i=k, and j≠l, then equation (1.2) defines "vertical relations"; and if i≠k, then equation (1.2) defines "horizontal relations". The measure of the "vertical" and of the "horizontal" relations is a mutual possibility of the occurrence of the membership functions, connected to the correspondent relation.

The set of the linguistic variables is considered as optimal, when the total measure of "horizontal relations" is maximized, subject to the minimum of the "vertical relations".

Hence, one can define a fitness function for the GA1 which will optimize the number and shape of membership functions as a maximum of the quantity, defined by equation (1.2), with minimum of the quantity, defined by equation (1.1).

The chromosomes of the GA1 for optimization of linguistic variables according to Equations (1.1) and (1.2) have the following structure:

$$\underbrace{[l_{X_1}, \ldots, l_{Y_n}]}_{m+n}\underbrace{[\alpha_{X_1}, \ldots, \alpha_{Y_n}]}_{m+n}\underbrace{[T_{X_1}, \ldots, T_{Y_N}]}_{m+n}$$

Where:

$l_{X(Y)_i} \in [1, L_{MAX}]$ are genes that code the number of membership functions for each linguistic variable $X_i(Y_i)$;

$\alpha_{X(Y)_i}$ are genes that code the overlap intervals between the membership functions of the corresponding linguistic variable $X_i(Y_i)$; and

$T_{X(Y)_i}$ are genes that code the types of the membership functions for the corresponding linguistic variables.

Another approach to the fitness function calculation is based on the Shannon information entropy. In this case instead of the equations (1.1) and (1.2), for the fitness function representation one can use the following information quantity taken from the analogy with information theory:

$$\begin{aligned} H^j_{X_i} &= -p^j_{X_i}\log(p^j_{X_i}) \\ &= -p(x_i \mid x_i = \mu^j_{X_i})\log[p(x_i \mid x_i = \mu^j_{X_i})] \\ &= -\frac{1}{N}\sum_{t=1}^{N}\mu^j_{X_i}(x_i(t))\log[\mu^j_{X_i}(x_i(t))] \end{aligned} \tag{1.1a}$$

and

$$\begin{aligned} H^{(j,l)}_{X_i|X_k} &= H\left(x_i \mid_{x_i=\mu^j_{X_i}, x_k=\mu^l_{X_k}}\right) \\ &= -\frac{1}{N}\sum_{t=1}^{N}\left[\mu^j_{X_i}(x_i(t)) * \mu^l_{X_k}(x_k(t))\right] \\ &\quad \log\left[\mu^j_{X_i}(x_i(t)) * \mu^l_{X_k}(x_k(t))\right] \end{aligned} \tag{1.2a}$$

In this case, GA1 will maximize the quantity of mutual information (1.2a), subject to the minimum of the information about each signal (1.1a). In one embodiment the combination of information and probabilistic approach can also be used.

In case of the optimization of number and shapes of membership functions in Sugeno—type FIS, it is enough to include into GA chromosomes only the input linguistic variables. The detailed fitness functions for the different types of fuzzy models will be presented in the following sections, since it is more related with the optimization of the structure of the rules.

Results of the membership function optimization GA1 are shown in FIGS. **6** and **7**. FIG. **6** shows results for input variables. FIG. **7** shows results for output variables. FIGS. **8**, **9**, **10** show the activation history of the membership functions presented in FIGS. **6** and **7**. The lower graphs of FIGS. **8**, **9** and **10** are original signals, normalized into the interval [0, 1]

Optimal Rules Selection

Rule Pre-selection Algorithm

The pre-selection algorithm selects the number of optimal rules and their premise structure prior optimization of the consequent part.

Consider the structure of the first fuzzy rule of the rule base

$$R^1(t) = \text{IF } x_1(t) \text{ is } \mu_1^1(x_1) \text{ AND } x_{l_2}(t) \text{ is } \mu_2^1(x_2) \text{ AND } \cdots \text{ AND } x_m(t) \text{ is } \mu_m^1(x_m)$$

$$\text{THEN } y_1(t) \text{ is } \mu_{m+1}^{\{l_{m+1}1\}}(y_1),\ y_2(t) \text{ is } \mu_{m+2}^{\{l_{m+2}2\}}(y_2), \cdots, y_n(t) \text{ is } \mu_{m+n}^{\{l_{m+n}1\}}(y_n),$$

Where:

m is the number of inputs;

n is the number of outputs;

$x_i(t)$, i=1, . . . , m are input signals;

$y_j(t)$, j=1, . . . , n are output signals;

$\mu_k^{l_k}$ are membership functions of linguistic variables;

k=1, . . . , m+n are the indexes of linguistic variables;

l_k=2, 3, . . . are the numbers of the membership functions of each linguistic variable;

$\mu_k^{\{l_k\}}$—are membership functions of output linguistic variables, upper index;

$\{l_k\}$ means the selection of one of the possible indexes; and

t is a time stamp.

Consider the antecedent part of the rule:

$R_{IN}^1(t)$=IF $x_1(t)$ is $\mu_1^1(x_1)$ AND $x_{1_2}(t)$ is $\mu_2^1(x_2)$ AND . . . AND $x_m(t)$ is $\mu_m^1(x_m)$

The firing strength of the rule R^1 in the moment t is calculated as follows:

$$R^1_{fs}(t)=\min[\mu_1^1(x_1(t)), \mu_2^1(x_2(t)), \ldots, \mu_m^1(x_m(t))]$$

for the case of the min-max fuzzy inference, and as

$$R_{fs}^1(t)=\Pi[\mu_1^1(x_1(t)), \Sigma_2^1(x_2(t)), \ldots, \mu_m^1(x_m(t))]$$

for the case of product-max fuzzy inference.

In general case, here can be used any of the T-norm operations.

The total firing strength $R_{\Theta s}^1$ of the rule, the quantity $R_{fs}^1(t)$ can be calculated as follows:

$$R_{fs}^1 = \frac{1}{T}\int_t R_{fs}^1(t)dt$$

for a continuous case, and:

$$R_{fs}^1 = \frac{1}{T}\sum_t R_{fs}^1(t)$$

for a discrete case.

In a similar manner the firing strength of each s-th rule is calculated as:

$$R_{fs}^s = \frac{1}{N}\int_t R_{fs}^s(t)dt, \text{ or } R_{fs}^s = \frac{1}{N}\sum_t R_{fs}^s(t), \quad (1.3)$$

where

$$s = 1, 2, \ldots, \prod_{i=1}^{m} l_i \text{ is a linear rule index}$$

N—number of points in the teaching signal or maximum of t in continuous case.

In one embodiment the local firing strength of the rule can be calculated in this case instead of integration, the maximum operation is taken in Eq. (1.3):

$$R_{fs}^s = \max_t R_{fs}^s(t) \quad (1.4)$$

In this case, the total strength of all rules will be:

$$R_{fs} = \sum_{s=1}^{L_0} R_{fs}^s,$$

where:

$$L_0 = \prod_{k=1}^{m} l_k \text{ - Number of rules in complete rule base}$$

Number of rules in complete rule base

Quantity R_{fs} is important since it shows in a single value the integral characteristic of the rule base. This value can be used as a fitness function which optimizes the shape parameters of the membership functions of the input linguistic variables, and its maximum guaranties that antecedent part of the KB describes well the mutual behavior of the input signals. Note that this quantity coincides with the "horizontal relations," introduced in the previous section, thus it is optimized automatically by GA1.

Alternatively, if the structure of the input membership functions is already fixed, the quantities R_{fs}^s can be used for selection of the certain number of fuzzy rules. Many hardware implementations of FCs have limits that constrain, in one embodiment, the total possible number of rules. In this case, knowing the hardware limit L of a certain hardware implementation of the FC, the algorithm can select $L \leqq L_0$ of rules according to a descending order of the quantities R_{fs}^s. Rules with zero firing strength can be omitted.

It is generally advantageous to calculate the history of membership functions activation prior to the calculation of the rule firing strength, since the same fuzzy sets are participating in different rules. In order to reduce the total computational complexity, the membership function calculation is called in the moment t only if its argument x(t) is within its support. For Gaussian-type membership functions, support can be taken as the square root of the variance value σ^2.

An example of the rule pre-selection algorithm is shown in the FIG. **11**, where the abscissa axis is an index of the rules, and the ordinate axis is a firing strength of the rule R_{fs}^s. Each point represents one rule. In this example, the KB has 2 inputs and one output. A horizontal line shows the threshold level. The threshold level can be selected based on the maximum number of rules desired, based on user inputs, based on statistical data and/or based on other considerations. Rules with relatively high firing strength will be kept, and the remaining rules are eliminated. As is shown in FIG. **11**, there are rules with zero firing strength. Such rules give no contributions to the control, but may occupy hardware resources and increase computational complexity. Rules with zero firing strength can be eliminated by default. In one embodiment, the presence of the rules with zero firing strength may indicate the explicitness of the linguistic variables (linguistic variables contain too many membership functions). The total number of the rules with zero firing strength can be reduced during membership functions construction of the input variables. This minimization is equal to the minimization of the "vertical relations."

This algorithm produces an optimal configuration of the antecedent part of the rules prior to the optimization of the rules. Optimization of the consequential part of KB can be applied directly to the optimal rules only, without unnecessary calculations of the "un-optimal rules". This process can also be used to define a search space for the GA (GA2), which finds the output (consequential) part of the rule.

Optimal Selection of Consequental Part of KB with GA2

A chromosome for the GA2 which specifies the structure of the output part of the rules can be defined as:

$$[I_1 \ldots I_M],\ I_i=[I_1, \ldots, I_n],\ I_k=\{1, \ldots, l_{Y_k}\},\ k=1, \ldots, n$$

where:

I_i are groups of genes which code single rule;

I_k are indexes of the membership functions of the output variables;

n is the number of outputs; and

M is the number of rules.

In one embodiment the history of the activation of the rules can be associated with the history of the activations of membership functions of output variables or with some intervals of the output signal in the Sugeno fuzzy inference case. Thus, it is possible to define which output membership functions can possibly be activated by the certain rule. This allows reduction of the alphabet for the indexes of the output variable membership functions from $_1\{1, \ldots, l_{Y_1}\}, \ldots, \{1, \ldots, l_{Y_n}\}_1^N$ to the exact definition of the search space of each rule:

$$\{l^{min}_{Y_1}, \ldots, l^{max}_{Y_1}\}_1, \ldots, \{l^{min}_{Y_n}, \ldots, l^{max}_{Y_n}\}_1, \ldots, \{l^{min}_{Y_1}, \ldots, l^{max}_{Y_1}\}_N, \ldots, \{l^{min}_{Y_n}, \ldots, l^{max}_{Y_n}\}_N$$

Thus the total search space of the GA is reduced. In cases where only one output membership function is activated by some rule, such a rule can be defined automatically, without GA2 optimization.

In one embodiment in case of Sugeno 0 order FIS, instead of indexes of output membership functions, corresponding intervals of the output signals can be taken as a search space.

For some combinations of the input-output pairs of the teaching signal, the same rules and the same membership functions are activated. Such combinations are uninteresting from the rule optimization view point, and hence can be removed from the teaching signal, reducing the number of input-output pairs, and as a result total number of calculations. The total number of points in the teaching signal (t) in this case will be equal to the number of rules plus the number of conflicting points (points when the same inputs result in different output values).

FIG. **12**A shows the ordered history of the activations of the rules, where the Y-axis corresponds to the rule index, and the X-axis corresponds to the pattern number (t). FIG. **12**B shows the output membership functions, activated in the same points of the teaching signal, corresponding to the activated rules of FIG. **12**A. Intervals when the same indexes are activated in FIG. **12**B are uninteresting for rule optimization and can be removed. FIG. **12**C shows the corresponding output teaching signal. FIG. **12**D shows the relation between rule index, and the index of the output membership functions it may activate. From FIG. **12**D one can obtain the intervals $[l^{min}_{Y_j}, l^{max}_{Y_j}]^j$, j=1, . . . , N where j is the rule index, for example if j=1, $l^{min}_{Y_1}=6$, $l^{max}_{Y_1}=8$.

FIGS. **13**A–F show plots of the teaching signal reduction using analysis of the possible rule configuration for three signal variables. FIGS. **13**A–C show the original signals. FIGS. **13**D–F show the results of the teaching signal reduction using the rule activation history. The number of points in the original signal is about 600. The number of points in reduced teaching signal is about 40. Bifurcation points of the signal, as shown in FIG. **12**B are kept.

FIG. **14** is a diagram showing rule strength versus rule number for 12 selected rules after GA2 optimization. FIG. **15** shows approximation results using a reduced teaching signal corresponding to the rules from FIG. **14**. FIG. **16** shows the complete teaching signal corresponding to the rules from FIG. **14**.

Fitness Evaluation in GA2

The previous section described optimization of the FIS, without the details into the type of FIS selection. In one embodiment, the fitness function used in the GA2 depends, at least in part, on the type of the optimized FIS. Examples of fitness functions for the Mamdani, Sugeno and/or Tsukamoto FIS models are described herein. One of ordinary skill in the art will recognize that other fuzzy models can be used as well.

Define error E^p as a difference between the output part of teaching signal and the FIS output as:

$$E^p = \frac{1}{2}(d^p - F(x_1^p, x_2^p, \ldots, x_n^p))^2 \text{ and } E = \sum_p E^p,$$

where $x_1^p, x_2^p, \ldots, x_n^p$ and d^p are values of input and output variables in the p training pair, respectively. The function $F(x_1^p, x_2^p, \ldots, x_n^p)$ is defined according to the chosen FIS model.

Mamdani Model

For the Mamdani model, the function $F(x_1^p, x_2^p, \ldots, x_n^p)$ is defined as:

$$F(x_1, \ldots, x_n) = \frac{\sum_{l=1}^{M} \bar{y}^l \prod_{i=1}^{n} \mu_{j_i}^l(x_i)}{\sum_{l=1}^{M} \prod_{i=1}^{n} \mu_{j_i}^l(x_i)} = \frac{\sum_{l=1}^{M} \bar{y}^l z^l}{\sum_{l=1}^{M} z^l}, \quad (1.5)$$

where

$$z^l = \prod_{i=1}^{n} \mu_{j_i}^l(x_i)$$

and $\bar{y}^l$ is the point of maximum value (called also as a central value) of $\mu_y^l(y)$, Π denotes the selected T-norm operation.

Sugeno Model Generally

Typical rules in the Sugeno fuzzy model can be expressed as follows:

IF x_1 is $\mu^{(l)}_{j_1}(x_1)$ AND x_2 is $\mu^{(l)}_{j_2}(x_2)$ AND . . . AND x_n is $\mu^{(l)}_{j_n}(x_n)$

THEN $y=f^l(x_1, \ldots, x_n)$,

where l=1, 2, . . . , M—the number of fuzzy rules M defined as {number of membership functions of x_i input variable}× {number of membership functions of x_2 input variable}× . . . ×{number of membership functions of x_n input variable}.

The output of Sugeno FIS is calculated as follows:

$$F(x_1, x_2, \ldots, x_n) = \frac{\sum_{l=1}^{M} f^l \prod_{i=1}^{n} \mu_{j_i}^l(x_i)}{\sum_{l=1}^{M} \prod_{i=1}^{n} \mu_{j_i}^l(x_i)}. \quad (1.6)$$

First-Order Sugeno Model

Typical rules in the first-order Sugeno fuzzy model can be expressed as follows:

IF x_1 is $\mu^{(I)}_{j_1}(x_1)$ AND x_2 is $\mu^{(I)}_{j_2}(x_2)$ AND . . . AND x_n is $\mu^{(I)}_{j_n}(x_n)$

THEN $y=f^I(x_1, \ldots x_n)=p_1{}^{(I)}x_1+p_2{}^{(I)}x_2+ \ldots p_n{}^{(I)}x_n+r^{(I)}$,

(Output variables described by some polynomial functions.)

The output of Sugeno FIS is calculated according equation (1.6).

Zero-Order Sugeno Model

Typical rules in the zero-order Sugeno FIS can be expressed as follows:

IF x_1 is $\mu^{(I)}_{j_1}(x_1)$ AND x_2 is $\mu^{(I)}_{j_2}(x_2)$ AND . . . AND x_n is $\mu^{(I)}_{j_n}(x_n)$

THEN $y=r^{(I)}$,

The output of zero-order Sugeno FIS is calculated as follows

$$F(x_1, x_2, \ldots, x_n) = \frac{\sum_{l=1}^{M} r^l \prod_{i=1}^{n} \mu_{j_i}^l(x_i)}{\sum_{l=1}^{M} \prod_{i=1}^{n} \mu_{j_i}^l(x_i)} \quad (1.7)$$

Tsukamoto Model

The typical rule in the Tsukamoto FIS is:

IF x_1 is $\mu^{(I)}_{j_1}(x_1)$ AND x_2 is $\mu^{(I)}_{j_2}(x_2)$ AND . . . AND x_n is $\mu^{(I)}_{j_n}(x_n)$

THEN y is $\mu_k{}^{(I)}(y)$,

where $j_1 \epsilon I_{m_1}$ is the set of membership functions describing linguistic values of x_1 input variable; $j_2 \epsilon I_{m_2}$ is the set of membership functions describing linguistic values of x_2 input variable; and so on, $j_m \epsilon I_{m_n}$ is the set of membership functions describing linguistic values of x_n input variable; and $k \epsilon O$ is the set of monotonic membership functions describing linguistic values of y output variable.

The output of the Tsukamoto FIS is calculated as follows:

$$F(x_1, \ldots, x_n) = \frac{\sum_{l=1}^{M} y^l \prod_{i=1}^{n} \mu_{j_i}^l(x_i)}{\sum_{l=1}^{M} \prod_{i=1}^{n} \mu_{j_i}^l(x_i)} = \frac{\sum_{l=1}^{M} y^l z^l}{\sum_{l=1}^{M} z^l}, \quad (1.8)$$

where $z^l = \prod_{i-1}^{n} \mu_{j_i}^l(x_i)$ and $z^l = \mu_k^{(l)}(y^l)$

Refinement of the KB Structure with GA

Stage 4 described above generates a KB with required robustness and performance for many practical control system design applications. If performance of the KB generated in Stage 4 is, for some reasons, insufficient, then the KB refinement algorithm of Stage 5 can be applied.

In one embodiment, the Stage 5 refinement process of the KB structure is realized as another GA (GA3), with the search space from the parameters of the linguistic variables. In one embodiment the chromosome of GA3 can have the following structure:

$\{[\Delta_1,\Delta_2,\Delta_3]\}^L$; $\Delta_i \epsilon [-\mathrm{prm}_i^j, 1-\mathrm{prm}_i^j]$; i=1,2,3; j=1,2, . . . , L, where L is the total number of the membership functions in the system

In this case the quantities Δ_i are modifiers of the parameters of the corresponding fuzzy set, and the GA3 finds these modifiers according to the fitness function as a minimum of the fuzzy inference error. In such an embodiment, the refined KB has the parameters of the membership functions obtained from the original KB parameters by adding the modifiers $\mathrm{prm}^{new}{}_i = \mathrm{prm}_i + \Delta_i$.

Different fuzzy membership function can have the same number of parameters, for example Gaussian membership functions have two parameters, as a modal value and variance. Iso-scalene triangular membership functions also have two parameters. In this case, it is advantageous to introduce classification of the membership functions regarding the number of parameters, and to introduce to GA3 the possibility to modify not only parameters of the membership functions, but also the type of the membership functions, form the same class. Classification of the fuzzy membership functions regarding the number of parameters is presented in the Table 2.

TABLE 2

	Class		
One parametric	Two parametric	Three parametric	Four parametric
Crisp	Gaussian Isosceles triangular Descending linear Ascending linear Descending Gaussian Ascending Gaussian	Non symmetric Gaussian Triangular	Trapezoidal Bell

GA3 improves fuzzy inference quality in terms of the approximation error, but may cause over learning, making the KB too sensitive to the input. In one embodiment a fitness function for rule base optimization is used. In one embodiment, an information-based fitness function is used. In another embodiment the fitness function used for membership function optimization in GA1 is used. To reduce the search space, the refinement algorithm can be applied only to some selected parameters of the KB. In one embodiment refinement algorithm can be applied to selected linguistic variables only.

The structure realizing evaluation procedure of GA2 or GA3 is shown in FIG. **17**. In FIG. **17**, the SC optimizer **17001** sends the KB structure presented in the current chromosome of GA2 or of GA3 to FC **17101**. An input part of the teaching signal **17102** is provided to the input of the FC **17101**. The output part of the teaching signal is provided to the positive input of adder **17103**. An output of the FC **17101** is provided to the negative input of adder **17103**. The output of adder **17103** is provided to the evaluation function calculation block **17104**. Output of evaluation function calculation block **17104** is provided to a fitness function input of the SC optimizer **17001**, where an evaluation value is assigned to the current chromosome.

In one embodiment evaluation function calculation block **17104** calculates approximation error as a weighted sum of the outputs of the adder **17103**.

In one embodiment evaluation function calculation block **17104** calculates the information entropy of the normalized approximation error.

Optimization of KB Based on Plant Response

In one embodiment of Stages 4 and 5 the fitness function of GA can be represented as some external function Fitness=f(KB), which accepts as a parameter the KB and as output provides KB performance. In one embodiment, the function f includes the model of an actual plant controlled by the system with FC. In this embodiment, the plant model in addition to plant dynamics provides for the evaluation function.

In one embodiment function f might be an actual plant controlled by an adaptive P(I)D controller with coefficient gains scheduled by FC and measurement system provides as an output some performance index of the KB.

In one embodiment the output of the plant provides data for calculation of the entropy production rate of the plant and of the control system while the plant is controlled by the FC with the structure from the the KB.

In one embodiment, the evaluation function is not necessarily related to the mechanical characteristics of the motion of the plant (such as, for example, in one embodiment control error) but it may reflect requirements from the other viewpoints such as, for example, entropy produced by the system, or harshness and or bad feelings of the operator expressed in terms of the frequency characteristics of the plant dynamic motion and so on.

FIG. **18** shows one embodiment the structure-realizing KB evaluation system based on plant dynamics. In FIG. **18**, and SC optimizer **18001** provides the KB structure presented in the current chromosome of the GA2 or of the GA3 to an FC **18101**. the FC is embedded into the KB evaluation system based on plant dynamics **18100**. The KB evaluation system based on plant dynamics **18100** includes the FC **18101**, an adaptive P(I)D controller **18102** which uses the FC **18101** as a scheduler of the coefficient gains, a plant **18103**, a stochastic excitation generation system **18104**, a measurement system **18105**, an adder **18106**, and an evaluation function calculation block **18107**. An output of the P(I)D controller **18102** is provided as a control force to the plant **18103** and as a first input to the evaluation function calculation block **18107**. Output of the excitation generation system **18104** is provided to the Plant **18103** to simulate an operational environment. An output of the Plant **18103** is provided to the measurement system **18105**. An output of the measurement system **18105** is provided to the negative input of the adder **18106** and together with the reference input Xref forms in adder **18106** control error which is provided as an input to the P(I)D controller **18102** and to the FC **18101**. An output of the measurement system **18105** is provided as a second input of the evaluation function calculation block **18107**. The evaluation function calculation block **18107** forms the evaluation function of the KB and provides it to the fitness function input of SC optimizer **18001**. Fitness function block of SC optimizer **18001** ranks the evaluation value of the KB presented in the current chromosome into the fitness scale according to the current parameters of the GA2 or of the GA3.

In one embodiment, the evaluation function calculation block **18107** forms evaluation function as a minimum of the entropy production rate of the plant **18103** and of the P(I)D controller **18102**.

In one embodiment, the evaluation function calculation block **18107** applies Fast Fourier Transformation on one or more outputs of the measurement system **18105**, to extract one or more frequency characteristics of the plant output for the evaluation.

In one embodiment, the KB evaluation system based on plant dynamics **18100** uses a nonlinear model of the plant **18103**.

In one embodiment, the KB evaluation system based on plant dynamics **18100** is realized as an actual plant with one or more parameters controlled by the adaptive P(I)D controller **18102** with control gains scheduled by the FC **18101**.

In one embodiment plant **18103** is a stable plant.

In one embodiment plant **18103** is an unstable plant.

The output of the SC optimizer **18001** is an optimal KB **18002**.

Teaching Signal Acquisition

In the previous sections it was stated that the SC optimizer **242** uses as an input the teaching signal which contains the plant response for the optimal control signal.

FIG. **19** shows optimal control signal acquisition. FIG. **19** is an embodiment of the system presented in the FIGS. **1** and **2**, where the FLCS **140** is omitted and plant **120** is controlled by the P(I)D controller **150** with coefficient gains scheduled directly by the SSCQ **130**.

The structure presented in FIG. **19** contains an SSCQ **19001**, which contains an GA (GA0). The chromosomes in the GA0 contain the samples of coefficient gains as $\{k_P, k_D, k_I\}^N$. The number of samples N corresponds with the number of lines in the future teaching signal. Each chromosome of the GA0 is provided to a Buffer **19101** which schedules the P(I)D controller **19102** embedded into the control signal evaluation system based on plant dynamics **19100**.

The control signal evaluation system based on plant dynamics **19100** includes the buffer **19101**, the adaptive P(I)D controller **19102** which uses Buffer **19101** as a scheduler of the coefficient gains, the plant **19103**, the stochastic excitation generation system **19104**, the measurement system **19105**, the adder **19106**, and the evaluation function calculation block **19107**. Output of the P(I)D controller **19102** is provided as a control force to the plant **19103** and as a first input to the evaluation function calculation block **19107**. Output of the excitation generation system **19104** is provided to the Plant **19103** to simulate an operational environment. An output of Plant **19103** is provided to the measurement system **19105**. An output of the measurement system **19105** is provided to the negative input of the adder **19106** and together with the reference input Xref forms in adder **19106** control error which is provided as an input to P(I)D controller **19102**. An output of the measurement system **19105** is provided as a second input of the evaluation function calculation block **19107**. The evaluation function calculation block **19107** forms the evaluation function of the control signal and provides it to the fitness function input of the SSCQ **19001**. The fitness function block of the SSCQ **19001** ranks the evaluation value of the control signal presented in the current chromosome into the fitness scale according to the current parameters of the GA0.

An output of the SSCQ **19001** is the optimal control signal **19002**.

In one embodiment, the teaching for the SC optimizer **242** is obtained from the optimal control signal **19002** as shown in FIG. **20**. In FIG. **20**, the optimal control signal **20001** is provided to the buffer **20101** embedded into the control signal evaluation system based on plant dynamics **20100** and as a first input of the multiplexer **20001**. Control signal evaluation system based on plant dynamics **20100** includes a buffer **20101**, an adaptive P(I)D controller **20102** which uses the buffer **20101** as a scheduler of the coefficient gains, a plant **20103**, a stochastic excitation generation system **20104**, a measurement system **20105** and an adder **20106**. On output of the P(I)D controller **20102** is provided as a control force to the plant **20103**. An output of the excitation generation system **20104** is provided to the plant **20103** to

simulate an operational environment. An output of plant **20103** is provided to the measurement system **29105**. An output of the measurement system **20105** is provided to the negative input of the adder **20106** and together with the reference input Xref forms in adder **20106** control error which is provided as an input to P(I)D controller **20102**. An output of the measurement system **20105** is the optimal plant response **20003**. The optimal plant response **20003** is provided to the multiplexer **20002**. The multiplexer **20002** forms the teaching signal by combining the optimal plant response **20003** with the optimal control signal **20001**. The output of the multiplexer **20002** is the optimal teaching signal **20004** which is provided as an input to SC optimizer **242**.

In one embodiment optimal plant response **20003** can be transformed in a manner that provides better performance of the final FIS.

In one embodiment high and/or low and/or band pass filter is applied to the measured optimal plant response **20003** prior to optimal teaching signal **20004** formation.

In one embodiment detrending and/or differentiation and/or integration operation is applied to the measured optimal plant response **20003** prior to optimal teaching signal **20004** formation.

In one embodiment other operations which the person skill of art may provide is applied to the measured optimal plant response **20003** prior to optimal teaching signal **20004** formation.

Simulation Results

FIGS. **21** **37** shows results of fuzzy control of nonlinear dynamic system under stochastic excitation as an illustration of the example of teaching signal approximation with the optimal FC.

The dynamic system used for the results in FIGS. **21**–**37** is described by the equations of motion of a coupled nonlinear oscillator:

$$\begin{cases} \ddot{x} + 2\beta_1\dot{x} + \omega_1^2(1-ky)x = 0 \\ \ddot{y} + 2\beta_2\dot{y} + \omega_2^2 y + \frac{\pi^2}{2l}(x\ddot{x} + \dot{x}^2) = \frac{1}{M}u(t) + \xi(t) \end{cases},$$

where:

$u(t)=k_p e+k_d \dot{e}+k_i \int_0 e(t)dt$ ($e=y_{ref}-y$) is a controlling force; and

$\xi(t)$ is a stochastic excitation.

The entropy production rate of the dynamic system is:

$$\frac{dS_x}{dt} = 2\beta_1\dot{x}\cdot\dot{x}, \quad \frac{dS_y}{dt} = 2\beta_2\dot{y}\cdot\dot{y};$$

The kinetic energy is:

$$T = \frac{\dot{x}^2}{2} + \frac{\dot{y}^2}{2},$$

The potential energy is:

$$U = U_x + U_y, \; U_x = \frac{1}{2}\omega_1^2 x^2(1-ky), \; U_y = \frac{1}{2}\omega_2^2 y^2,$$

The total energy is: T+U.

The control system's entropy production rate is:

$$\frac{dS_c}{dt} = k_d \dot{e}^2.$$

Model parameters used for simulation are:

β_1	0.3
ω_1	1.5
k	4
β_2	0.3
ω_2	4
l	0.5
M	5

Initial conditions are taken as:

$[x_0=1; y_0=0; \dot{x}_0=0; \dot{y}_0=0]$

Stochastic excitation used for the simulations is Raleigh noise, obtained using a stochastic filter. A time history and the histogram of such a noise is shown in FIG. **21**.

The GA parameters used in the SSCQ **130** for the simulation results are: PS: 200; GN: 100; Pcr=0.9; Pmut=0.006; and two point crossover was used. The results of the stochastic simulations under different types of control are presented in the FIGS. **22**–**37**.

FIG. **21** shows the stochastic excitation as a left subplot showing time history, and a right subplot showing the normalized histogram.

FIG. **22** shows the free oscillations under stochastic excitation

FIG. **23** shows the free oscillations without excitation

FIG. **24** shows the P(I)D control under stochastic excitation

FIG. **25** shows the P(I)D gains and control force, obtained with P(I)D control under stochastic excitation

FIG. **26** shows the P(I)D control without excitations

FIG. **27** shows the P(I)D gains and control force, obtained with P(I)D control without excitation

FIG. **28** shows the output of plant with P(I)D gains adjusted with SSCQ with minimum of plant entropy production

FIG. **29** shows the P(I)D gains adjusted with SSCQ with minimum of plant entropy production, and corresponding control force

FIG. **30** shows the output of plant with P(I)D gains adjusted with FC obtained using AFM, and as a teaching signals the results of SSCQ with minimum of plant entropy production

FIG. **31** shows the control gains and control force obtained with AFM

FIG. **32** shows the output of plant with P(I)D gains adjusted with FC obtained using SC optimizer, and as a teaching signals the results of SSCQ with minimum of plant entropy production

FIG. **33** shows the control gains and control force obtained with SC optimizer

FIG. **34** shows a comparison of the control gains obtained with SC optimizer and with AFM

FIG. **35** shows a comparison of the plant controlled variable obtained with the SC optimizer and with the AFM controller

FIG. **36** shows the plant entropy obtained with AFM based FC and with the SC optimizer based FC

FIG. **37** shows the plant entropy production obtained with AFM based FC and with SC optimizer based FC

SC optimizer **242** in the simulation results corresponding to FIGS. **21**–**C17** uses the Mamdani type fuzzy model with 4 membership functions for the first input, 4 membership functions for the second input, 5 membership functions for the third input, 3 membership functions for the first and second outputs, and 6 membership functions for the third output. The number of membership functions as, well as their types, were obtained by genetic optimization. For the AFM, the number of membership functions for the inputs was specified manually (7 membership functions per each

input). The numbers of the membership functions for outputs is simply equal to the number of rules, e.g. 51 membership functions for each output.

FIGS. **37** and **36** show that the intended fitness function (plant entropy) with the SC optimizer-based control is reduced better than with AFM-based control.

Swing dynamic system simulation results, Motion under fuzzy control with one P(I)D Controller. Comparison between back propagation FNN and SC optimizer control results

The previous example showed simulated control of a stable plant. The SC optimizer **242** can also be used to optimize a KB for an unstable object as, for in one embodiment, a nonlinear swing dynamic system. The nonlinear equations of motion of the swing dynamic system are:

$$\begin{cases} \ddot{\theta} + 2\frac{\dot{l}}{l}\dot{\theta} + \frac{g}{l}\sin\theta = 0 \\ \ddot{l} + 2k\dot{l} - l\dot{\theta}^2 - g\cos\theta = \frac{1}{m}\left(k_p \cdot e_l + k_d \cdot \dot{e}_l + k_i \cdot \int e_l dt + \xi(t)\right) \end{cases} \quad (38)$$

Here $\xi(t)$ is the given stochastic excitation (a white noise). Equations of entropy production are the following:

$$\frac{dS_\theta}{dt} = 2\frac{\dot{l}}{l}\dot{\theta}\cdot\dot{\theta};\ \frac{dS_l}{dt} = 2k\dot{l}\cdot\dot{l}; \quad (39)$$

The system (**38**) is a globally unstable system (in Lyapunov sense).

In this example only the second state variable (the length l) is controlled, and behavior of the first state variable (the rotation angle θ) is considered only for the reference.

The fitness function for the unstable swing is configured to minimize the entropy production rate in the plant and to minimize the entropy production rate in the control system. The final form of the fitness function of control in this case is:

$$f = (S_P - S_C)\left(\frac{dS_P}{dt} - \frac{dS_C}{dt}\right) \quad (40)$$

For the simulation, initial conditions and system parameters were specified as shown in Table 3 below.

TABLE 3

l_0	$\dot{l}_0$	θ_0	$\dot{\theta}_0$	k	m	Rs
2	0	π/4	0	1	1	l = 5

FIG. **38** shows the swing system and its equations of motion. FIG. **39** shows the excitation as a band limited white noise. This excitation was used for the teaching signal acquisition. FIG. **40** shows the results of the approximation of the teaching signal for different values of the control error and for derivative of the control error. The "o" symbols in FIG. **40** demonstrate the teaching signal. The solid line is a result of the approximation of the signal with back propagation-based FNN. The thin line in FIG. **40** is the result of the approximation of the teaching signal with the SC optimizer **242**. The results of the approximation can be summarized in the following Table 4:

TABLE 4

Parameter	FNN	Scoptimizer
FIS type	Sugeno zero order	
Number of inputs	Two inputs: control error, derivative of control error	
Number of outputs	Three outputs: K_P, K_D, K_I	
Number of membership functions for inputs	[8 × 8], Manual setting	[4 × 6], Numbers obtained automatically
Type of membership functions	Triangular	
Fuzzy And operator	Product	
Number of rules	64	24
Approximation error (Sufficient value for control quality is 0.1)	0.01 (<0.1)	0.05 (<0.1)

FIGS. **41**, **42**, **43**, **44**, **45**, **46** show the simulation results. The simulation results can be summarized as follows. Approximation error of the FNN is smaller than approximation error of the SC optimizer, but both values are sufficient. For the FNN, it is necessary to manually define number of membership functions for each input variable. The number of rules obtained with the FNN is greater than number of rules obtained with the SC optimizer. The stochastic excitation acting on the system in this case is the same as was used for the preparation of the teaching signal as well as a reference signal. The results are summarized in Table 5 below

TABLE 5

	P(I)D		FNN		SCoptimizer	
	Range	Deviation	Range	Deviation	Range	Deviation
'e'	4.025	0.57	3.503	0.5	3.513	0.54
'de'	6.972	0.61	7.743	0.56	7.834	0.55
'θ'	2.136	0.42	2.091	0.38	2.093	0.37
'l'	4.025	0.57	3.503	0.5	3.513	0.54
'i'	8.026	0.63	8.534	0.58	8.620	0.57
'dSp'	50.028	3.92	50.419	4.41	50.535	4.38
'Sp'	25.453	3.34	29.829	2.8	23.253	2.81
'dSc'	78.148	7.33	43.373	3.67	47.306	3.6
'Sc'	53.396	7.04	29.899	2.44	21.075	2.42
'U'	30.231	1.8	24.313	1.45	21.374	1.28
'Kp'	0.000	0	2.993	0.45	2.251	0.39
'Kd'	0.000	0	0.960	0.16	1.016	0.08
'Ki'	0.000	0	3.628	0.43	3.052	0.35
$(S_p - S_c)$* *$(\dot{S}_p - \dot{S}_c)$	266.58	44.51	16.99	1.12	18.35	1.17

Both the FNN controller and the SC optimizer-based controller are better than the P(I)D controller. The FNN approximates the teaching signal with redundant accuracy, and, as a result, better performance with the same conditions as used for teaching signal acquisition, but control signals are unstable near equilibrium points. The SC optimizer control has better performance with respect to entropy production, and control gains have simpler physical realization. The output of the SC optimizer-based controller is stable near equilibrium points. The KB prepared with the SC optimizer uses 24 rules, and has almost the same performance (according to the selected fitness function) as the FNN based FC with 64 rules

For analysis of the robustness of the simulated FC, the simulations were repeated with a new excitation signal, having longer duration, and different trajectory using the same distribution as was used for the teaching signal acquisition. The excitation used in this case is shown in FIG. **47**.

The results of the intended fitness function are shown in FIG. **48**. FIG. **48** shows that the fitness function performance of the SC optimizer is better than the fitness function performance of the FNN-based approach. FIG. **49** shows the controlled state variable dynamics. The Output of the SC optimizer in this case has a smaller deviation from the set point. Figure SW **13** shows the coefficient gain scheduler dynamics. The behavior of the coefficient gains obtained with the SC optimizer shows smaller deviation, especially around equilibrium points. Controller output is stable in case of SC optimizer control. The other control parameters are summarized in the following Table 6:

TABLE 6

	P(I)D		FNN		SCoptimizer	
	Range	Deviation	Range	Deviation	Range	Deviation
'e'	4.65	0.44	4.76	0.5	4.83	0.5
'de'	12.13	1.64	13.73	2.15	13.82	2.14
'θ'	3.01	0.46	2.58	0.39	2.58	0.36
'l'	8.78	2.87	8.61	2.81	8.59	2.77
'j'	9.68	1.43	8.38	1.37	8.44	1.23
'dSp'	293.81	11.16	81.55	5.14	68.97	4.19
'Sp'	410.96	111.83	380.81	105.09	307.81	84.96
'dSc'	269.01	12.54	146.54	9	142.06	8.38
'Sc'	1346.37	370.21	1103.19	310.01	1046.69	293.11
'U'	65.32	8.92	40.61	8.89	42.37	7.77
'Kp'	0.00	0	4.64	0.86	2.74	0.48
'Kd'	0.00	0	0.99	0.16	1.07	0.12
'Ki'	0.00	0	3.65	0.7	3.74	0.42
$(S_p - S_c)^* *(S_p - S_c)$	124838.92	6974.98	33307.25	4022.85	24103.82	3709.82

Table 6 shows that both the FNN controller and the SC optimizer-based controller are better than the P(I)D controller regarding fitness function performance. Due to over learning, the FNN controller becomes unstable with unknown excitation, and asymptotically looses control under the intended fitness function. The SC optimizer control works better under unknown conditions, thus the FC prepared with a KB produced by the SC optimizer **242** is more robust regarding variations of the excitation signal from the same distribution.

In the following example in addition to unknown excitation, a new reference signal in introduced as a harmonic signal obtained by the following equation:

$$Rs(t) = 5 + 4\sin\left(\frac{2\pi}{50}t\right) + 0.5\sin(2\pi t) \tag{41}$$

The reference signal according to Equation (41) is shown in the FIG. **51**. Control results using the reference signal of FIG. **51** are shown in FIGS. **52**–**18** and summarized in Table 7.

TABLE 7

	P(I)D		FNN		SCoptimizer	
	Range	Deviation	Range	Deviation	Range	Deviation
'e'	4.65	0.44	4.76	0.5	4.83	0.5
'de'	12.13	1.64	13.73	2.15	13.82	2.14
'θ'	3.01	0.46	2.58	0.39	2.58	0.36
'l'	8.78	2.87	8.61	2.81	8.59	2.77
'j'	9.68	1.43	8.38	1.37	8.44	1.23
'dSp'	293.81	11.16	81.55	5.14	68.97	4.19
'Sp'	410.96	111.83	380.81	105.09	307.81	84.96
'dSc'	269.01	12.54	146.54	9	142.06	8.38
'Sc'	1346.37	370.21	1103.19	310.01	1046.69	293.11
'U'	65.32	8.92	40.61	8.89	42.37	7.77
'Kp'	0.00	0	4.64	0.86	2.74	0.48
'Kd'	0.00	0	0.99	0.16	1.07	0.12
'Ki'	0.00	0	3.65	0.7	3.74	0.42
$(S_p - S_c)^* *(S_p - S_c)$	124838.92	6974.98	33307.25	4022.85	24103.82	3709.82

Table 7 shows that the FC prepared with a KB generated by the SC optimizer **242** is more robust in the presence of reference signal variation. Thus, the SC optimizer creates a robust KB for FC and reduces the number of rules in comparison with a KB created with other approaches. The KB created by the SC optimizer **242** automatically has a relatively more optimal number of rules based. The KB created by the SC optimizer **242** tends to be smaller and thus

more computationally efficient. The KB created by the SC optimizer tends to be more robust for excitation signal variation as well as for reference signal variation.

Swing dynamic system simulation results, Motion under fuzzy control with two P(I)D Controllers. Comparison between back propagation FNN and SC optimizer control results

In one embodiment two state variables (the angle θ and the length l) are controlled, and two types of stochastic excitations are used.

Gaussian excitation (a white noise) is acting along θ-axis, and non-Gaussian (Rayleigh) excitation is acting along l-axis. Initial conditions: θ_0=0.25, l_0=2.5, $\dot{\theta}_0$=0, $\dot{l}_0$=0.01, and reference signals: θ=0.4; l=3.5. In this example we see Sugeno 0 FIS with four inputs and six outputs variables. Input variables are: control error, derivative of control error for two P(I)D Controllers (along θ and l-axes). Output variables are control gains for P(I)D θ and P(I)D l correspondingly. For fuzzy simulation in this case we have chosen fitness function which minimizes a control error.

Tables 43, 44 and FIGS. **56**, **57**, **58**, **59** and **60** show the simulation results.

Table 8 shows dynamic and thermodynamic characteristics of swing motion along θ-axis.

TABLE 8

	P(I)D		FNN		SCoptimizer	
	Range	Deviation	Range	Deviation	Range	Deviation
'e'	0.2311	0.0368	0.2744	0.0330	0.2082	0.0271
'de'	0.3401	0.0615	0.6906	0.0924	0.3580	0.0576
'θ'	0.2311	0.0368	0.2744	0.0330	0.2082	0.0271
'θ'	0.3464	0.0619	0.6919	0.0924	0.3592	0.0577
'dSp'	0.0272	0.0019	0.1353	0.0101	0.0361	0.0024
'Sp'	0.0093	0.0012	0.0444	0.0049	0.0114	0.0015
'dSc'	0.1593	0.0258	0.7304	0.0733	0.2297	0.0294
'Sc'	0.5705	0.1558	0.9173	0.2805	0.6036	0.1582
'U'	1.8772	0.3107	3.0092	0.4544	3.0419	0.4139
'Kp'	0	0	12.7595	1.3437	4.7755	0.6805
'Kd'	0	0	12.7159	3.2428	7.0913	1.6870
'Ki'	0	0	16.8095	2.2770	9.9998	1.5148
$(S_p - S_c)^* *(\dot{S}_p - \dot{S}_c)$	0.0707	0.0087	0.3402	0.0320	0.0799	0.0091

Table 9 shows dynamic and thermodynamic characteristics of swing motion along l-axis.

TABLE 9

	P(I)D		FNN_P(I)D		SCoptimizer	
	Range	Deviation	Range	Deviation	Range	Deviation
'e'	2.7487	0.5118	1.9356	0.2385	2.1212	0.2694
'de'	3.5462	0.5347	5.1765	0.5602	2.9937	0.3848
'l'	2.7487	0.5118	1.9356	0.2385	2.1212	0.2694
'i'	3.5471	0.5349	5.1770	0.5602	2.9938	0.3848
'dSp'	11.6337	1.6373	27.5628	2.3988	9.0148	1.2071
'Sp'	17.222	2.8356	18.9126	2.6774	8.9580	1.1389
'dSc'	29.0804	4.0928	59.0850	4.6245	27.8549	3.8679
'Sc'	43.0811	7.0611	42.0118	6.6106	28.8407	3.6452
'U'	22.6100	4.1190	33.4908	4.5510	25.2402	4.0567
'Kp'	0	0	11.9993	2.0805	4.4347	0.7776
'Kd'	0	0	13.5328	1.6818	3.8774	0.4960
'Ki'	0	0	20.3707	3.1219	9.8635	1.2870
$(S_p - S_c)^* *(\dot{S}_p - \dot{S}_c)$	119.9456	22.1278	213.0406	18.1487	157.4477	22.3259

In Tables 10 and 11 and in FIGS. **61**, **62** results of robustness investigations are shown using the FC with the same KB (obtained from the teaching signal for the given above initial conditions) in the new situation, where new initial conditions, new reference signals, new noises amplitudes and new time of simulation are considered.

TABLE 10

	P(I)D		FNN		SCoptimizer	
	Range	Deviation	Range	Deviation	Range	Deviation
'e'	1.7058	0.0770	—	—	1.6025	0.0599
'de'	1.4721	0.1053	—	—	—	0.1179
'θ'	1.7058	0.0770	—	—	1.6025	0.0599
'θ'	1.4775	0.1053	—	—	2.1911	0.1179
'dSp'	2.3699	0.1136	—	—	7.8942	0.3266
'Sp'	1.6819	0.0764			3.8596	0.1592
'dSc'	6.5034	0.4078	—	—	10.4666	0.5201
'Sc'	11.1231	1.1647	—	—	11.1151	1.0726
'U'	6.0736	0.3156	—	—	11.8522	0.5232
'Kp'	0	0	—	—	8.4882	0.7814
'Kd'	0	0	—	—	9.2615	1.5437
'Ki'	0	0	—	—	9.9899	1.5492
$(S_p - S_c)^* *(\dot{S}_p - \dot{S}_c)$	14.7445	0.9209	—	—	13.5519	0.5222

In this case the output of FC_FNN gives unacceptable control of the swing motion.

TABLE 11

	P(I)D		FNN_P(I)D		Scoptimizer	
	Range	Deviation	Range	Deviation	Range	Deviation
'e'	3.6429	0.1447	—	—	3.5974	0.1420
'de'	3.7624	0.2177	—	—	4.4991	0.2403
'l'	3.6429	0.1447	—	—	3.5974	0.1420
'i'	3.7631	0.2170			4.4991	0.2404
'dSp'	19.5747	1.1262	—	—	30.6159	1.4965
'Sp'	18.9028	0.9256	—	—	23.1497	1.1836
'dSc'	97.8403	5.6594	—	—	94.1772	4.6575
'Sc'	95.0564	4.6141	—	—	72.0488	3.6436
'U'	36.7835	0.8077	—	—	28.7214	1.0880
'Kp'	0	0	—	—	9.9998	0.5328

TABLE 11-continued

	P(I)D		FNN_P(I)D		Scoptimizer	
	Range	Deviation	Range	Deviation	Range	Deviation
'Kd'	0	0	—	—	8.6156	0.6355
'Ki'	0	0	—	—	9.4755	0.8124
$(S_p - S_c)^* *(S_p - S_c)$	2.9475	166.9512	—	—	1.4757	75.4050

In Table 11, the FC_FNN gives unacceptable control of the swing motion under unknown conditions. The simulation results show that the FC with the KB generated by the SC optimizer is more effective and robust than P(I)D and FNN control under new conditions such as different excitations, different reference signal and different initial conditions.

Although the foregoing has been a description and illustration of specific embodiments of the invention, various modifications and changes can be made thereto by persons skilled in the art, without departing from the scope and spirit of the invention as defined by the claims attached hereto.

What is claimed is:

1. A method for optimizing a knowledge base in a soft computing controller, comprising:

selecting a fuzzy model by selecting one or more parameters, said one or more parameters comprising at least one of a number of input variables, a number of output variables, a type of fuzzy inference model, and a teaching signal;

optimizing linguistic variable parameters of a knowledge base according to said one or more parameters to produce optimized linguistic variables;

ranking rules in said rule base according to firing strength;

eliminating rules with relatively weak firing strength leaving selected rules from said rules in said rule base; and

optimizing said selected rules, using said fuzzy model, said linguistic variable parameters and said optimized linguistic variables, to produce optimized selected rules.

2. The method of claim **1**, further comprising optimizing said selected rules using a derivative-based optimization procedure.

3. The method of claim **1**, further comprising optimizing parameters of membership functions of said optimized selected rules to reduce approximation errors.

* * * * *